Ethernet Fronthaul and Time-Sensitive Networking for 5G and Beyond Mobile Networks

A Thesis Submitted to the University of Kent

for the Degree of Doctor of Philosophy in Electronic Engineering

By

Mohamad Kenan Al-Hares

March, 2019

Abstract

Ethernet has been proposed to be used as the transport technology in the future fronthaul network. For this purpose, a model of switched Ethernet architecture is developed and presented in order to characterise the performance of an Ethernet mobile fronthaul network. The effects of traditional queuing regimes, including Strict Priority (SP) and Weighted Round Robin (WRR), on the delay and delay variation of LTE streams under the presence of background Ethernet traffic are investigated using frame inter-arrival delay statistics. The results show the effect of different background traffic rates and frame sizes on the mean and Standard Deviation (STD) of the LTE traffic frame inter-arrival delay and the importance of selecting the most suitable queuing regime based on the priority level and time sensitivity of the different traffic types. While SP can be used with traffic types that require low delay and Frame Delay variation (FDV), this queuing regime does not guarantee that the time sensitive traffic will not encounter an increase in delay and FDV as a result of contention due to the lack of pre-emptive mechanisms. Thus, the need for a queuing regime that can overcome the limitations of traditional queuing regimes is shown.

To this extent, Time Sensitive Networking (TSN) for an Ethernet fronthaul network is modelled. Different modelling approaches for a Time Aware Shaper (TAS) based on the IEEE 802.1Qbv standard in Opnet/Riverbed are presented. The TAS model is assumed to be the scheduling entity in an Ethernet-based fronthaul network model, located in both the Ethernet switches and traffic sources. The TAS with/without queuing at the end stations has been presented as well. The performance of the TAS is compared to that of SP and WRR and is quantified through the FDV of the high priority traffic when this contends with lower priority traffic. The results show that with the TAS, contention-induced FDV can be minimized or even completely removed. Furthermore, variations in the processing times of networking equipment, due to the envisaged softwarization of the next generation mobile network, which can lead to time variation in the generation instances of traffic in the Ethernet fronthaul network (both in the end-nodes and in

switches/aggregators), have been considered in the TAS design. The need for a Global Scheduler (GS) and Software Defined Networking (SDN) with TAS is also discussed.

An Upper Physical layer functional Split (UPS), specifically a pre-resource mapper split, for an evolved Ethernet fronthaul network is modelled. Using this model and by incorporating additional traffic sources, an investigation of the frame delay and FDV limitations in this evolved fronthaul is carried out. The results show that contention in Ethernet switch output ports causes an increase in the delay and FDV beyond proposed specifications for the UPS and other time sensitive traffic, such as legacy Common Public Radio Interface (CPRI)-type traffic. While TAS can significantly reduce or even remove FDV for UPS traffic and CPRI-type traffic, it is shown that TAS design aspects have to carefully consider the different transmission characteristics, especially the transmission pattern, of the contending traffic flows. For this reason, different traffic allocations within TAS window sections are proposed. Furthermore, it is demonstrated that increased link rates will be important in enabling longer fronthaul fibre spans (more than ten Kilometres fibre spans with ten Gigabit Ethernet links). The results also show that using multiple hops (Ethernet switches/aggregators) in the network can result in a reduction in the amount of UPS traffic that can be received within the delay and FDV specifications. As a result, careful considerations of the fibre span length and the number of hops in the fronthaul network should be made.

Acknowledgements

I would foremost like to thank my supervisor Prof. Nathan Joseph Gomes, for his valuable guidance, encouragement, support and feedback throughout the years of my PhD.

I thank Dr. Philippos Assimakopoulos, for his help, support and being a very good collaborator and friend.

I acknowledge the financial support from the Engineering and Physical Sciences Research Council (EPSRC) for three years of my PhD study.

I would like to acknowledge as well the iCIRRUS and NIRVANA Projects for contributing to my general knowledge and experience through meetings and collaborative work.

I would like to thank Mr. Simon Hill and Dr. Howard Thomas from Viavi Solutions for providing the probing system that was used in the measurements of Chapter 3. I would like as well to thank very much Dr. Daniel Muench from ADVA Optical Networking for valuable discussions and a productive collaboration.

I would like to thank my mother and father, Amira Alnatour and Ali Al-Hares, and my family and friends.

List of Publications

Publications that have resulted directly from the work reported in this thesis:

[P1] M.K. Al-Hares, P. Assimakopoulos and N. J. Gomes, "Ethernet Fronthaul Transport of an Upper-Physical Layer Functional Split using Time-Aware Shaping," IEEE/ACM Trans. Netw, Submitted.

My contribution in this journal paper includes the upper physical layer split modelling and implementation, design and configuration of the simulated scenarios, analysis and write up of the paper.

[P2] M. K. Al-Hares, P. Assimakopoulos, D. Muench, and N. J. Gomes, "Modeling Time Aware Shaping in an Ethernet Fronthaul," in *IEEE* Global. commun. Conf *(GLOBECOM)*, Singapore, 2017 pp. 1-6.

My contribution in this conference paper covers the time aware shaper modelling and implementation, design and configuration of the simulated scenarios, analysis and write up for most parts of the paper.

[P3] M. K. Al-Hares, P. Assimakopoulos, D. Muench, and N. J. Gomes, "Traditional Queuing Regimes and Time-aware Shaping Performance Comparison in an Ethernet Fronthaul Network," in *IEEE Int. Conf. on Transp .Optic.Net*. (ICTON) ,Girona, Spain, 2017.

My contribution in this conference paper includes the time aware shaper modelling and implementation, design and configuration of the simulated scenarios and write up of the paper.

[P4] P. Assimakopoulos, G.S. Birring, M.K. Al-Hares, N.J. Gomes "Ethernet-based fronthauling for cloud radio access networks ," in *IEEE Int. Conf. on Transp .Optic.Net*. (ICTON), Spain, Girona, 2017.

My contribution in this conference paper covers part of the time sensitive networking section.

[P5] M. K. Al-Hares, P. Assimakopoulos, D. Muench and N. J. Gomes,"Scheduling in an Ethernet Fronthaul Network," in *European Conf. on Networks and Commun. (EUCNC)*, Oulu, Finland, 2017.

My contribution in this conference paper includes the time aware shaper modelling and implementation, design and configuration of the simulated scenarios, analysis and the paper write up.

[P6] P. Assimakopoulos, M.K. Al-Hares, and N.J. Gomes, "Switched Ethernet fronthaul architecture for cloud-radio access network", in *OSA/IEEE J. Optical Commun. and Netw*., vol: 8, no. 12, pp. B135-B146, Dec. 2016.

In this journal paper, my contribution includes parts of the measurements and the analysis sections.

[P7] M. K. Al-Hares, P. Assimakopoulos, S. Hill, and N. J. Gomes "The Effect of Different Queuing Regime On a Switched Ethernet Fronthaul," in *IEEE Int. Conf. on Transp .Optic.Net*. (ICTON), Trento, Italy, 2016, pp. 1-4.

In this conference paper, my contribution includes the testbed implementation, measurements, results analysis and write up for most parts of the paper.

[P8] N. J. Gomes, P. Assimakopoulos, M. K. Al-Hares, Usman Habib, and Shabnam Noor "The new flexible mobile fronthaul: Digital or analog, or both? ," in *IEEE Int. Conf. on Transp .Optic.Net*. (ICTON) , Trento, Italy, 2016.

My contribution in this conference paper covers part of the digital fronthaul section.

[P9] P. Assimakopoulos, M. K. Al-Hares, S. Hill, A. Abu-Amara, and N. J. Gomes, "Statistical distribution of packet inter-arrival rates in an Ethernet fronthaul," in *IEEE Int. Conf. on Commun. Workshops (ICC)*, Kuala Lumpur, Malaysia, 2016.

In this conference paper, my contribution covers parts of the measurements and the analysis sections.

[D1] iCIRRUS deliverable D3.1, Peter Turnbull, Howard Thomas, Daniel Venmani Philippe Chanclou, Volker Jungnickel, Luz Fernandez del Rosal, Mike Parker, Philippos Assimakopoulos, Mohamad Kenan Al-Hares, Nathan Gomes" intelligent Converged network consolIdating Radio and optical access aRound USer equipment".Available:http://www.icirrus-5gnet.eu/wp-content/uploads/2016/02/D3-1-Verification-of-Ethernet-.pdf.

My contribution in this deliverable includes the Ethernet fronthaul testbed and the delay analysis.

Table of Content

1 INTRODUCTION 8

1.1 Cloud Radio Access Network 8

1.2 Research Aims and Motivation 12

1.3 Structure of the Thesis 14

2 BACKGROUND THEORY 16

2.1 Cloud Radio Access Network (C-RAN) in the 5G 16

2.1.1 Architecture Review 16

2.1.2 C-RAN with CPRI Fronthaul Interface 18

2.1.3 C-RAN with Ethernet Fronthaul Network 21

2.1.4 Timing and Synchronization in the Ethernet Fronthaul Network 23

2.1.5 Radio over Ethernet Encapsulations and Mappings 25

2.1.6 LTE and 5G Stack and Functionality 27

2.1.7 Different Functional Split Proposals 30

2.1.8 Data Rate Requirements in the Ethernet Fronthaul Interface 33

2.2 Fronthaul Requirements and Key Performance Indicators (KPIs) 35

2.2.1 Delay and Frame Delay Variation in the Ethernet Fronthaul Interface 35

2.2.2 Latency Imbalance 36

2.3 Traditional Queuing Regimes in the Ethernet Fronthaul 37

2.3.1 Weighted Round Robin 37

2.3.2 Strict Priority 38

2.4 Time Sensitive Networking 39

2.4.1 Time Aware Shaping (802.1Qbv) 39

2.4.2 Frame Pre-emption (802.1Qbu) 41

2.5 Opnet/Riverbed Simulation Platform 42

3 ETHERNET FRONTHAUL NETWORK WITH TRADITIONAL QUEUING REGIMES. 45

3.1 Introduction 45

3.2 Latency in the Ethernet Fronthaul 46

3.3 Measurements Setup 47

3.4 Testbed Results and Comparisons 49
3.4.1 WRR Queuing Regime Results 50
3.4.2 Strict Priority Queuing Regime Results 52
3.4.3 Comparison with Single-Queue Case 54
3.4.4 Different LTE Data Rate Comparison 56

3.5 Asymmetric Delay and Time Inaccuracy in the Network 57

3.6 Conclusion 59

4 MODELLING AND PERFORMANCE STUDY FOR THE TIME AWARE SHAPER (TAS) 60

4.1 Introduction 60

4.2 Bridge Aware Time Aware Shaper Design 61

4.3 Initial Results 64

4.4 TSN and Traditional Queuing Regimes Comparison 66
4.4.1 Constant Background Frame Size Scenario 66
4.4.2 Variable Frame Size Scenario 67

4.5 Network Aware Time Aware Shaper Design 70

4.6 Initial Results 74

4.7 TSN and Traditional Queuing Regimes Comparison 75
4.7.1 Variable Frame Size Scenario (SP and TAS comparison) 77
4.7.2 Variable Burst Size Scenario (SP and TAS comparison) 77
4.7.3 Variable and Constant Burst Size Scenario (SP, WRR and TAS comparison) 79

4.8 Buffering Protection 81

4.9 Global Scheduler with TAS 83

4.10 Conclusion 85

5 UPPER-PHY SPLIT MODELLING IN OPNET/RIVERBED WITH DIFFERENT TRAFFIC AND TRANSPORT USE CASES IN THE ETHERNET FRONTHAUL 88

5.1 Introduction 88

5.2 Upper-PHY Split Modelling in Riverbed 89
5.2.1 LTE-AS Module 90
5.2.2 UPS Module 91
5.2.3 Statistics Implementation in Opnet/Riverbed 93

5.3 Fronthaul Scenarios 94
5.3.1 Initial Results 97
5.3.2 Upper-PHY Split Traffic with Statistically Distributed Background Traffic 99
5.3.3 Mixed Ethernet Fronthaul Traffic Scenario 100

5.4 Time Aware Shaper in the Fronthaul Network 102
5.4.1 UPS and Uniformly Distributed Background Traffic 103
5.4.2 Mixed Traffic Scenario 104
5.4.3 Mixed Traffic with Different Time Section Allocation Scenario 106
5.4.4 Buffering in the Ethernet Fronthaul 108
5.4.5 Buffering in the Multi-Hop Ethernet Fronthaul 110

5.5 Conclusion 113

6 CONCLUSIONS AND FUTURE WORK 115

6.1 Conclusions 115

6.2 Main Contributions of the Thesis 119

6.3 Future Work 121

BIBLIOGRAPHY 124

List of abbreviations

APTS	Assisted Partial Timing Support
BBU	Baseband Unit
BE	Best Effort
BES	Best Effort Section
BESS	Best Effort Subsection
BTS	Base Transceiver Station
CU	Central Unit
CPRI	Common Public Radio Interface
C-RAN	Cloud Radio Access Network
CDF	Cumulative Distribution Function
CRC	Cyclic Redundancy Clock
C&M	Control and Management
CoS	Class of Service
CRC	Cyclic Redundancy Check
DU	Distributed Unit
D-RAN	Distributed Radio Access Network
EPC	Evolved Packet Core
FDV	Frame Delay variation
FRP	Frame Result Packet
FPGA	Field Programmable Gate Arrays
GbE	Gigabit Ethernet
Gbps	Gigabits-per-second
GP	Guard Period
GNSS	Global Navigation Satellite System
GS	Global Scheduler
GUI	Graphical User Interface
HOP	Hold Period
HDLC	High level Data Link Control
HP	High Priority
HARQ	Hybrid Automatic Repeat request
LoS	Line of Sight
LP	Low Priority
MIMO	Multiple-Input Multiple-Output
MCS	Modulation and Coding Scheme
NFV	Network Function Virtualization

NAS	Non-access stratum
OAI	Open Air Interface
OFDM	Orthogonal Frequency Division Multiplexing
PS	Protected Section
PLL	Phased-Locked Loop
PTP	Precision Time Protocol
PSS	Protected Subsection
PRE	Packet Routing Engine
PDCP	Packet Data Convergence Protocol
PRTC	Primary Reference Time Clock
QAM	Quadrature Amplitude Modulation
QPSK	Quadrature Phase Shift Keying
RRS	Radio Remote System
RLC	Radio Link Control
RRU	Remote Radio Unit
RCC	Radio Cloud Centre
RAU	Radio Aggregation Unit
RF	Radio Frequency
RoE	Radio-over-Ethernet
RRH	Remote Radio Head
RRC	Radio Resource Control
RAT	Radio Access Technology
RAN	Radio Access Network
SP	Strict Priority
SFP	Small Form-factor Pluggable
SAP	service access point
SyncE	Synchronous Ethernet.
SDN	Software Defined Network
SDAP	Service Data Adaptation Protocol
TAS	Time Aware Shaper
TB	Transport Block
UPS	Upper Physical Layer split
WFQ	Weighted Fair Queuing

Table of Figures

Figure.1.1 Traditional Access Network. 8

Figure.1.2. Distributed Radio Access Network (D-RAN). 9

Figure.1.3. Cloud Radio Access Network (C-RAN). 10

Figure.1.4.Cloud Radio Access Network (C-RAN) with Ethernet fronthaul network. 11

Figure.2.1. Centralized RAN architecture with Fronthaul and Backhaul. 17

Figure.2.2. CPRI protocol architecture overview [7]. 19

Figure.2.3. CPRI frame architecture overview [2]. 20

Figure.2.4. Ethernet Fronthaul architecture with dedicated VLANs for addressing of RUs or sectors within RUs [14]. 22

Figure.2.5. Frequency Synchronization by Physical Layer Clock Recovery (SyncE) [7]. 23

Figure.2.6. Four Messages in 1588/PTP standard [7]. 25

Figure.2.7. RoE with different traffic types [32]. 26

Figure.2.8. RoE Frame Structure [32]. 26

Figure.2.9. LTE User and Control Plane Stack [35] 27

Figure.2.10. 5G NR User and Control Plane Stack [36]. 29

Figure.2.11. Functional Split Points between Central Unit (CU) and Distributed Unit (DU) [16] 30

Figure.2.12. Weighted Round Robin (WRR) example with three equal weights queues. 37

Figure.2.13. Strict Priority (SP) example with different priority queues. 38

Figure.2.14. Generic Time Window, Window Section and Subsection Plan based on IEEE 802.1Qbv. 40

Figure.2.15. Pre-emptive and Non-pre-emptive transmission. 41

Figure.2.16. Node Model Editor. 43

Figure.2.17. Part of State Machine of Transmit/Receive Functionality in PHY Module [46]. . 44

Figure.2.18. Overall Functionality Structure in Opnet/Riverbed. 44

Figure.3.1. Main Delay Parameters in a Switched Ethernet Fronthaul. Note that T is Based on the Delay Definitions Shown in (a), i.e. it includes Serialisation Delays. Higher LTE Protocol Layers are not shown in the Figure. 46

Figure.3.2. Testbed used for the Measurement Procedure. PRE=Packet Routing Engine, GbE=Gigabit Ethernet,SFP=Small Form-Factor Pluggable. 48

Figure.3.3. Forwarding Mode in the Ethernet switch. 49

Figure.3.4. Cut through Mode. 49

Figure.3.5. Comparison for mean and STD of frame inter-arrival delays of the LTE traffic with different WRR weights and background traffic data rates and a frame size of 1500 bytes. .. 51

Figure.3.6. Comparison for mean and STD of frame inter-arrival delays of the LTE traffic with different background traffic frame sizes and WRR weights at a data rate 215 Mbps. The "LTE" trace corresponds to transmitting only the LTE traffic (i.e. no background traffic). 51

Figure.3.7. Mean and STD of frame inter-arrival delays of the LTE traffic under SP regime for different frame sizes and background traffic data rates (105 Mbps, 450Mbps). 53

Figure.3.8. CCDFs for the mean of the inter-arrival frame delays of the LTE traffic under SP regime with different frame sizes and background traffic data rates (105 Mbps, 450Mbps). 53

Figure.3.9. Comparison for the mean of the frame inter-arrival delay of the LTE traffic for equal-weight (Wrr4) and No-priority cases with different LTE traffic bandwidths and different background traffic data rates with frame sizes 500 bytes. 55

Figure.3.10. Comparison for the mean of the frame inter-arrival delay of the LTE traffic for equal-weight (Wrr4) and No-priority cases with different background traffic data rates and 4000 bytes frame size. 55

Figure.3.11. Comparison for the mean of the frame inter-arrival delay of the LTE traffic for equal-weight (Wrr4) and No-priority cases with different LTE traffic bandwidths and different background traffic data rates with frame sizes 500 bytes. The "LTE" trace corresponds to transmitting only the LTE traffic (i.e. no background traffic). 56

Figure.3.12. Measured delay estimates for the fronthaul obtained through PTP timestamping. Two of the traces indicate erroneous values for the fronthaul delay (a stable error), while one is close to the actual value, which is approximately 37.7 μs. 58

Figure.3.13. Measured delay for fronthaul traffic by using two in-line probes and with no contending traffic. 58

Figure.4.1. TAS implementation in Opnet. TG1 generates the HP traffic while TG2 the LP traffic. 62

Figure.4.2. Implemented algorithm for the scheduler in the switch in Opnet. 63

Figure.4.3. Transmitted traffic in the protected window by TG. 65

Figure.4.4. Average and peak FDV for the PTP traffic with SP and TAS with different GPs. The background traffic source is constant frame-rate and constant frame size. 67

Figure.4.5. Average and peak FDV for the PTP traffic with SP and TAS with different GPs. The background traffic source is constant frame-rate with a varying frame size following a normal distribution with mean of 1000 octets and variance of 200 octets. 68

Figure.4.6. Average and peak FDV for the PTP traffic with SP and TAS with different GPs. The background traffic source is constant frame-rate with a varying frame size following a normal distribution with mean of 1000 octets and variance of 500 octets.....69
Figure.4.7. Zoom-in in the region of GPs from 0 to 1 μs for the results of Fig. 4.6. The inset shows worse- case PTP timestamping error that would result from the peak FDV values.....69
Figure.4.8. Durations of the HP sections in (a) the end-station and (b) the switch. 72
Figure.4.9. TAS implementation in Opnet. TG1 generates the HP traffic while TG2 the LP traffic. 73
Figure.4.10. Implemented algorithm for the scheduler in the end-station in Opnet. 73
Figure.4.11. Traffic in the network with TAS (taken from the utilization statistic in Opnet)...74
Figure.4.12. TG2 Traffic in the network with the queuing (taken from the utilization statistic in Opnet). 75
Figure.4.13. Implementation flow chart of the Bursty background traffic. 76
Figure.4.14. Average and peak FDV for the PTP traffic with SP and TAS with different GPs. The background traffic source is bursty with variable frame size. 77
Figure.4.15. High priority traffic emulating PTP transmissions and background traffic with constant frame size and variable burst size.....78
Figure.4.16. High priority traffic emulating PTP transmissions and background traffic with constant frame size and constant burst size.....79
Figure.4.17. High priority traffic emulating PTP transmissions and background traffic with variable frame and burst size. 80
Figure.4.18. PS duration definition with buffering protection in a) the end station.....82
b) the bridge (switch). 82
Figure.4.19. Comparison of frame delay results with buffering protection, with and without the modified PS design shown in Fig.4.18.....83
Figure.4.20. Scheduling design concept. SDN: Software-defined networking; GS:, Global Scheduler; SW: Ethernet switch; PTP: Precision-time protocol; BC: Boundary clock; GM: Grand master; PDCP: Packet data convergence protocol; RLC: Radio link control; MAC: Media-access control; PHY: Physical layer. 84
Figure.4.21. Number of transmitted frames in case of GS deployment in the network.....85
Figure.5.1. Implementation of the UPS in the Ethernet fronthaul network (Block diagram). .91
Figure.5.2. Implementation of the UPS in Opnet/Riverbed.....92
Figure.5.3. UPS Module pseudocode.....93
Figure.5.4. ROE Frame Structure in Opnet/Riverbed.....93
Figure.5.5. Ethernet Frame Structure in Opnet/Riverbed.....93

Figure.5.6. Statistics Implementation in Opnet. 94
Figure.5.7. the simulation set-up of the Ethernet fronthaul.....95
Figure.5.8. Cpri-type traffic implementation flow chart in Opnet. 96
Figure.5.9. Baseline delay and FDV of the UPS and CPRI traffic. 98
Figure.5.10. UPS traffic delay and FDV for scenario described in 5.3.2. 100
Figure.5.11. UPS & CPRI traffic delay and FDV with the existence of background traffic for scenario described in 5.3.3. 101
Figure.5.12. Simulation set-up of the Ethernet fronthaul with TAS.....102
Figure.5.13. TAS section allocations in: (A) UPS and background traffic scenario; (B) Mixed traffic scenario (case 1); (C) Mixed traffic scenario (case 2); (D) Mixed traffic with different time sections allocation scenario.....103
Figure.5.14. Frame delay & FDV of UPS traffic for scenario described in 5.4.1. 104
Figure.5.15. Frame delay & FDV of UPS traffic for scenario B with TAS. 106
Figure.5.16. Frame delay and FDV of UPS traffic for scenario described in 5.4.2.....107
Figure.5.17. CDF of the UPS FDV in the Mixed Traffic with Different Time Sections Allocation scenario.....109
Figure.5.18. Zoomed UPS FDV's CDF results. 110
Figure.5.19. the simulation set-up of the Ethernet fronthaul with TAS and five hops. 111
Figure.5.20. CDF of the UPS FDV in the mixed traffic with 10Gbps links, different Number of hops and 64% utilization. 112

List of Tables

Table. I The Requirements of the Data Rate for the Different Functional Split [49]……34

Table. II Requirements of the Delay and FDV for the Different Functional Split Points.……36

Table. III Delay, FDV, Queuing Delay and Queuing Delay Variation for the Results of Figure.4.3 ……65

Table. IV Background Traffic Settings for Scenario 5.3.3……101

Table. V Percentage Traffic within Specifications with Different Ethernet Links Lengths for 64% Utilization ……110

Table. VI Percentage Traffic within Specifications with Different Ethernet Links Lengths (13, 10 &7 Km) and Number of Hops for 64% utilization……112

1 Introduction

1.1 Cloud Radio Access Network

The Radio Access Network (RAN) has evolved through generations of mobile networks to provide a higher data rate and Quality of Service (QoS) with less deployment cost and more flexibility and dynamicity [1]. With the traditional RAN, both baseband and radio processing are located in the same unit and integrated in the base station, see Fig .1.1. The main limitation of this access network is that it can serve a particular number of antennas located within specific geographical areas and the cost of expanding the coverage or increasing the capacity is very high. To increase the coverage or the capacity in this network, new base stations should be installed which incur a high cost due to the equipment, management, installation and rental cost, and a high power consumption [2]. To overcome this limitation, Distributed RAN (D-RAN) has been proposed [1].

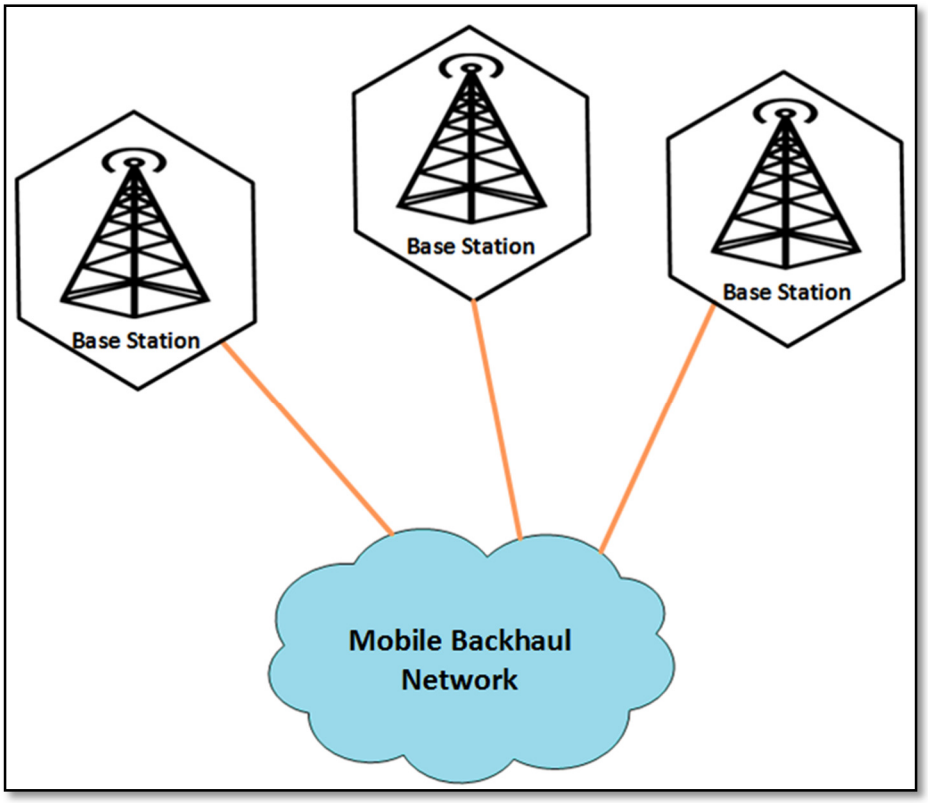

Figure.1.1 Traditional Access Network.

In D-RAN, the baseband and radio processing are separated into two units. The baseband processing is performed in the Baseband Unit (BBU) and the radio processing is carried out in the Remote Radio Head (RRH) [3], as shown in Fig. 1.2. This separation allowed more flexibility in the network planning and coverage. The limitation of this access network is that only one RRH is connected to each BBU. To improve the flexibility and efficiency of the access network, the Cloud Radio Access Network (C-RAN) has been proposed [4]. With C-RAN, the BBUs are centralized in one location and serve a number of RRHs as shown in Fig. 1.3.

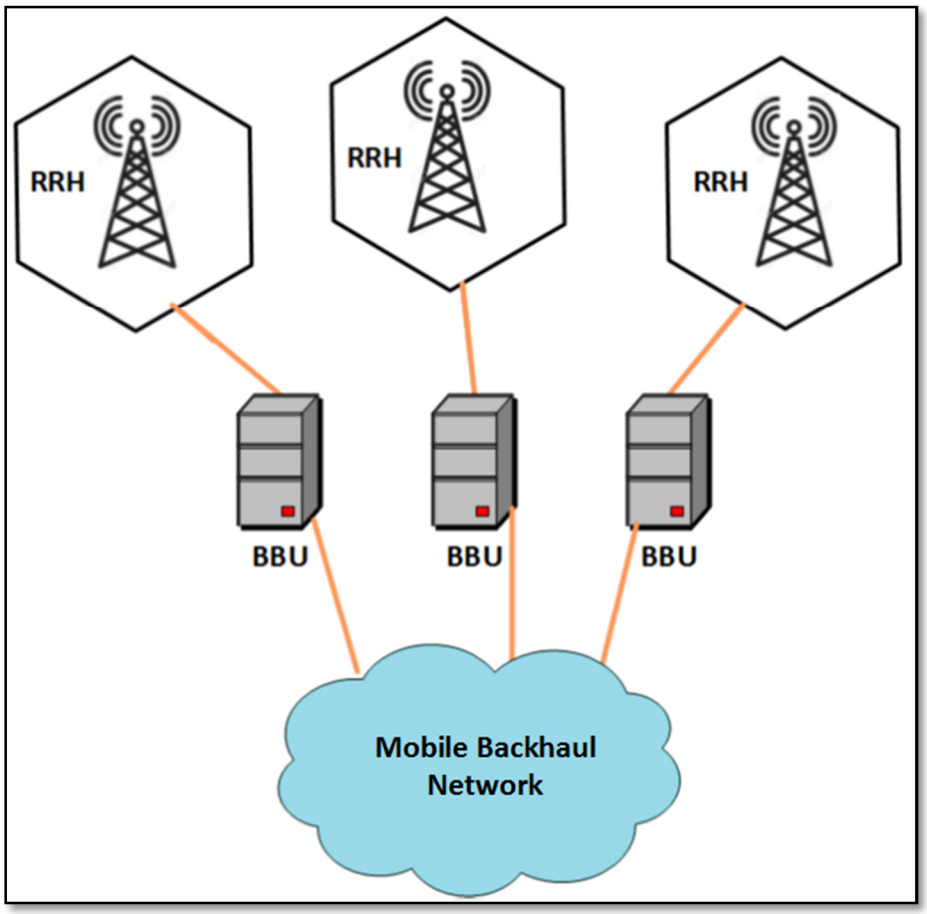

Figure.1.2. Distributed Radio Access Network (D-RAN).

The C-RAN has many advantages, such as [5] [6]:

- Improving the capacity and coverage of the network.
- Allowing network self-optimization and configuration.
- Permitting high manageability through Software Defined Networking (SDN).

- Allowing the use of cloudification and virtualization techniques to improve the use of the processing resources available in the access network.
- Improving the network scalability.
- Reducing deployment and running costs.

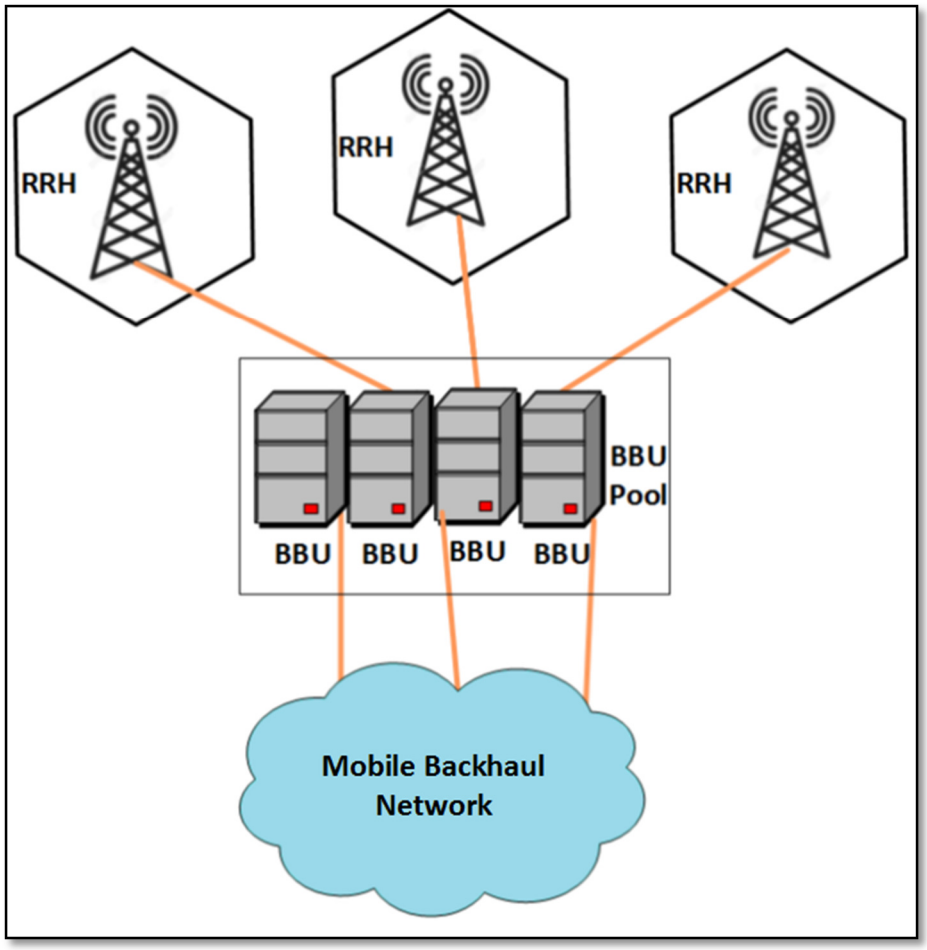

Figure.1.3. Cloud Radio Access Network (C-RAN).

The transport network between the BBU and RRH is called the fronthaul. The fronthaul should fulfil the data rate and ultra-low latency requirements of the mobile network and enable flexible and low cost deployment and high efficiency in its resource utilization [7]. The data rate in the fronthaul network can be ten times the actual user data rate.

While analogue fronthaul has the advantage of high spectral efficiency and low latency, it suffers from different channel impairments such as noise and distortion [8].

Digital fronthaul network is more robust against such impairments and widely used and produced. On the other hand, some digital fronthaul implementations have delay issues and high bandwidth requirements [9].

An Ethernet fronthaul network has been proposed to be used in the future C-RAN. Using Ethernet technology has many advantages such as allowing for statistical multiplexing gains, network virtualization, monitoring, orchestration and SDN, and low cost deployment [9]. Fig. 1.4 shows a C-RAN with an Ethernet fronthaul network. The traffic is transmitted in the Ethernet fronthaul through the switching units to the targeted RRHs through allocated Virtual Local Area Networks (VLANs). On the other hand, using Ethernet may lead to a lack of synchronization, increased delay and delay variation due to contention, and mapping inefficiency [10].

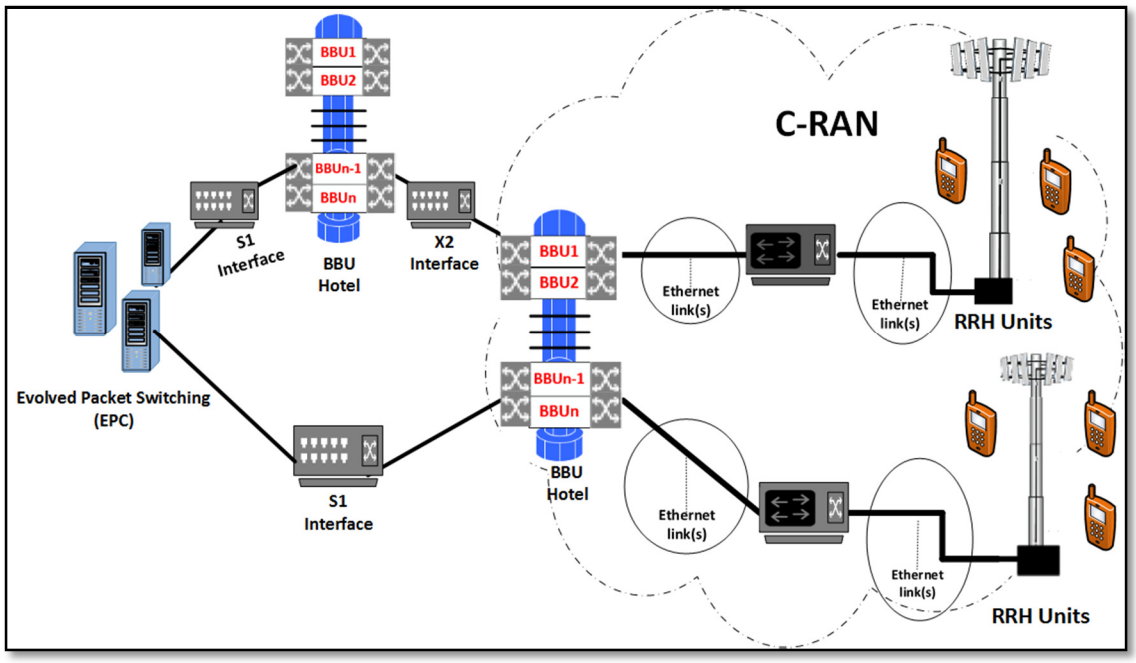

Figure.1.4.Cloud Radio Access Network (C-RAN) with Ethernet fronthaul network.

In current C-RANs, In-phase and Quadrature (IQ) samples are transmitted from the BBU to the RRH by using either the CPRI [11] or Open Base Station Architecture Initiative (OBSAI) [12] industry standards. As a result of the time domain samples transmission in CPRI, fronthaul has high data rate requirements. In addition, CPRI has stringent latency requirements due to its timing and synchronization mechanisms [9]. The transmission of CPRI traffic leads to the absence of any possibility to achieve statistical multiplexing

gain due to the continuous transmission of time-domain waveform samples [2]. To reduce the data rate and relax the latency requirements, eight main functional splits points have been proposed [7]. The selection of the functional split point depends on several factors such as the reduction of fronthaul bit-rate, delay requirements and the support of radio techniques such as multiple-input multiple-output (MIMO), massive MIMO and Coordinated Multipoint (CoMP) [13] , [14].

1.2 Research Aims and Motivation

Identifying the main limitations of the available scheduling techniques in the current Ethernet networks and modelling, analysing and testing selected queuing and scheduling techniques in the Ethernet fronthaul network is one of the main aims of this work. Another main aim is to model and examine a selected functional split proposal in the Ethernet fronthaul network

The Ethernet fronthaul network has been proposed as a transport medium in the C-RAN. Many challenges exist to the use of Ethernet technology in the fronthaul network, such as the lack of synchronization and the induced delay and Frame Delay Variation (FDV) due to the processing, contention and transport link [9]. As a result, new standards, techniques and technologies have been proposed to overcome these challenges.

This work aims to discuss in detail the delay and FDV of different time sensitive traffic, CPRI, Precision Time Protocol (PTP) and Upper Physical layer Split (UPS) traffic, in particular, in the Ethernet fronthaul network.

The work investigates the limitations of the current queuing regimes, in particular Strict Priority (SP) and Weighted Round Robin (WRR). While SP and WRR can be potentially used with a range of traffic types and applications to schedule their transmission over the Ethernet network, they might not be able to fulfil the requirement of many time sensitive traffic flows such as those carrying PTP and CPRI, causing a significant delay and FDV for the frames in such flows.

It is interesting to investigate this aspect and accordingly decide on the best Time Sensitive Networking (TSN) standard that can be used in the Ethernet fronthaul and allows each flow to be transmitted within its specifications.

Implementing and designing a Time aware shaper (TAS) in a simulation platform environment (Opnet/Riverbed) and investigating its performance with different time sensitive traffic such as PTP, CPRI and UPS traffic is another aim for this work. Different traffic types with different frame sizes, data rates and transmission pattern should be transmitted alongside the time sensitive traffic in a range of contention scenarios to test the performance of TAS, with most of the applicable contention scenarios in the proposed fronthaul network. It is interesting to investigate and report the advantages and limitations of TAS with each of these time sensitive traffic types and the potential solutions for these limitations. The importance and need for the Global scheduling in the Ethernet fronthaul network is interesting to be discussed and explored as well as self-configured and optimized network which are necessary to allow the use of the different techniques and standards in the transport and wireless parts.

The UPS is not investigated enough in the literature [15] and according to the 3GPP it is an interesting split point as it is the closest split point to the antenna which can lead to statistical multiplexing gains. It also readily allows for joint processing techniques in both downlink and uplink and offers centralized aggregation for the transmission of 4G and 5G New Radio (NR) signals [16].

Modelling and implementing the UPS in Opnet/Riverbed and investigating the effect of the contention in different scenarios where traffic with different types, rates and transmission patterns transmitted alongside the UPS traffic on the delay and FDV of the UPS traffic is a point of interest and can be an important reference for any future development for the fronthaul network. Investigating the ability of TAS to absorb the UPS FDV due to the contention while maintaining the delay within requirements is another aim of this work.

Having the UPS and TAS implemented and deployed in the same network, and reporting the performance, is interesting as it gives a complete picture and allows reporting the delay and FDV of UPS in a possible fronthaul network structure.

A multi-hop scenario is a potential use case in the Ethernet fronthaul [11] and for that reason, this case will be covered as well together with UPS traffic and TAS.

Note that the used data and link rates in the different scenarios in this thesis are already used in the 4G fronthaul and can be used in the 5G network. Due to the limitations in the software and hardware platforms, the high link and data rates of the 5G fronthaul have not been used. The results in some scenarios are scaled to the 5G high rates. The investigated queuing regimes (SP, WRR) can be used in both 4G and 5G fronthaul while the implemented and tested scheduling regime (TAS) has been proposed to be used in 5G and beyond networks. In addition, the implemented functional split is proposed to be deployed in the 5G and beyond fronthaul networks.

1.3 Structure of the Thesis

The thesis is divided into six chapters. More specifically:

Chapter 2 presents the background theory for the thesis, including among others, the theory of C-RAN, fronthaul requirements and KPIs, proposed functional distribution in fronthaul, queuing regimes and time sensitive networking.

Chapter 3 shows the effect of the traditional queuing regimes, SP and WRR, on the different LTE performance measures. Testbed of Ethernet fronthaul with LTE and background traffic sources is presented. The effect of WRR and SP on the mean and standard deviation (STD) of the inter-arrival frame delay of LTE traffic with a range of contention scenarios that have different background traffic rates and frame sizes is measured. In addition, a special case of single queue and equal WRR weights is investigated and a different LTE traffic rates case is presented.

Chapter 4 demonstrates a different modelling approach for TAS based on the 802.1Qbv standard and the performance of the TAS with different traffic types such as PTP, CPRI-type traffic and split traffic. Different contention scenarios are presented considering different frame sizes and traffic rates. The ability of TAS in absorbing the FDV of the PTP traffic is compared with the other traditional queuing regimes, SP and WRR, in this

chapter and the importance of the SDN and GS in the Ethernet fronthaul with TAS is also investigated.

Chapter 5 presents a study for the UPS traffic in the Ethernet fronthaul network. Modelling for the UPS in the Opnet/Riverbed simulation platform is presented in this chapter. The effect of different traffic types such as CPRI-type traffic and randomized background traffic on the delay and FDV of the UPS traffic in the Ethernet fronthaul is examined. Different time section allocation scenarios for UPS traffic with TAS and the use of buffering in the Ethernet fronthaul are also analysed. Different link rates and lengths with various number of hops in Ethernet fronthaul scenarios are simulated and analysed in this chapter.

Chapter 6 demonstrates the main contribution of the thesis and discusses future work.

2 Background Theory

2.1 Cloud Radio Access Network (C-RAN) in the 5G

2.1.1 Architecture Review

The exponential growth in the number of mobile network users [7] and their increasing bandwidth requirements, force the service providers to invest more resources and equipment. Areas with dense network users such as shopping malls or main train stations increase the stress on the base stations that serve them and lead to the need to install more base stations in these areas by the operators to fulfil the needs and improve the quality of service. Installing more base stations has a high cost, requires a lot of radio planning efforts to avoid any interference and has low power efficiency [5].

C-RAN has been proposed to accommodate the ultra-dense mobile users' bandwidth requirements in the next generation of the mobile network and overcome the high energy consumption. It allows as well the use of advanced techniques such as cloudification and virtualization which aggregate the resources on a pool level and allocate it on demand, which can lead to an efficient use of the available processing resources and reduce the power consumption [17], [18].

In addition, the network implementation and running cost can significantly be reduced and the operation can be more straightforward as the processing is centralised with C-RAN. Furthermore, the deployment and management of different radio techniques such as coordinated multipoint (CoMP) become simpler and more practical with C-RAN since the baseband units are centralized [9].

Fig. 2.1 shows the architecture of the C-RAN. The C-RAN consists of Baseband Unit (BBU) pool, Remote Radio Head (RRH) and transport network called fronthaul.

A BBU pool is located in a centralized location such as a data centre and consists of many BBUs. The BBU pool has high computational and processing capabilities that can be

allocated dynamically to the RRHs based on the network need. The main responsibility of the BBU is processing the LTE data and transmitting it to the RRH.

With the proposed functional split, some of the functionalities moved from the Central Unit (CU) to the Distributed Unit (DU). The different proposals of the functional splitting are explained in details in sub-section 2.1.7 [9].

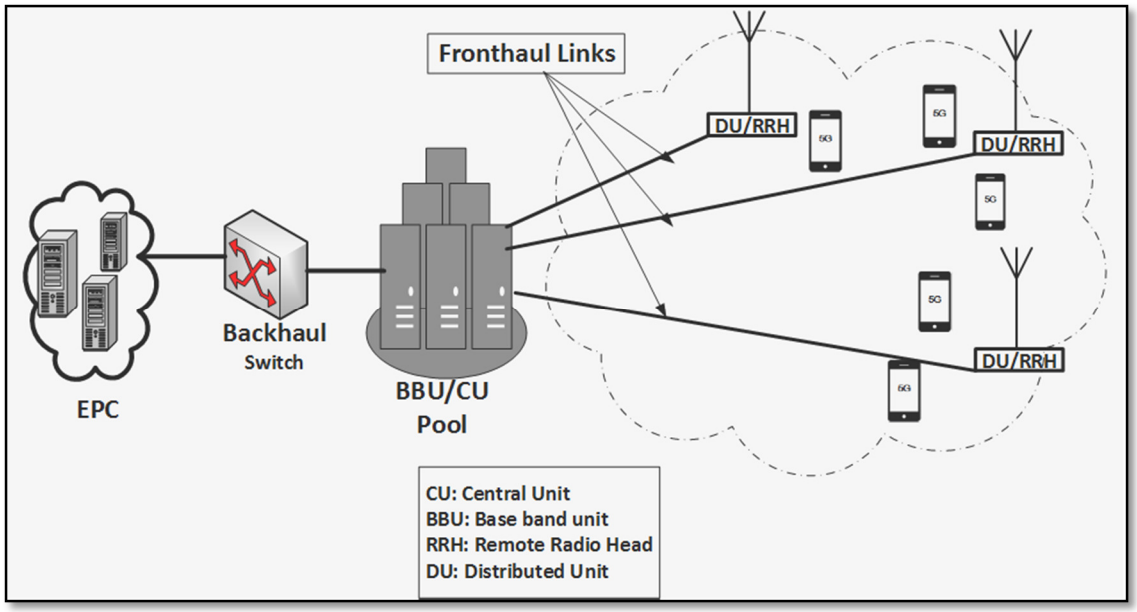

Figure.2.1. Centralized RAN architecture with Fronthaul and Backhaul.

The transport network (fronthaul network) in the C-RAN, that provides the connectivity between the BBU and the RRH, should guarantee low delay and delay variation and high capacity to fulfil the requirements of the different applications that are envisioned by 5G and require ultra-low latency and high data rate [19]. Fronthaul network should has low deployment and management cost as well. For this purpose, different technologies have been proposed.

Using millimetre wave communication in the fronthaul network has the advantage of the low cost and simple and straightforward deployment since it does not require pre-existed infrastructure between the network nodes. On the other hand, it can cause more latency and latency variations in the fronthaul due to the need for multiple hops to keep the Line of Sight (LoS) path in each mmWave transport link [20]. Optical fibre communication is elected to be used in the fronthaul as the most suitable technology

since it can provide the highest data rate among all possible technologies. On the other hand, this technology has a high implementation cost and suffers from the lack of flexibility in the deployment [2].

There are many challenges in deploying the C-RAN such as [2] , [21]:

- Strict delay, Frame Delay Variation (FDV) and synchronization requirements.
- High data rate and bandwidth requirements.
- Implementing the virtualization and cloudification techniques in the BBU pool.

2.1.2 C-RAN with CPRI Fronthaul Interface

The Common Public Radio Interface (CPRI) is a result of industry collaboration to define the interface specification between the REC (Radio Equipment Protocol) and RE (Radio Equipment) [7]. For the transmission of the user plan, synchronization, Control and Management information (C&M) between the REC and RE and between the REs, CPRI defines two protocol layers L1 and L2 [22].

As shown in Fig. 2.2, L1 defines the optical and electrical transmission and time division multiplexing, while L2 defines control and management through Ethernet and High level Data Link Control (HDLC).

The CPRI interface supports the following types of traffic:

- IQ Data: User plane information in the form of in-phase and quadrature modulated data (digital baseband signals).
- Synchronization: Synchronization data used for frame and time alignment.
- L1 Inband Protocol: Signalling information related to the used links in the network.
- C&M data: control and management information to be exchanged between the different entities in the network.
- Protocol Extensions: Reserved for any protocol extension in the future.

CPRI has a constant bit rate which can go from 614.4 Mb/s up to 24.33 Gb/s see Fig. 2.3 and each link consists of a fixed-bandwidth time division-multiplexed (TDM) connection see Fig. 2.2. This interface can support different topologies such as tree and ring topologies [10].

As shown in Fig. 2.3, the basic frame duration in CPRI is 260 ns and each one of them consists of 16 words. The word length depends on the CPRI line rate. The hyper frame consists of 256 basic frames and 150 hyper frames make a radio frame. The duration of the radio frame in CPRI is 10 ms.

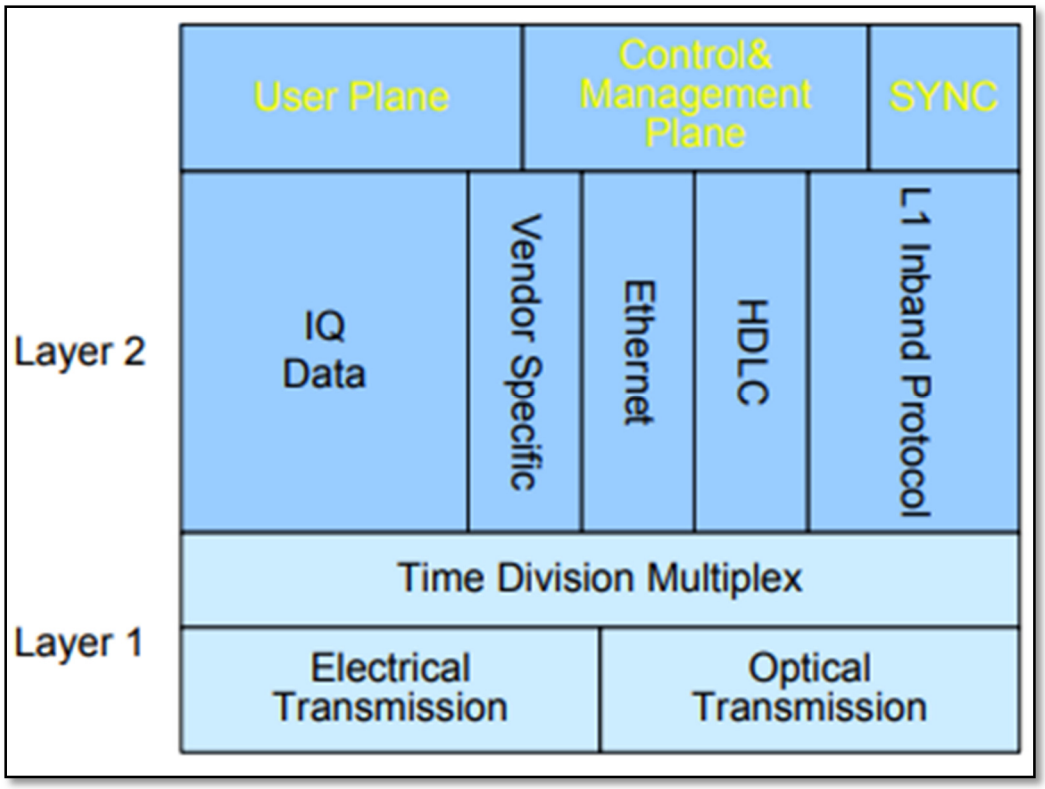

Figure.2.2. CPRI protocol architecture overview [7].

While CPRI is a successful industrial collaboration to transmit In-phase and Quadrature (I/Q) data from the REC to RE, the interface has many disadvantages such as consuming large bandwidth and the low efficiency in using the available bandwidth (lack in the statistical multiplexing gain) due to the constant bit rate on the link (continuous radio waveform) [23].

In the Ethernet fronthaul network, CPRI has been proposed to be encapsulated in the Ethernet frames and sent over the Ethernet fronthaul network [11]. IEEE 1914.3, Radio

over Ethernet (RoE), (this standard will be explained in detail in Section 2.1.5) is an intermediate structure agnostic encapsulation that is used to allow the encapsulation of the I/Q data in the Ethernet frames. Two types of RoE encapsulation have been proposed [11].

- Size based encapsulation, where CPRI frames are assembled and encapsulated in the payload of the Ethernet frames until the payload size is reached.
- Time based encapsulation, where a specific period of the I/Q transmission time is assembled and encapsulated in the Ethernet frames payload.

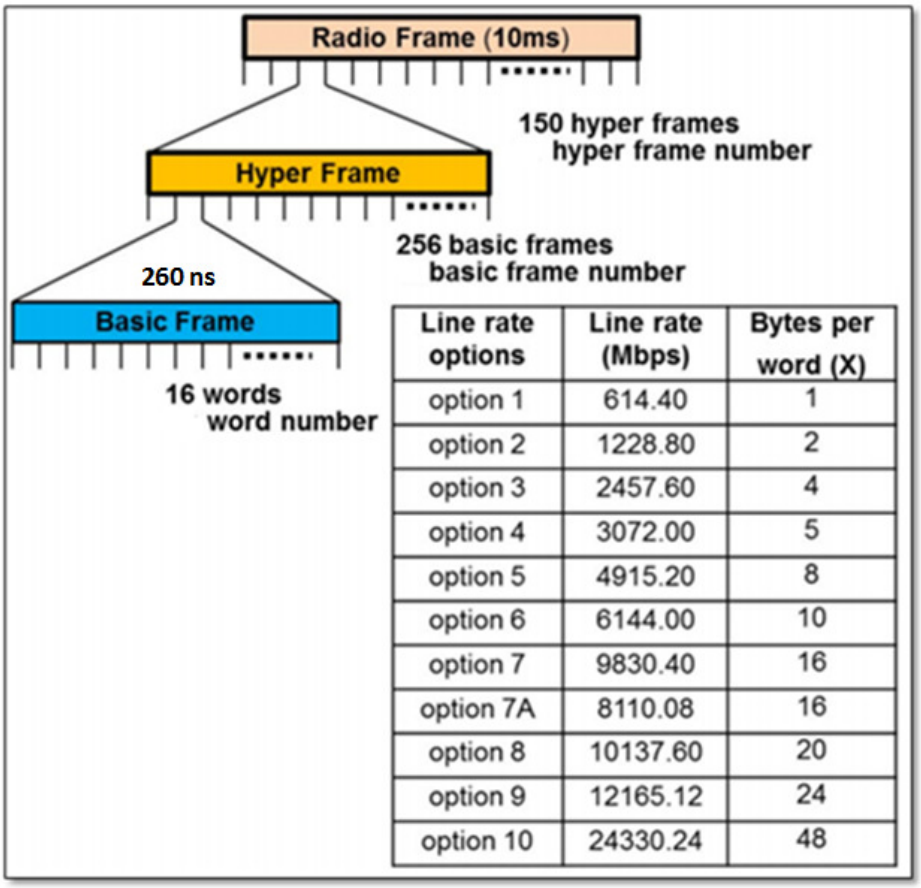

Line rate options	Line rate (Mbps)	Bytes per word (X)
option 1	614.40	1
option 2	1228.80	2
option 3	2457.60	4
option 4	3072.00	5
option 5	4915.20	8
option 6	6144.00	10
option 7	9830.40	16
option 7A	8110.08	16
option 8	10137.60	20
option 9	12165.12	24
option 10	24330.24	48

Figure.2.3. CPRI frame architecture overview [2].

Using Ethernet with CPRI is attractive since it allows the use of low cost industrial standard equipment, has a standardised Operations, Administration and Maintenance (OAM) and the ability to monitor the network performance through compatible hardware probes. On the other hand, meeting the delay and jitter requirements of CPRI

with the structure and nature of the Ethernet networks is challenging [11] and for this purpose, different time sensitive networking standards such as Time Aware Shaping (TAS) (see section 2.4.1) and Frame pre-emption (see Section in 2.4.2) have been proposed to schedule and manage the traffic in the Ethernet network to meet CPRI requirements [24].

The other challenge in encapsulating CPRI in Ethernet is that CPRI synchronisation information will be lost due to Ethernet framing. The synchronization should be implemented in the network to compensate for this issue and maintain CPRI requirements [25].

2.1.3 C-RAN with Ethernet Fronthaul Network

Ethernet technology has been proposed as a potential transport technology in the next generation of the radio access network. As mentioned in Section 1.1, the future cloud radio access network has high requirements in terms of the data rate, latency and synchronization.

Fig. 2.4 shows an example of Ethernet fronthaul with dedicated Virtual Local Area Network (VLAN) trunking [26]. The Baseband Unit (BBU) encapsulates the I/Q samples or the proposed functional split LTE data (see Section 2.1.7) in the Ethernet frames and sends them over trunk links to the Ethernet switches and then over other trunk links toward the RRHs. The different Remote Radio Heads (RRHs) and/or sectors within RRHs are addressed through VLAN ids, with the use of dedicated VLANs. The transmitted traffic types can be either sent separately on different VLANs or group of traffic types that have similar requirements or specifications such as having the same priority can be transmitted through a particular VLAN. The first trunk in Fig. 2.4 is set in the R1 link while the second trunk is set on the R2 link [25].

The main advantages of deploying Ethernet in C-RAN are [27]:

- The low cost deployment for the operators and vendors where off-the-shelf (OTS) equipment can be used.
- Ability to treat traffic with different priority and classes.
- Usability with different network topologies.

- Agnostic to any functional changes in the network.
- The ability to use the statistical multiplexing and achieve high use of the available bandwidth.
- The possible structural convergence with backhaul and midhaul.

On the other hand, the main limitations of using Ethernet in the fronthaul network are [28]:

- Ethernet has no inherent support for synchronisation of frequency, phase or time.
- Delay and FDV due to contention between different traffic streams in the network bridges can violates the specifications of the time sensitive traffic (more details in subsection 2.4).

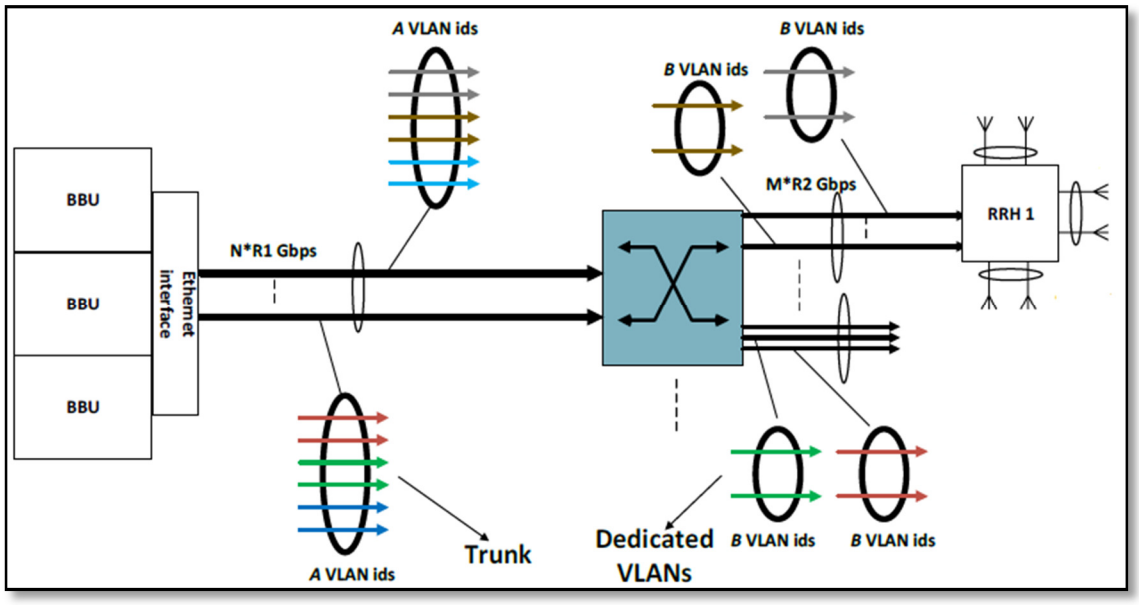

Figure.2.4. Ethernet Fronthaul architecture with dedicated VLANs for addressing of RUs or sectors within RUs [14].

2.1.4 Timing and Synchronization in the Ethernet Fronthaul Network

Two main synchronization techniques are used in networks to provide frequency, time and phase synchronization. The first technique is the Physical Layer approach: synchronous Ethernet (Sync E), which provides frequency synchronization [29], while the second technique is a Packet based approach, Precision Timing Protocol (PTP), which provides time and phase synchronisation [30].

- **Synchronous Ethernet (Sync E)**

Synchronous Ethernet (SyncE) is an ITU-T standard (G.8265) that supports the transmission of the clock synchronization over the physical layer of the Ethernet network. In this physical layer technology, the synchronization clock is sent over the physical layer of the Ethernet network and recovered by the receiver node to adjust its internal clock accordingly. Fig. 2.5 shows the Sync E transmission in the Ethernet network. The phased-locked loop (PLL) of the network node (switch) receives the bit sequence from the master clock (primary reference clock (PRC)) clean it from the jitter and extract the timing information to adjust the local oscillator according to it and transmit the data. All the nodes apply clock recovery mechanisms in their physical layer functionality to obtain the clock information and feed their own PLL. Most Ethernet devices do not provide a high precision clock and do not use the incoming timing information, rather they use free-running oscillators [29].

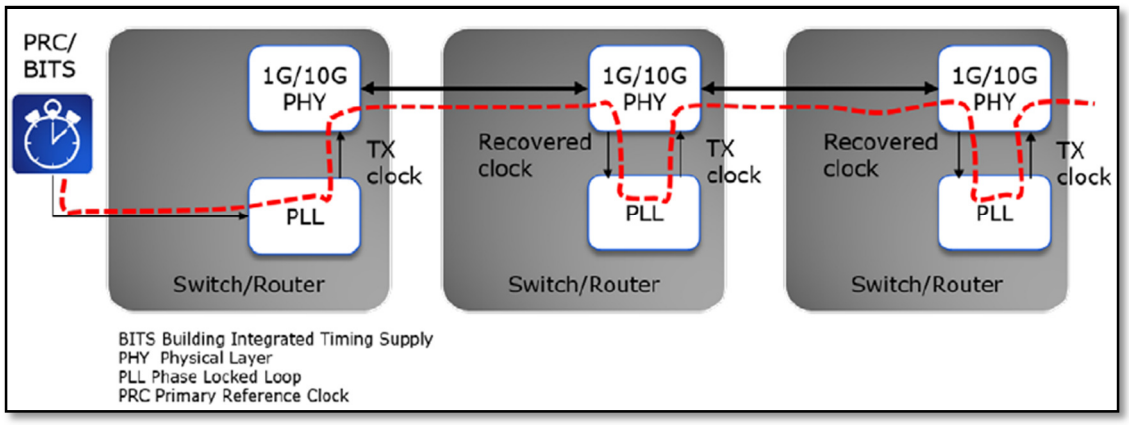

Figure.2.5. Frequency Synchronization by Physical Layer Clock Recovery (SyncE) [7].

- **Packet based approach, Precision Timing Protocol (PTP)**

IEEE1588 or Precision Time Protocol (PTP) is a standardised protocol defined by the IEEE and then adopted and developed by the different industrial sectors including the telecom networks. Different synchronization profiles are under the definition of ITU-T Q13/SG15 [30].

This standard has a packet-based approach where the packet or frame path delay is measured between the clock source (master) and the device that needs to be synchronized (slave) with the use of time stamping. The measured delay between the master and slave allows the system to fix the time offset.

In this standard, four messages are sent between the master and slaves in the network in order for the slave to be able to calculate the path delay [7], see Fig. 2.6.

The first message is the sync message (T1): this message is time stamped in the master and sent to the slave. At T2, the slave keeps the time that sync message is received in at the slave station.

The second message is Delay_req: this message is stamped by the slave node with the exact time when the Delay_req (T3) message is sent back to the master station.

The third message is Delay_resp: this message is stamped in the Master with the time when it receives the Delay_req (T4) and sent back to the slave station.

The slave is now capable of calculating the mean path delay since it has all the required information. The mean path delay (D_{mp}) is given by:

$$D_{mp} = \frac{((T_2 - T_1) + (T_4 - T_3))}{2} \qquad (1)$$

The variability of the frame delay in the network due to the contention in the network bridges (switches) is one of the main challenges in using PTP in the Ethernet fronthaul network. The different time stamps should reflect the delay in the network without any delay or FDV due to the queuing or contention in the network switches output queues which can lead to delay asymmetry [31].

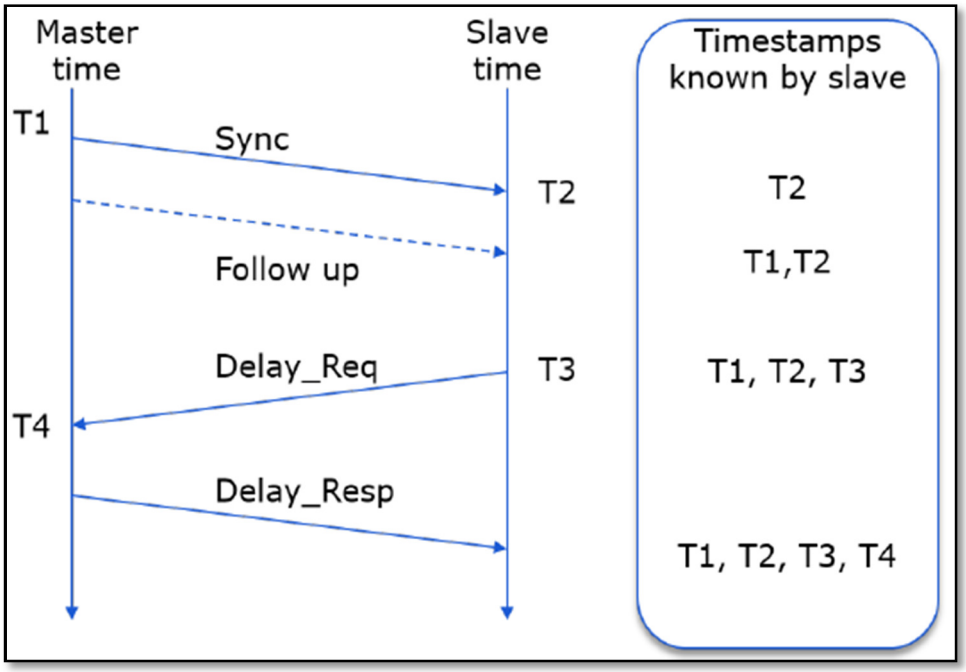

Figure.2.6. Four Messages in 1588/PTP standard [7].

2.1.5 Radio over Ethernet Encapsulations and Mappings

The Radio over Ethernet (RoE) standard, IEEE 1914.3, has been introduced to allow the transmission of I/Q user-plane data, vendor-specific data, and control and management (C&M) information channels over the Ethernet-based switched networks. The received data is encapsulated in the RoE frame and passed to the Ethernet to be encapsulated and sent over the Ethernet network [32].

Different RoE mappers are proposed for different types of transmitted traffic over Ethernet networks, see Fig. 2.7. The structure-agnostic mapper is designed to accommodate any digitized radio data transmitted over Ethernet network. The structure-aware mapper is designed specifically for the Common Public Radio Interface (CPRI). The native mode mapper is implemented for digitized radio in-phase and quadrature (I/Q) payload and control data channels [33].

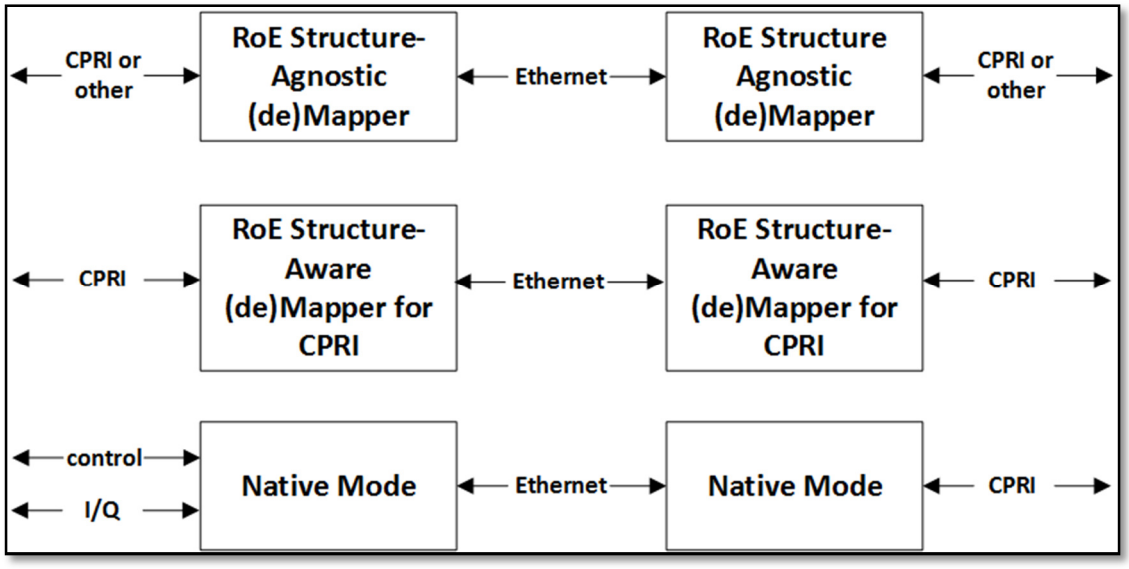

Figure.2.7. RoE with different traffic types [32].

Fig. 2.8 shows the RoE frame format and its fields. The fields of the RoE header are:

- Sub Type (subtype) field: 8 bits used to define 13 sub-types.
- Flow ID (flow identifier) field: 8 bits used to define the flow ID between two RoE nodes (RoE node, node that support RoE standard).
- Length (length) field: 16 bits are used to specify the frame length, not that the 2 most significant bits (MSBs) are reserved for future use by this standard.
- Order Info (time Stamp/seq Num) field: 32 bits used to assign the order information to each flow. The order information can be a sequence number or a time stamp.
- Payload bytes: The received data from the upper layer depends on the selected RoE mapper.

The results in [33] show that RoE encapsulation and its header can cause a small increase in the latency.

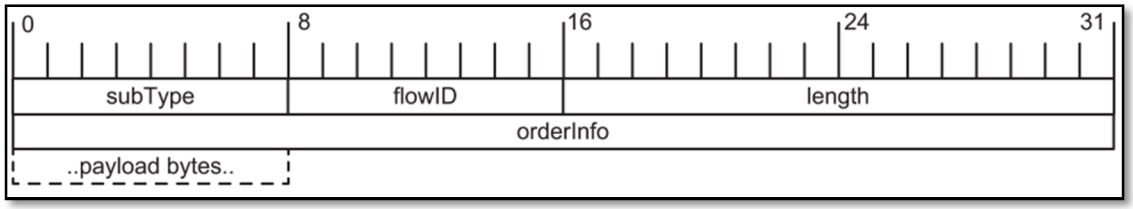

Figure.2.8. RoE Frame Structure [32].

2.1.6 LTE and 5G Stack and Functionality

The protocol stack for the user plane of the Evolved Universal Terrestrial Radio Access Network (E-UTRAN) is shown in Fig. 2.9. The Internet Protocol (IP) packets that are received from the Public-Data Network Gateway (P-GW) are transported transparently (their peer entities are located within the EPC) by the entities in the user plane. The IP layer communicates with its peer entity at the P-GW and the Application layer communicates with the one in the PDN. The protocol stack for the control plane is shown in Fig. 2.9 as well. The control plane contains the same entities as the user plane but with the Radio Resource Controller (RRC) [34] .

- **Packet Data Control Protocol (PDCP)**

The PDCP protocol processes the messages of the control plane and IP packets in the user plane.

The main functions of PDCP are [34]

- Header Compression and decompression.
- Ciphering and deciphering for the Control plane messages.
- The Protocol Data Unit (PDU) sequence check and reordering for the PDUs.

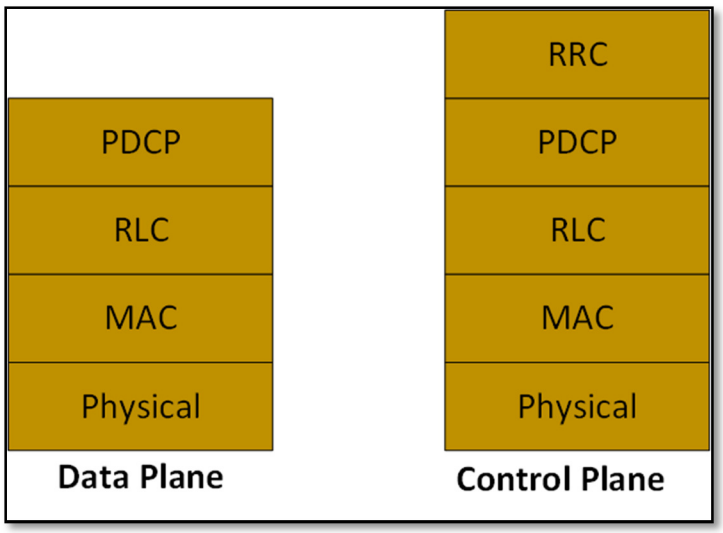

Figure.2.9. LTE User and Control Plane Stack [35] .

- **Radio Link Control (RLC)**

This Layer is located between the PDCP layer and the MAC layer and is connected to the MAC layer by using logical channels and with PDCP through service access points (SAP) [34] . This layer has many important functionalities such as:

- Segmentation and concatenation: Reformat and construct the PDCP PDU in order to construct the RLC Service Data Unit (SDU).
- Reorder the received PDUs.

- **Medium Access Control (MAC)**

The MAC layer communicates with the RLC layer through logical channels and with the physical layer through the transport channels. The MAC layer performs many functionalities such as [34], [35]:

- Resources Scheduling.
- Multiplexing and Demultiplexing between logical and transport channels.
- Error correction through Hybrid Automatic Repeat Request (HARQ).
- Mapping between transport channels and logical channels.

- **Physical Layer (PHY)**

The PHY layer receives the MAC SDU and sends the LTE traffic to the User Equipment (UE). This layer has many important functionalities such as [35]:

- Error detection on the transport channels.
- Mapping of the transport channel onto physical channels.
- Power management on the physical channels.
- Modulation and demodulation of physical channels.
- Time and frequency synchronisation.
- MIMO and CoMP antenna processing.
- RF processing.

- **Radio Resource Controller (RRC)**

This layer is only used in the control plane and its functionality include [34] :

- Broadcasting the system information.
- RRC connection control: which includes establishment, modification and release of RRC connection, paging, initial security activation, establishment of signalling and data radio bearers, inter-LTE handover and configuration of lower layers.
- Inter-Radio Access Technology (RAT) mobility.
- Measurement configuration: Controls measurement reporting by the UE to assist handover decisions by the eNodeB.

In the 5G NR, the user plane contains the same layers of the LTE user plane (PHY, MAC, RLC, and PDCP) and has introduced a new layer called Service Data Adaptation Protocol (SDAP) as shown in Fig. 2.10. This new layer has the following functionality: [36]:

- Mapping between QoS flow and data radio bearer;
- Marking QoS flow ID in both DL and UL packets.

On the other hand, the 5G NR control plane is identical to the LTE control plane.

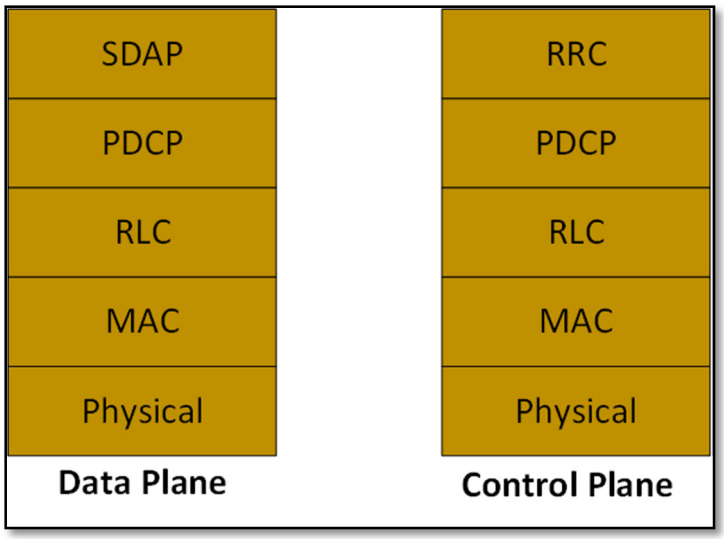

Figure.2.10. 5G NR User and Control Plane Stack [36].

2.1.7 Different Functional Split Proposals

One of the main challenges in the development of the C-RAN is the excessive bandwidth requirements of the transmitted sampled waveforms signals such as CPRI over the fronthaul network [37]. For this purpose, different functional splits have been proposed and are under investigation. With the function split, specific amount of functionalities, based on the split point, are moved from the CU to the DU.

A particular reduction in the bandwidth requirements based on the split point can be achieved with the proposed functional splits (the reduction in the bandwidth requirements with each split will be explained in details in Section 2.1.8).

In addition, some of them can offer a better mobility management, allow the use of different radio techniques and improve the overall radio performance. The selection of split point can greatly change the transport design and overall C-RAN architecture [38]. It should be noted that frequency domain splits (e.g. the pre-IFFT split) transport frequency domain samples (instead of the sampled time waveforms) resulting in reduced sample widths (number of bits per sample) and the avoidance of oversampling. As a result, data rate requirements are significantly reduced. The data rate requirements reduced as the split point moved toward the higher layers.

According to the 3GPP [16], eight splits points have been proposed (see Fig. 2.11):

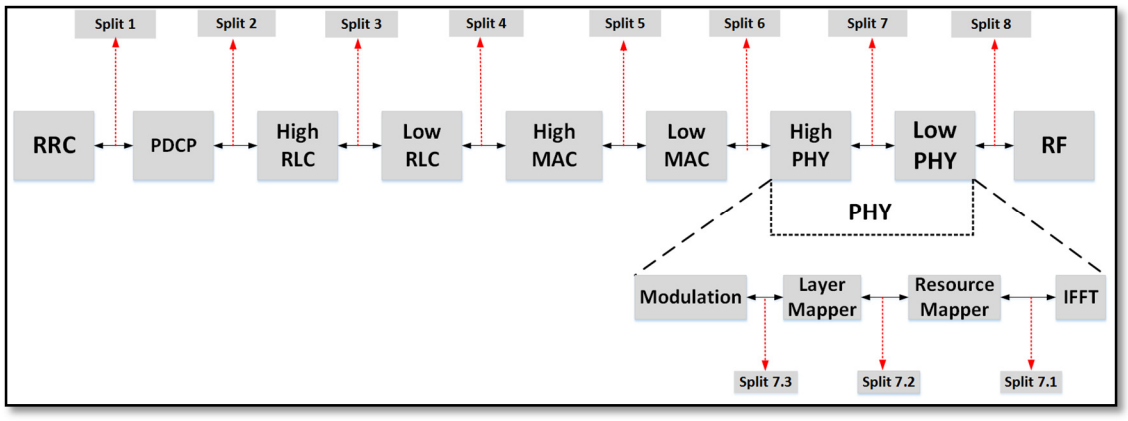

Figure.2.11. Functional Split Points between Central Unit (CU) and Distributed Unit (DU) [16] .

- **Option 2 (PDCP-HIGH RLC)**

In this split option, RRC, PDCP are in the central unit (CU) while the RLC, MAC, PHY and RF are in the DU. The entire user plane is in the DU while the Radio Resource Management (RRM) is centralized.

In addition, this split does not support some of the inter-cell coordination features. On the other hand, a significant reduction in the bandwidth requirements and efficient mobility management can be achieved with this split option [15] , [39] .

This split allows a flexible mobility with coordinated different technologies in the CU and is considered straightforward in regards to the implementation as it is already been standardized for LTE Dual Connectivity [15] , [39] , [40]. In [41], PDCP-RLC split has been implemented in Open Air Interface (OAI) and the increase in the throughput with different Modulation and Coding Scheme (MCS) has been shown.

- **Option 3 (intra RLC split)**

In this split option, low RLC (partial functionality of RLC), MAC, PHY and RF are in the distributed unit. PDCP and high RLC are in the central unit. Two implementation approaches have been introduced for this split, one of them is a split based on the Automatic Repeat Request (ARQ) and the other one is a split based on TX RLC and RX RLC [15].

- **Option 4 (RLC-MAC split)**

In this split option, RRC, PDCP and RLC are in the central unit. MAC, PHY and RF are in the DU. The possibility of virtualizing the RLC can lead to a significant improvement in the storage and processing utilization sharing. On the other hand, this split has very strict delay requirement in the downlink [15], [42].

- **Option 5 (intra MAC split)**

In this split, the lower part of the MAC layer (Low-MAC), PHY layer and RF are in the DU while higher part of the MAC layer (High-MAC), RLC and PDCP are in the CU. This split has a complex interface between DU and CU and could lead to limitations with some CoMP schemes [15] .

- **Option 6 (MAC-PHY split)**

In this split, the MAC and the upper layers are in the CU while PHY and RF are in the DU. This split can lead to a lower data rate in comparison to the intra PHY splits (as discussed in the following) but has a very strict delay requirements as the HARQ and many other time critical procedures are done in the CU [15], [43]. In [44] and [45], a software-emulated Option-6 split was presented. The concentration in [45] on the latency performance while in [44], the Ethernet data rate contributions from different transport channels is studied. The focus in [42] is the operational capabilities of the software defined with a functional split in real-time operation.

- **Option 7 (intra PHY split)**

With this split, part of the PHY functionality with the RF moved to the DU while the rest of PHY functionality and the upper layers are centralized. This split has three different options [37], [16], [15] :

- Option 7-1 (Low PHY): In this split option, the Fast Fourier Transformation (FFT) is included in the DU. This split achieves some improvement in terms of the bandwidth requirements (Up to four times reduction in the data rate) but the traffic is still constant as the element resource mapping is executed in the CU.
- Option 7-2 (Low PHY/High PHY): In this split option, the resource element mapper is placed in the DU which in effect can introduce a greater reduction in the bandwidth requirements (up to ten times reduction in the data rate) but on the other hand might require subframe level timing interaction between the separated parts of the PHY layer. This split point offers as well multi-vendor interoperability. The exact location of this split in the physical layer is still not specified yet and there is a lot of interest to investigate this split point with different use cases. In [10], UPS is implemented in the hardware and the split point after the Forward Error Correction (FEC) (After FEC in the DU). The implementation considers the physical layer only and the LTE higher layers are not implemented. This paper [10] examined the latency optimized and overhead optimized approaches for encapsulating the UPS traffic in Ethernet frames.

- Option 7-3 (High PHY): In this split option, the scrambling, modulation and layer mappers are included in the DU. This split can reduce the bandwidth requirements in the fronthaul network in comparison to other lower layers splits and has the robustness in case of non-ideal transmission and mobility.

- **Option 8 (PHY-RF split)**

Known as well as the BBU-RRH split, in this split, the RF is located in the DU while the higher layers are located in the CU [15]. This split allows the separation between the RF and the PHY layer and supports the different radio techniques such as CoMP and MIMO and load balancing since most of the LTE protocol stack is centralized. On the other hand, this split has a high data rate requirements due to the transmission of the digitized I/Q samples [16].

- **Flexible Functional Split**

The flexible functional split has been proposed to allow the use of different functional split points in the Ethernet fronthaul based on the different factors or measures such as the need to support specific QoS (Delay, FDV) for specific service or to fulfil specific bandwidth demands in a given geographical area [16]. In [46], an algorithm has been proposed to select the most appropriate functional split based on the inter-cell interference in the network. The flexible functional split allows to take the benefit of different split points and minimize the effect of its limitations on the network performance. It also allows real time performance optimisation, load management and enables the use of different technologies such as SDN and NFV in the network [37], [16].

2.1.8 Data Rate Requirements in the Ethernet Fronthaul Interface

Future 5G network is expected to offer a high capacity to accommodate the highly dense networks and fulfil the applications, coverage and availability requirements [47]. Such requirements may demand up to 1000 times the current available capacity and can potentially leads to the use of a range of radio techniques such as massive Multiple Input, Multiple Output (MIMO) (currently MIMO uses up to 8x8 antennas in 3GPP release 10 and above, but with massive MIMO that will be significantly extended, e.g. up to 64x64) and Coordinated Multi Point (CoMP) [48] , [47].

In highly dense networks, a large number of cells are expected to be deployed [7]. The deployment of the small cell in the future 5G network plays an important role to fulfil the coverage and availability requirements. The deployment of the Small cells is estimated to be increased by up to 40% by 2020 [2].

Table. I shows the data rate requirements for different functional split points in the future C-RAN with 20% load and 8x8 MIMO [49]. These splits points are explained in details in Subsection 2.1.7 [7] , [49]. The data rate requirement is seen to increase as the split move towards the lower layer in the LTE protocol stack where the requirements of CPRI is 49.125.45 Gbps (Note that CPRI data rate here is scaled to project the requirements for eight antennas and 100 MHz bandwidth). The actual (user) data rate is close to the presented value with the PDCP-RLC split (small increase due to LTE protocol overheads can be neglected). The data rate of MAC-PHY split is less than the data rate with option 7-2 (Low PHY) since the data is a bit sequence and not quantized I/Q data like in the case of option 7-2. The data rate with option 7-2 split is five times less than the data rate with option 7-1 (Low PHY /High PHY) while the data rate with option 7-1 split is four times less than CPRI data rate (pre-IFFT split).

Table. I

The Requirements of the Data Rate for the Different Functional Split [49]

Split Point	Downlink data rate Gbps	Uplink data rate Gbps
PDCP-RLC Split	0.8	0.8
RLC-MAC Split	0.8	0.8
MAC-PHY Split	0.8	0.8
Option 7-2 (Low PHY) Split	2.5	2.5
Option 7-1 (Low PHY /High PHY) Split	12.2	12.2
CPRI	49.125	49.125

2.2 Fronthaul Requirements and Key Performance Indicators (KPIs)

2.2.1 Delay and Frame Delay Variation in the Ethernet Fronthaul Interface

The delay and the FDV are among the most important challenges in implementing the Ethernet fronthaul network for the next generation of the access network. The delay and FDV in the Ethernet fronthaul network include the processing delay, fabric delay and delay variation in the BBU/CU and the Ethernet switching and aggregation units, the delay due to the propagation in the network, and the delay and FDV due to the queuing and contention in the Ethernet network equipment. The fabric delay (processing delay) in the Ethernet switches is the time that it takes the switching units to forward the frames to the output ports in the switch. Many factors affect the fabric delay such as the switching unit architecture and the traffic loading [51]. The FDV (also called PDV (packet delay variation)) is the absolute value of the difference between the delay of two consecutive frames or packets belonging to the same stream [52]. The absolute difference in the arriving time between two consecutive frames is called inter-arrival frame delay.

Latency and FDV are very critical as they can affect the radio performance and network synchronization. The HARQ procedure and the ability to use the different radio techniques such as CoMP and Massive MIMO can be severely affected by the high delay and FDV. The HARQ has a specific time limit to be met or otherwise will be triggered and re-transmission will occur in the network. The PTP synchronisation mechanism can be significantly affected as well with the varied delay and FDV [7]. In the next sub-section, the delay asymmetry problem in the Ethernet fronthaul network for the PTP traffic will be explained. Different scheduling techniques have been discussed in Section 2.3 to overcome the delay and FDV problem in the Ethernet fronthaul.

Table. II shows the delay and FDV requirements for the different functional split points. It can be noticed that the delay and FDV requirements becomes stricter toward the lower split points [53].

Table. II

Requirements of the Delay and FDV for the Different Functional Split Points.

Split-Point	One Way Delay (Max) (Without CoMP)	One Way Delay (Max) (With CoMP)	One Way FDV (Max)
PDCP-RLC Split	30 ms	60 ms	not yet defined
RLC-MAC Split	6 ms	6 ms	+/- 163 ns
MAC-PHY Split	250µs	75	+/- 163 ns
UPPER PHY Split	250µs	75	+/- 163 ns
LOWER PHY Split	250µs	75	+/- 163 ns
CPRI	250µs	75	+/- 16 ns

2.2.2 Latency Imbalance

The delay imbalance between the downlink and the uplink in the Ethernet fronthaul can cause a significant effect on the performance of the PTP which will have an effect as a result on time and phase synchronization in any network. The delay imbalance in the Ethernet fronthaul can come from either the processing, queuing or contention in the active equipment such as BBU, RRH and Ethernet switches or the transmission medium such us using different cable lengths in the uplink and downlink [24].

Assisted Partial Timing Support (APTS) was developed by Microsemi is an interesting architecture to overcome the asymmetry problem by using a Global Navigation Satellite System (GNSS) in conjunction with the PTP system [34]. In this architecture, the incoming PTP flow is time stamped by the GNSS used by the core Primary Reference Time Clock (PRTC). The PTP flow from the core PTRC to the edge is configured as a unicast protocol and calibrated for time error by the local edge PRTC GNSS [54].

2.3 Traditional Queuing Regimes in the Ethernet Fronthaul

2.3.1 Weighted Round Robin

Weighted Round Robin (WRR) is a network scheduling regime that allows the transmission of specific amounts of traffic from each port in the bridge or switch based on the assigned weight and Class of Service (CoS) to each traffic flow. The amount of traffic can be represented by either the number of frames (Frame based) or by the number of bytes (Byte based). The traffic is first classified into different service classes such as real time and interactive and then assigned to the queue associated with the class of service [55]. Fig. 2.12 shows an example of weighted round robin where three different traffic flows are assigned the same CoS and weights. In this example, each queue transmits the same number of frames every time unit. The main advantage of WRR is that it allows the balance in the transmission from each queue in the switch and makes sure every transmitted traffic flow in the network has some access to the available bandwidth based on the assigned weight. Allowing all the queues to transmit traffic based on the assigned weight prevents the bandwidth starvation for the low priority queues.

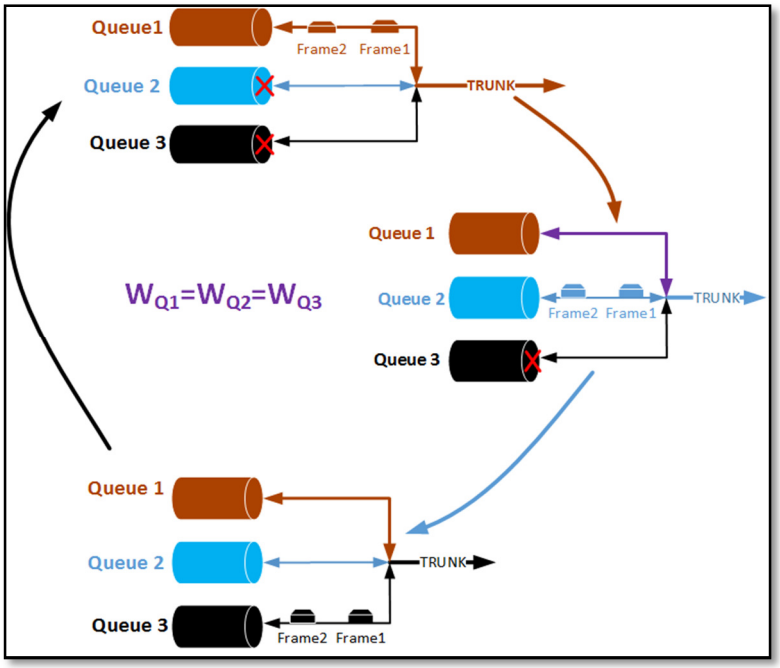

Figure.2.12. Weighted Round Robin (WRR) example with three equal weights queues.

2.3.2 Strict Priority

Strict Priority (SP) is a network scheduling regime that allows the traffic with high priority to be transmitted with minimum delay and FDV. The traffic is classified according to the CoS and assigned to different queues in the switch. The highest priority queue is served first and transmits all its traffic [56]. After that, the queue with less priority transmits its traffic [57]. If the high priority queue receives traffic during the transmission of the low priority queue, the former transmission will be stopped and the high priority traffic start its transmission. Fig. 2.13 shows an example of the strict priority case. The queue with priority 7 transmits all its traffic followed by the queue with priority 3 and the queue with priority 1. SP can be considered as a special case of WRR with a weight equal to zero for the lower priority stream(s). The main limitation of this queuing regime is that the queue with the lowest priority should wait for the other queues to transmit all their traffic before starting the transmission (queue with priority 1 in Fig. 2.13). Hence, the low priority queue can suffer a bandwidth starvation [58].

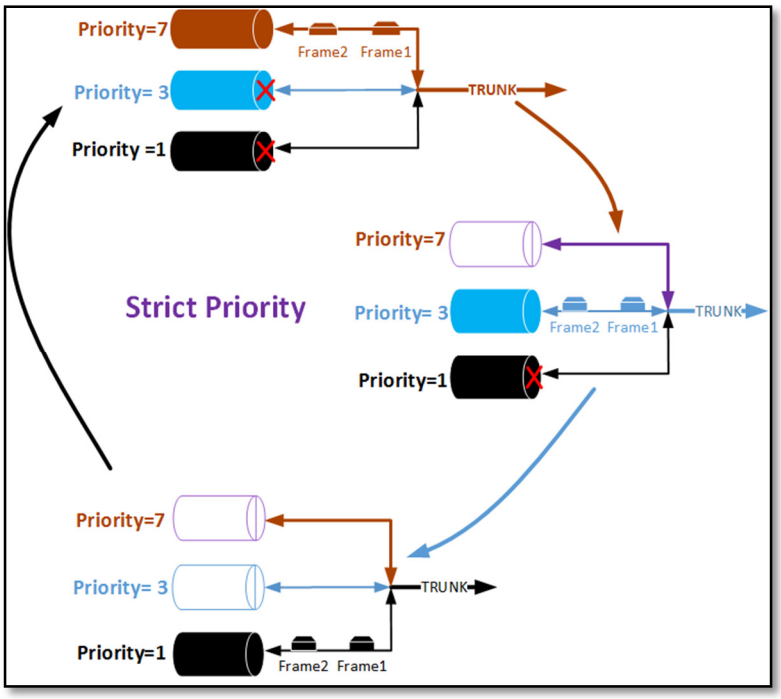

Figure.2.13. Strict Priority (SP) example with different priority queues.

2.4 Time Sensitive Networking

Time-Sensitive Network is an extension of standard Ethernet network which allows a deterministic data transmission over Ethernet network with bounded delay, FDV and frame loss. IEEE 802.1 Time Sensitive Networking (TSN) task group focuses on the development of different TSN standards such as Time Aware Shaping (IEEE 802.1Qbv) and Frame Pre-emption (IEEE 802.1Qbu) to allow latency and latency variation-sensitive streams to be transported within a switched (or bridged in 802.1Q nomenclature) network. The objective of these standards is to overcome the different performance issues in the current Ethernet networks and queuing regimes such as delay and FDV (delay and FDV related performance issues will be discussed in chapter 3) [59]. IEEE 802.1CM (Time Sensitive Networking for fronthaul) working group was introduced to adapt the TSN standards to be used in the Ethernet fronthaul network [60]. TSN for fronthaul defines two profiles, Profile A considers the strict priority and profile B extend profile A with the use of the frame pre-emption.

2.4.1 Time Aware Shaping (802.1Qbv)

The IEEE 802.1Qbv standard has been introduced as a solution to overcome the contention-induced FDV in network bridges and switches [40]. This standard allows time referenced transmissions from the traffic sources and network bridges based on non-overlapping assigned time sections defined within an explicit transmission window. For this reason, implementing this standard in the Ethernet network requires an overlaid time synchronization network [61].

As shown in Fig. 2.14, Time Aware Shaping (TAS) divides the Transmission Window (TW) into time sections and assigns time section to each traffic type. TAS allows the traffic to be transmitted from the traffic sources and/or pass through the Ethernet Bridge during its time section only. The traffic with High Priority (HP) is assigned to one TW section, while the lower priority traffic is assigned to another TW section. The section assigned to the HP traffic is termed the protected section (PS) while a best effort section (BES) is allocated to the lower priority traffic. To prevent the best effort traffic from overrunning into the PS, part of the transmission time after the BES will be idle and not assigned to

any traffic, in effect forming a guard period (GP). Each section can be divided into one or more sub-sections based on the number of transmitted streams within this time section [62].

The size of the sections and sub-sections is based on different factors, such as the number of transmitted streams in each time section and the required time to accommodate each stream within the TW [61]. PTP traffic is an example of high priority traffic, while Control and Management (C&M) is usually treated as a low priority traffic. It is possible within the section to assign priority levels to the different low or high priority streams and employ an "intra-section" scheduler such as SP, WRR or Weighted Fair Queuing (WFQ) [63].

In [64], an initial implementation has been done for TAS in the NS-3 simulation platform [65]. In this implementation, gating in the Ethernet switches has been performed to show the performance of TAS with CPRI traffic. The results show that TAS can reduce or even remove the FDV of CPRI traffic. According to the authors, the implementation did not follow the 802.1qbv standard in many aspects such as allowing only one frame at a time to be transmitted from the open windows in the switches. The implementation demonstrated only traffic (CPRI, Background traffic) with a specific rate and transmission pattern.

This standard is one of the potential standards to be used in the Ethernet fronthaul network to accommodate the time sensitive traffic. This standard is investigated further in Chapters 4 and 5, where its implementation and the simulation results for different contention scenarios are investigated and analysed.

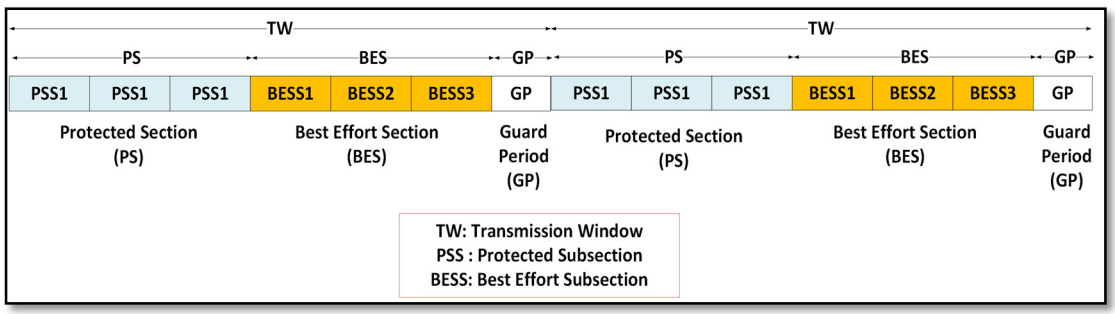

Figure.2.14. Generic Time Window, Window Section and Subsection Plan based on IEEE 802.1Qbv.

2.4.2 Frame Pre-emption (802.1Qbu)

The IEEE 802.1 Qbu standard has been introduced as a solution for the contention-induced delay and FDV in network bridges. This standard is part of the TSN working group which is under the umbrella of the 802.1 working group. The idea of this standard is to reduce the effect of the low priority traffic on the delay and FDV of the high priority traffic when they contented in the output ports by interrupting and pre-empting the transmission of a low priority frame [66]. Fig. 2.15 shows examples of pre-emptive and non-pre-emptive transmission in an Ethernet switch port.

In the non-pre-emptive case, the F_{Hp} should wait for the low priority frame to be transmitted and then be sent from the output port after that. In the pre-emptive transmission case, the low priority frame will be pre-empted and the High priority frame will be sent straight after hold period (HOP). The HOP is designed to accommodate 124 bytes, 60 bytes mCRC added by the MAC merge sublayer and 64 bytes data, which is the smallest possible fragment in this standard [67].

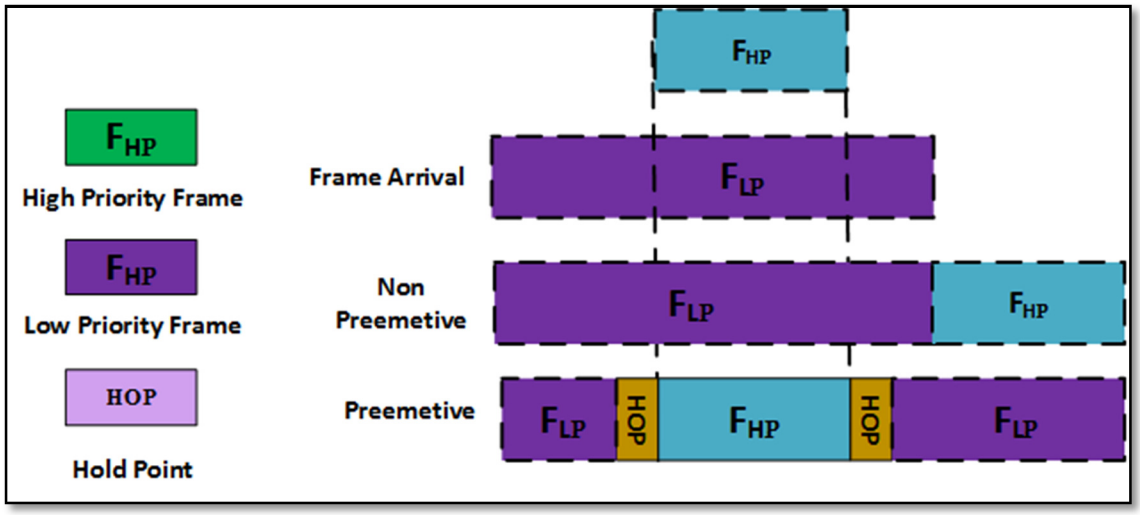

Figure.2.15. Pre-emptive and Non-pre-emptive transmission.

While this standard can reduce the effect of F_{LP} on the delay and FDV of F_{Hp}, this standard has several challenges and limitations which are (and not limited to) [68]:

- HOP size can be large enough to violate some traffic type's delay and FDV specifications.

- Significant overheads will be transmitted over the network as each frame partition should have specific header and CRC, this problem will occur more if jumbo frames are used in the transmission.

- Increase the complexity in the receiver as each frame should be checked whether it is a full frame or portion of a frame and the way it should be reassembled. The frame can be fragmented into different number of frames especially in multi-hop network.

- The switch output will be busy for a longer time and the overall processing in the switch will be higher.

2.5 Opnet/Riverbed Simulation Platform

Riverbed (OPNET previously) is a dynamic discrete event based simulation platform that has the ability to simulate the behaviour and the performance of different network types (models) such as Wireless, LTE …etc. The platform has a user-friendly Graphical User Interface (GUI) and is used widely by researchers, engineers and university students.

Each network model in Riverbed has a range of node models such as routers, switches computers, etc.., where each node model is made of different types of modules as shown in Fig. 2.16 [69].

The available modules include, processor queue transceiver and antenna modules. The processor module performs processing related to a specific protocol or algorithm on the received frame in the input stream and sends the packet out again on an output stream. The queue module is similar to the processor module but the queue module is provided with additional internal resources to facilitate the buffering and organization of packets. The buffering functionality allows the buffering in the module with full access and manageability for the queued packets. The queue module can be used as well to introduce delay to the transmitted traffic from the node.

Each module has a process model, the process model consists of a state machine where states are connected to each other as shown in Fig. 2.17. The functionality of the module

is associated with the way the state machine is designed and the module functions are implemented. The state machines and the functions in each module are programmed by using C/C++ with the possibility of modification or change to the existing code in order to implement a specific functionality or algorithm [69]. The overall functionality structure in Opnet/Riverbed is shown in Fig. 2.18.

The main focus of this work is the LTE model, particularly the eNodeB model, and the Ethernet model, particularly the Ethernet module in the Ethernet switch and server nodes.

While the LTE is modelled according to the 3GPP standards [70] [71] [72] [73] [74] the model has some limitations which are [69]:

- Radio Resource Control (RRC) message sizes are approximate.
- S1 interface messages sizes are approximate.
- The header compression capability of the Packet Data Convergence Protocol (PDCP) sub-layer is not an explicit model, it uses instead a probability distribution function based on a statistical model)
- Both closed-loop spatial multiplexing and multiuser MIMO and the closed loop uplink power control are not supported in this model.

Ethernet is modelled based on the IEEE 802.3 standard [75].

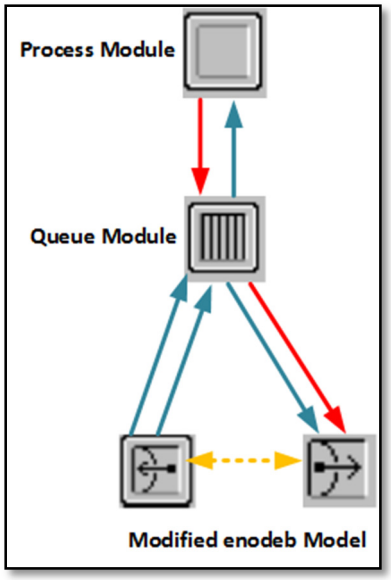

Figure.2.16. Node Model Editor.

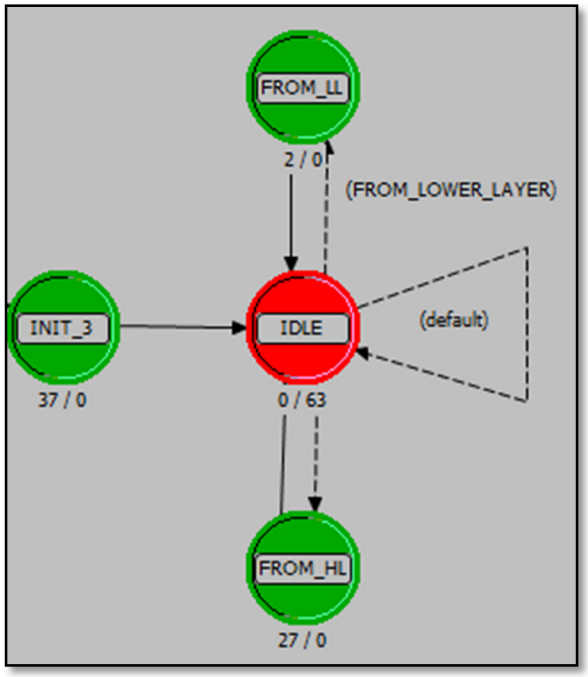

Figure.2.17. Part of State Machine of Transmit/Receive Functionality in PHY Module [46].

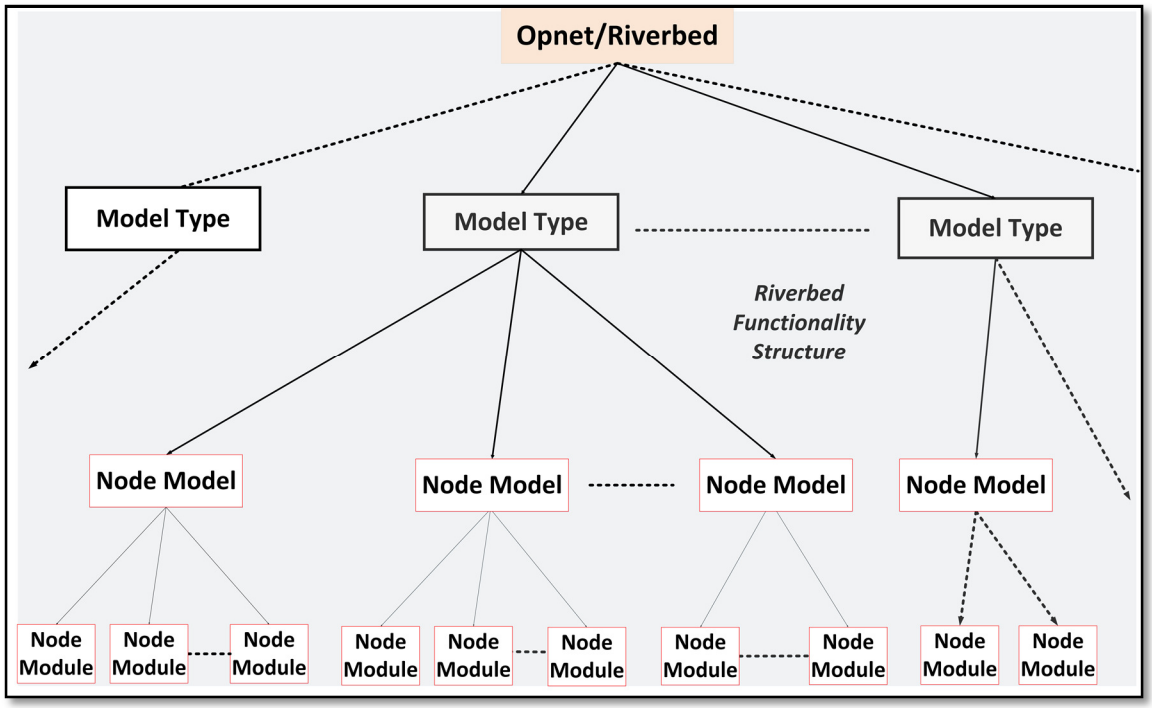

Figure.2.18. Overall Functionality Structure in Opnet/Riverbed.

3 Ethernet Fronthaul Network with Traditional Queuing Regimes.

3.1 Introduction

In this chapter, the effect of contention at the Ethernet switch ports in an Ethernet fronthaul network on the different performance measures of Long-Term Evolution (LTE) traffic will be presented. The LTE sampled radio waveform traffic is generated in a hardware testbed and transported over a switched Ethernet fronthaul together with background traffic, which represents traffic that might be generated by different functional splits in the access network. The switched Ethernet network consists of two store-and-forward Ethernet switches connected by fibre links. The focus of this study is the delay and standard deviation of the LTE traffic as the end to end latency and standard deviation cannot be guaranteed in the Ethernet fronthaul due to the contention in the Ethernet bridges' ports which can violates the delay and FDV requirements of different traffic types and network applications.

As mentioned in sub-section 2.3.2, the strict priority (SP) regime allows the high priority queue to use the whole available bandwidth to send its frames before allowing the lower priority queue to start its transmissions. Weighted Round Robin (WRR) allows more balanced transmission from each queue in the switch by permitting each queue to transmit traffic based on its assigned weight.

The performance of both queuing regimes in controlling the delay is investigated in previous work [76] and [77] , but it has not been investigated with an Ethernet fronthaul scenario where LTE sampled I/Q traffic contends with background traffic.

The main focus of this chapter is on the effect of deploying WRR and SP queuing regimes in the trunk ports of the Ethernet switches on the frame delay and inter-arrival delay of the LTE traffic, when it contends with background traffic. The performance obtained from each of these queuing regimes in improving the delay and Standard Deviation (STD) of the LTE traffic in the Ethernet fronthaul network is studied and compared.

The delay imbalance problem in the Ethernet fronthaul, due to the contention in the network bridges, is also explained and discussed.

3.2 Latency in the Ethernet Fronthaul

Fig. 3.1 shows an overview of the main delay components in a switched Ethernet network. The serialization delay *Tse*, is given by:

$$Tse=P/R, \qquad (1)$$

where *P* (bits) is the frame size and *R* (bits/s) is the supported interface speed. The propagation delay *Tp*, in fibre is given by:

$$T_p = \frac{d}{\left(\frac{c}{n}\right)} \qquad (2)$$

where *n* is the refractive index of silica (≈1.45), *c* is the speed of light in vacuum and *d* is the distance from BBU to RRH. The total physical layer end-to-end delay *T*, neglecting the inter-frame space, for a frame in a store-and-forward switching regime, is given by

$$T = (N+1)T_{se} + T_p + N(T_f + T_q) \qquad (3)$$

where *N* is the number of switches in the path, T_f is the fabric (processing) delay for each switch and T_q is the queuing delay in each switch.

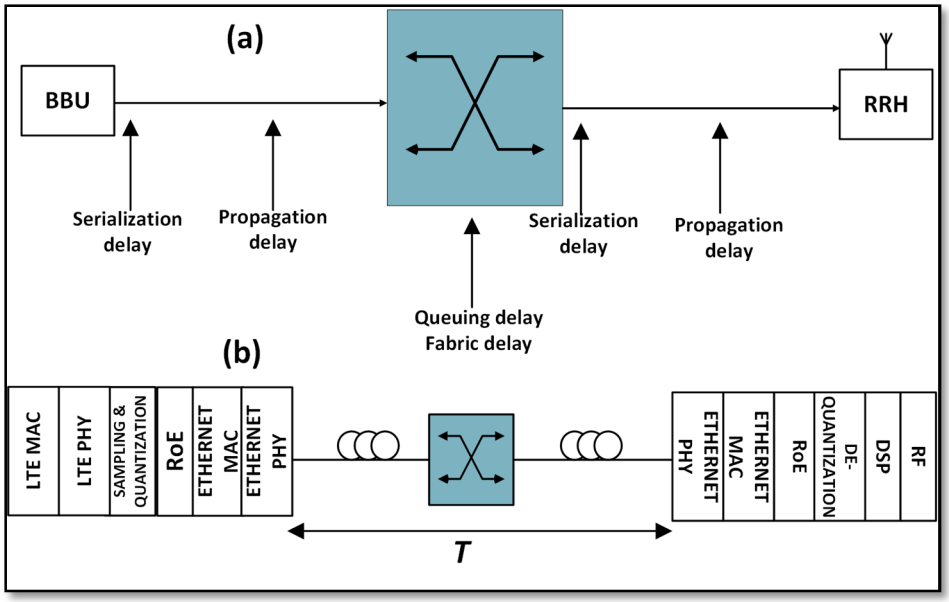

Figure.3.1. Main Delay Parameters in a Switched Ethernet Fronthaul. Note that T is Based on the Delay Definitions Shown in (a), i.e. it includes Serialisation Delays. Higher LTE Protocol Layers are not shown in the Figure.

3.3 Measurements Setup

Fig. 3.2 shows the testbed used for the measurement procedure. A workstation runs an emulated LTE base station (Amari LTE-100) that produces I/Q samples corresponding to a 5 MHz channel bandwidth (sampling rate of 6.25 MHz). The samples are then inserted into the payload section of a UDP/IP packet and transmitted over a layer 2 Ethernet network. The transmission is bursty, as the LTE source will buffer a number of OFDM symbols before transmitting the corresponding I/Q samples over the Ethernet link. The network comprises of two 3COM-5500G Ethernet switches [78] , operating in store-and-forward mode with standard 1000BASE long wavelength small form-factor pluggable (1000BASE-LX SFP) transceivers with LC connectors and single mode fibre (SMF) patchcords. The fibre link length in the testbed is 25 m (Note that the propagation delay does not have an effect on the inter-arrival frame delay and standard deviation). The packet stream containing the I/Q samples is received by an Ettus N210 RRH where it is digitally processed prior to up conversion and transmission over the wireless channel. A Viavi hardware-based traffic generator is used to generate bursty background traffic of different payload sizes (500 bytes, 1500 bytes, and 4000 bytes (jumbo frame)) and at variable data rates (45Mbps, 105 Mbps, 215 Mbps, and 450 Mbps). The two streams of traffic are assigned to different Virtual Local Area Network (VLAN) IDs and transmitted to the destination through a trunk link between the switches. The LTE traffic is captured using a number of Viavi in-line Ethernet probes that come in the form of 1000BASE-LX SFPs. A filter is applied that instructs the probe logic to capture all packet headers containing the destination MAC address and destination UDP port of the RRH. Once captured, the headers are timestamped (using a Viavi proprietary form of the Precision Time Protocol, PTP) and re-encapsulated (with the discovered network encapsulation), and with an additional Viavi proprietary header that includes the timestamp (in addition to other metadata fields). The captured packet headers are re-injected into the network as Frame Result Packets (FRPs) and sent to a Packet Routing Engine (PRE) which routes them to a management station for further processing. In the management station, the FRPs will be extracted by Wireshark. Additional fields include the SFP probe ID and FRP injection number, both of which are used as inputs to an in-house algorithm,

implemented in Matlab which can be used to extract more KPIs. The algorithm has been explained in [25].

The store-and-forward switching mode allows the switch to check the whole frame before forwarding it, while in the cut-through forwarding mode, the switch checks only the first 6 bytes of the frame that contains the destination MAC address. Using the store-and-forward mode allows the Ethernet switch to check for errors in the Ethernet frames and drop invalid ones, which results in a guaranteed high level of error-free data transmission. It allows as well flexible buffering in the switch in the case of queuing [79]. On the other hand, the store-and-forward switching mode causes more delay than the cut through mode since it stores the whole frame before forwarding it. Fig. 3.3 shows the forwarding mode in 3COM-5500G switch while Fig. 3.4 shows the cut through mode.

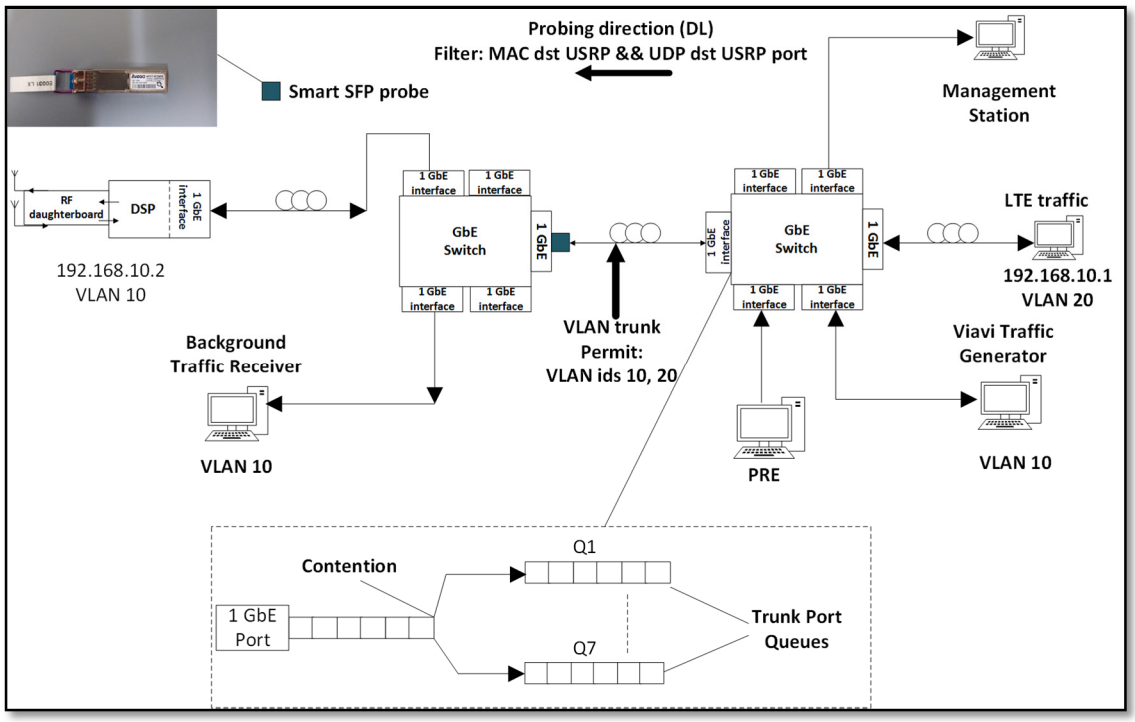

Figure.3.2. Testbed used for the Measurement Procedure. PRE=Packet Routing Engine, GbE=Gigabit Ethernet,SFP=Small Form-Factor Pluggable.

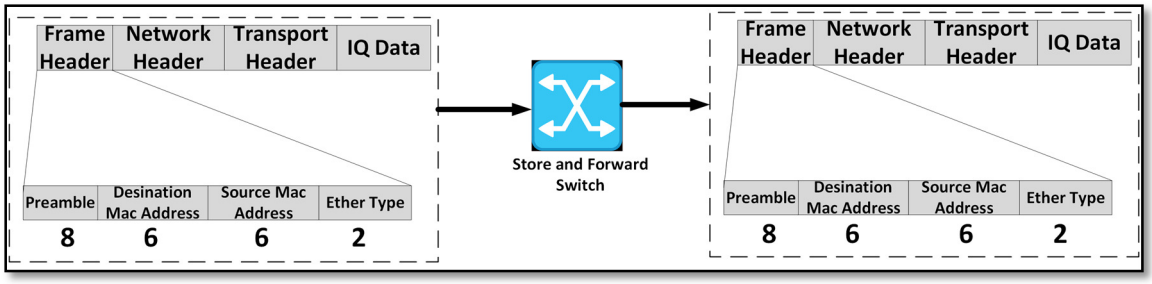

Figure.3.3. Forwarding Mode in the Ethernet switch.

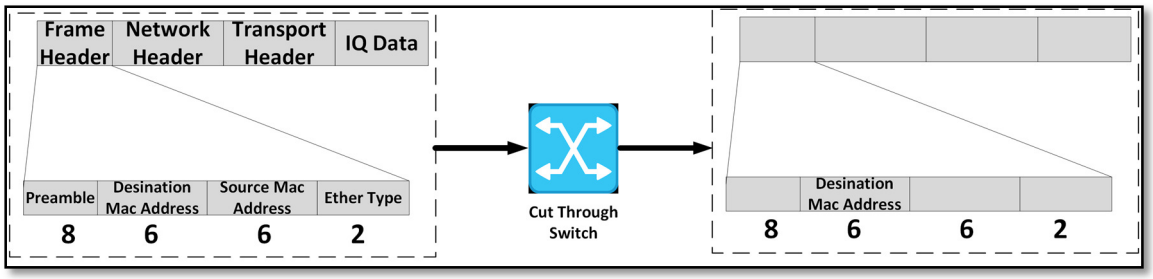

Figure.3.4. Cut through Mode.

3.4 Testbed Results and Comparisons

Here, the results from different queuing regimes, with a range of priority and weight combinations, different background traffic rates (45, 105, 215 and 450 Mbps) and frame sizes (500, 1500 and 4000 bytes) are presented. LTE data rate with all following scenarios is 200 Mbps. In the presented results, different packet-count-based WRR weight combinations are used: (WRR1: LTE 8, Background 2), (WRR2: LTE 8, Background 4), (WRR3: LTE 8, Background 6) and (WRR4: LTE 8, Background 8). The different weights that are allocated to the background traffic in this case represent the different weights that could be allocated to traffic with different priorities, such as PTP and functional split primitives for high priority traffic and time-insensitive traffic such as web browsing traffic for low priority traffic, that are proposed to be transmitted alongside the LTE traffic in the fronthaul network. The different data rates in this case are selected to show a range of load cases for the trunk link in the network. The frame sizes are chosen to show cases of different possible encapsulation for the I/Q traffic in the Ethernet frames (Standard and Jumbo frames) and the effect of that on the measured statistics. STD values are superimposed on the mean values in the form of error bars with many of

the presented results. The base line case which corresponds to transmitting just the LTE traffic (i.e. no background traffic) is indicated in all the following plots.

3.4.1 WRR Queuing Regime Results

In this section, the frame inter-arrival statistics for the LTE traffic when using a WRR regime in the switched Ethernet fronthaul are examined. The results in Fig. 3.5 show that increasing the weight of the background traffic causes the mean delay of the LTE stream to increase by approximately 2.6% on average for each weight increase and the STD increases by approximately 13.7% on average in each result. The increase in both the mean and STD for higher data rates is a result of the corresponding increase in the frame transmission rate of the background traffic which will cause the background traffic queue to be filled more often (note that the traffic source is bursty). The trend of the increase in both delay and STD is within the acceptable range. The increase in delay and STD for the different weight combinations for each data rate is simply a result of allocating more resources to the background traffic. Fig. 3.6 shows a comparison between different frame sizes with the background traffic data rate of 215Mbps. The results show that the delay and STD are increased with increasing frame size for the different background data rates. The results can be explained by the longer serialisation delays of larger frames resulting in them occupying the channel for longer.

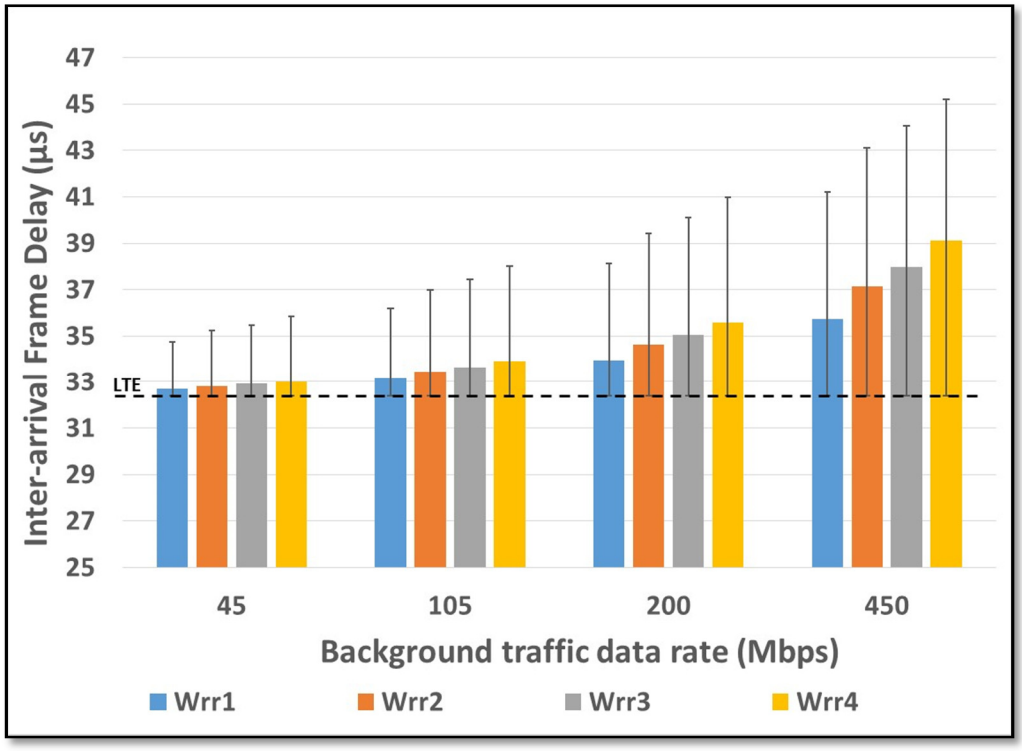

Figure.3.5. Comparison for mean and STD of frame inter-arrival delays of the LTE traffic with different WRR weights and background traffic data rates and a frame size of 1500 bytes.

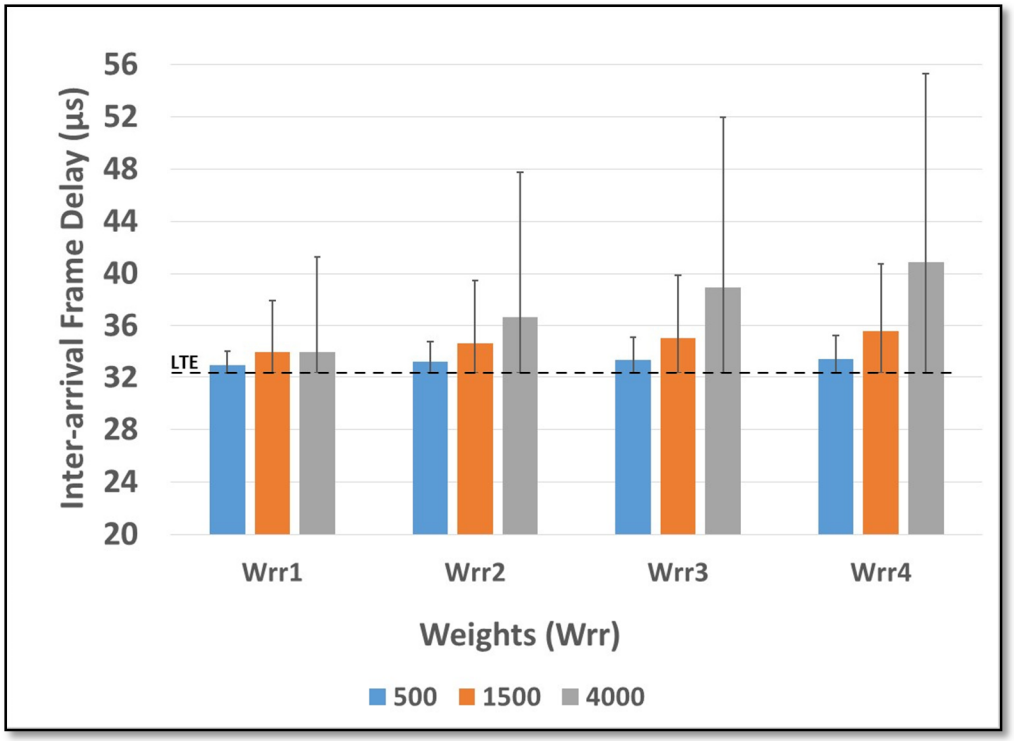

Figure.3.6. Comparison for mean and STD of frame inter-arrival delays of the LTE traffic with different background traffic frame sizes and WRR weights at a data rate 215 Mbps. The "LTE" trace corresponds to transmitting only the LTE traffic (i.e. no background traffic).

3.4.2 Strict Priority Queuing Regime Results

In this section, the frame inter-arrival statistics for the LTE traffic when using a SP regime in the switched Ethernet fronthaul are examined.

Fig. 3.7 shows the results of the mean and STD using SP for different frame sizes (500 bytes, 1000 bytes, 1500 bytes) and two different data rates (105 Mbps,450 Mbps) for each frame size, while Fig. 3.8 shows the corresponding Complementary Cumulative Distribution Functions (CCDFs).

when a background traffic frame is being serialized out of the switch port while a new LTE frame arrives in the queue (which until that point was unoccupied), the time that the LTE frame will have to wait, which is until the serialisation of the other frame is complete, will be greater for larger background frame sizes (and bounded by one background frame serialisation delay), resulting in an increase in the STD. The mean value on the other hand reduces, as with larger background frame sizes the occurrence of such an event is less likely (as, for the same load, the packet transmission rate is reduced). In Fig. 3.8, the contention occurrence probability with 500 bytes frames is approximately two times the occurrence probability with 1500 bytes frames with 450 Mbps data rate. Similarly, the occurrence probability with 1500 bytes frames is higher than the occurrence probability with 4000 bytes frames. On the other hand, the maximum inter-arrival frame delay peak value is occurred with the 4000 bytes frame size.

The results in Fig. 3.7 and Fig. 3.8 clearly show the effects of the lack of pre-emption on the inter-arrival delay mean and STD (the maximum increase in the STD with 4000 bytes and the maximum mean inter-arrival frame delay with 500 bytes) in this set-up.

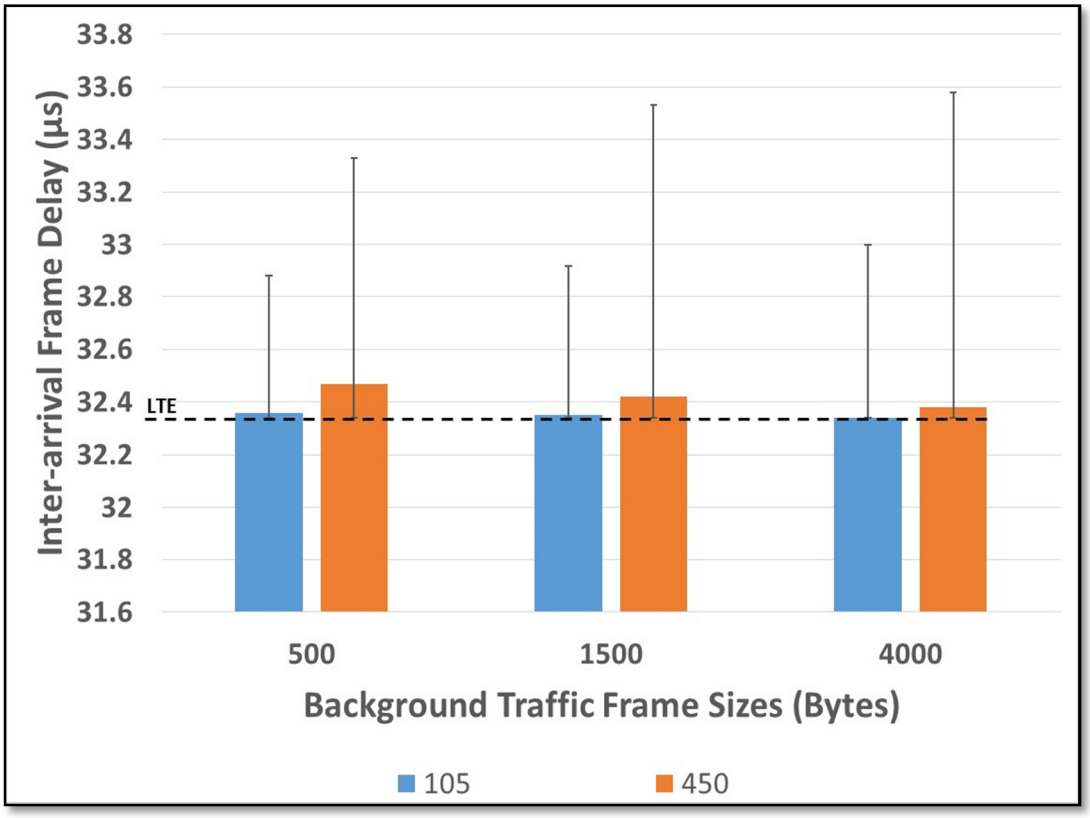

Figure.3.7. Mean and STD of frame inter-arrival delays of the LTE traffic under SP regime for different frame sizes and background traffic data rates (105 Mbps, 450Mbps).

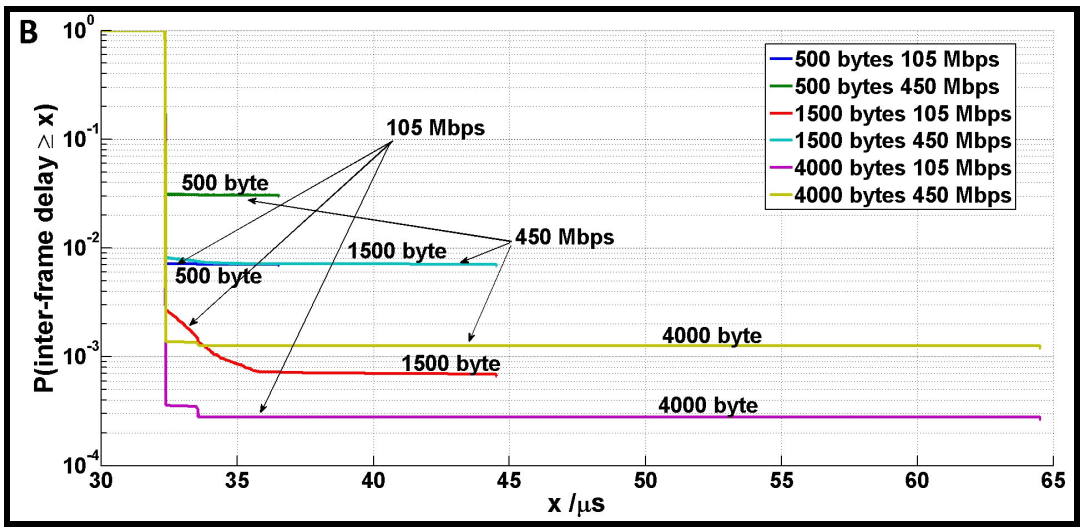

Figure.3.8. CCDFs for the mean of the inter-arrival frame delays of the LTE traffic under SP regime with different frame sizes and background traffic data rates (105 Mbps, 450Mbps).

3.4.3 Comparison with Single-Queue Case

The difference between using no-priority (i.e. a single queue) and WRR with equal-weights (i.e. two queues with equal priority) can also be investigated. These special cases are important for two main reasons. The first reason is that there might be cases where two streams have equal (or approximately equal) weight definitions when transported through the fronthaul since different types and numbers of traffic streams potentially can be transported. The second reason is that there is only a limited number of priority definitions at layer 2 which means that different streams may need to be accommodated by the same queue.

The results in Fig. 3.9 show that using no-priority in the network will cause higher mean delays than using two equal-weight queues for smaller frame sizes (not jumbo frame regimes) with 200 Mbps LTE traffic. On the other hand, the no-priority case will result in smaller mean delay than the equal-weights WRR case, when using jumbo frames in the background traffic, as can be seen in Fig. 3.10. Note that for the no-priority case, the delay does not change considerably between the two frame sizes in Figures 3.9 and 3.10. This is expected since a smaller frame size simply means that the traffic source will be transmitting a larger number of frames (in this case eight 500 byte frames instead of a single 4000 byte frame) over the same time interval. The delay of the equal weight case in Fig. 3.9 remains very low in value even at the higher data rates. Note that the delay here is bounded by the sum of the serialisation delays of the two traffic sources (approx. 36.4 µs) but the mean delay will also depend on how frequently frames from the two sources interact in the port (i.e. how often both queues are filled due to the bursty nature of the sources). Obviously, there is a clear increase in the delay for higher frame sizes for the equal weight case as now the serialisation time of each background frame will be higher (the serialization time of each background traffic frame is 32 µs in this case). With no priority case, the probability of LTE frame to wait 4000 bytes background traffic frame to be transmitted is less than the probability with WRR4 where the queuing regime is configured to allow equal number of frames from each traffic source to be transmitted (equal weight).

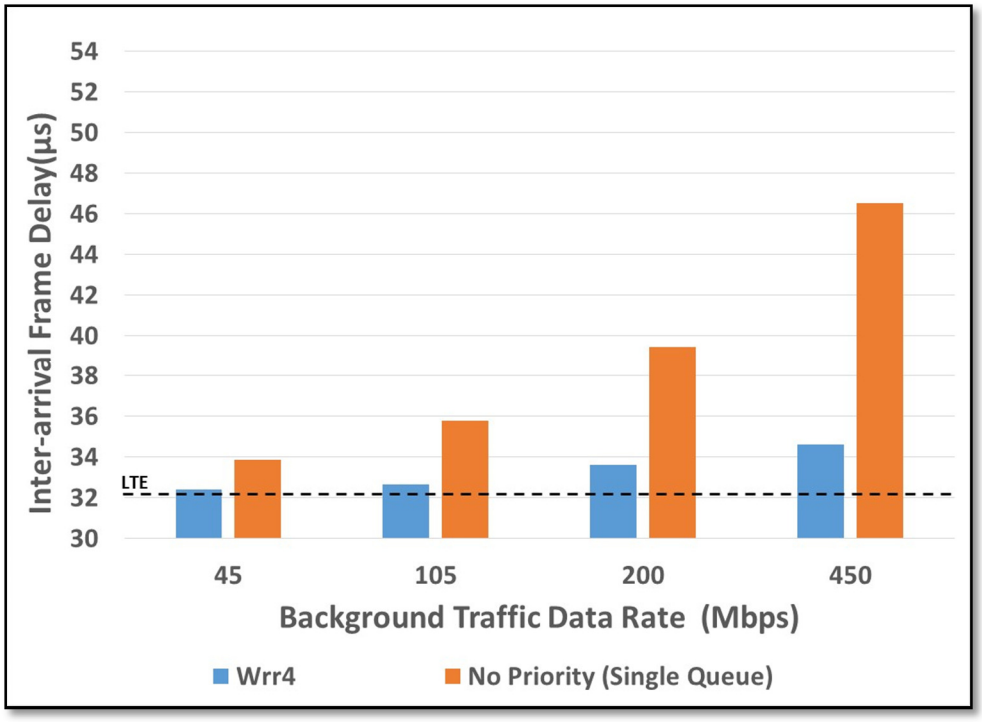

Figure.3.9. Comparison for the mean of the frame inter-arrival delay of the LTE traffic for equal-weight (Wrr4) and No-priority cases with different LTE traffic bandwidths and different background traffic data rates with frame sizes 500 bytes.

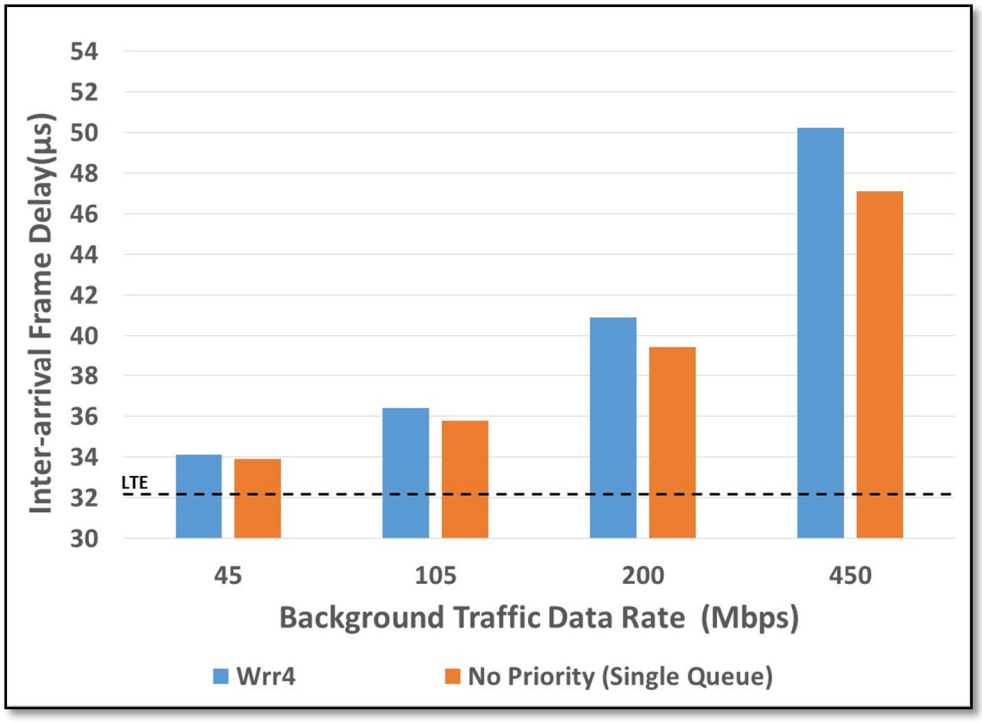

Figure.3.10. Comparison for the mean of the frame inter-arrival delay of the LTE traffic for equal-weight (Wrr4) and No-priority cases with different background traffic data rates and 4000 bytes frame size.

3.4.4 Different LTE Data Rate Comparison

In this section, the effect of contention between LTE traffic with different data rates and background traffic with different data rates and frame size of 500 byte on the LTE inter-arrival frame delay is investigated. Two LTE data rates have been tested, 200 Mbps (5 MHz bandwidth) and 400 Mbps (10 MHz bandwidth).

The results in Fig. 3.11 show that using higher LTE data rates can cause an increase in the inter-arrival frame delay for the LTE traffic as the contention events occur more frequently (more Ethernet frames are sent with the higher LTE bandwidth). The baseline values of the inter-arrival frame delay with 5MHz and 10MHz bandwidths are the same since the LTE frame sizes with both bandwidths are the same (4000 bytes frame size). With 4000 bytes background traffic frame size, the behaviour in relation to both cases (WRR4, No Priority) will be similar to figure 3.10 (inter-arrival frame delay is higher with WRR4). The inter-arrival frame delay will be higher with the higher bandwidth (higher with 10 MHz bandwidth in this case).

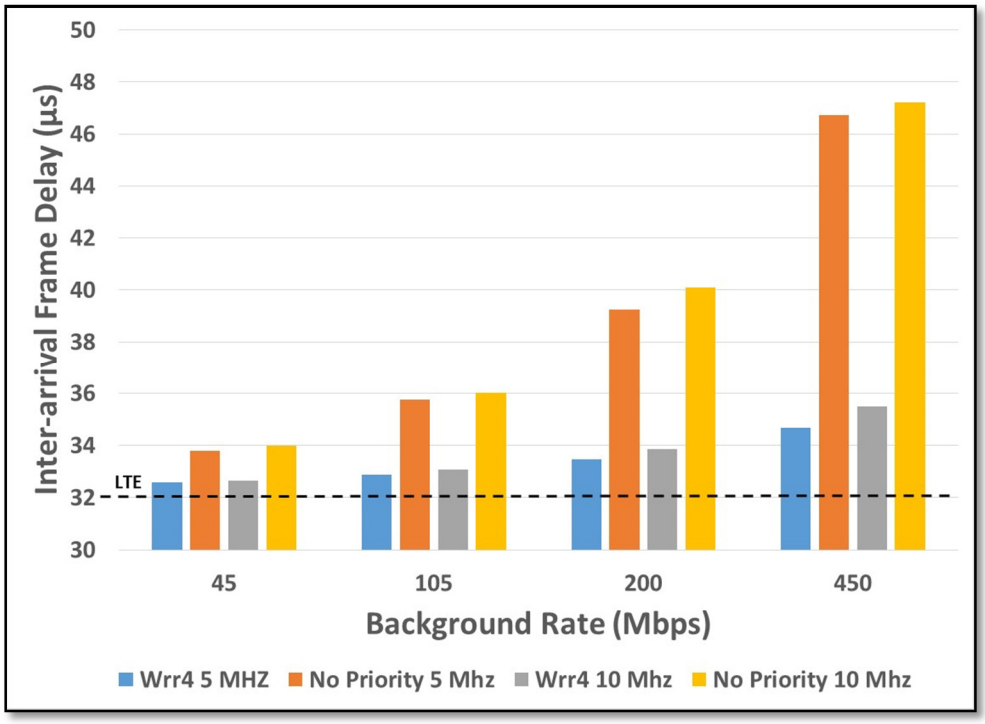

Figure.3.11. Comparison for the mean of the frame inter-arrival delay of the LTE traffic for equal-weight (Wrr4) and No-priority cases with different LTE traffic bandwidths and different background traffic data rates with frame sizes 500 bytes. The "LTE" trace corresponds to transmitting only the LTE traffic (i.e. no background traffic).

3.5 Asymmetric Delay and Time Inaccuracy in the Network

As mentioned in sub-section 2.1.5, to achieve proper operation of PTP in any network, the network should not have any delay asymmetry between the PTP grandmaster and the slave clocks. Delay asymmetry can be a result of network design (e.g., variability between uplink and downlink networking segments) or from different levels of contention between DL and UL paths. Whatever the source, the result will be an error in the time-stamping equal to one-half of the delay asymmetry. This error will remain constant until the next timing update takes place. Fig. 3.12 shows three different estimates for the delay through the fronthaul obtained by time-stamping through PTP. Note that all estimates are relatively stable, but there is a large offset between them. Two of the estimates are wrong (indicated as stable PTP errors), while the actual fronthaul delay (approximately 37.7 µs) is more accurately estimated during a time period in which contention does not take place. One method of overcoming the contention issue is to make use of bursting, and transmitting the PTP packets during "silent" periods in between the bursts. Note that bursting is not a necessary method to gain an uncontended time period. For a transmission scheme where the I/Q data traffic is transmitted at a constant frame rate instead, a scheduler could be used to transmit the PTP packets during silent periods between LTE-carrying frames. But, with a bursting implementation, a scheduler that transmits the PTP packets is possibly a lower complexity implementation.

The lack of accuracy of the time reference in the testbed limits the ability to measure the FDV by using two in-line probes since the probes will not be time-aligned. Fig. 3.13 shows the latency of the LTE traffic in the network measured by two probes. The traffic in this measurement does not contend with any other traffic. The results show a high variation in the delay due to the inaccuracy in the probes' timing, where the variation is around 50% of the baseline value. This issue can be solved by using an internal or external time reference with higher accuracy.

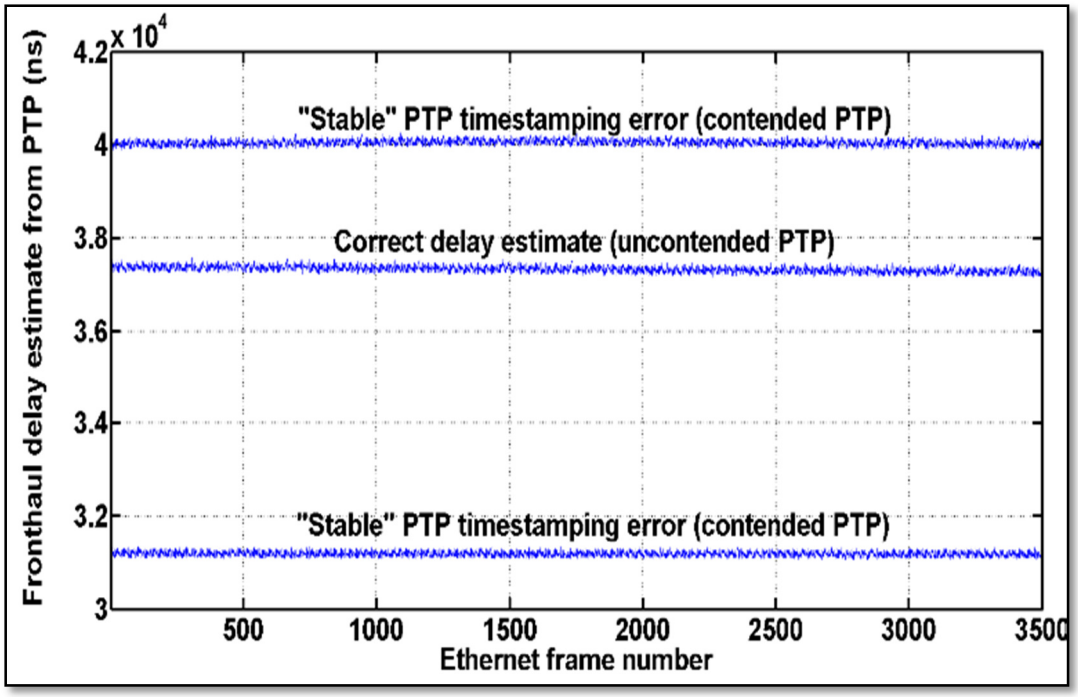

Figure.3.12. Measured delay estimates for the fronthaul obtained through PTP timestamping. Two of the traces indicate erroneous values for the fronthaul delay (a stable error), while one is close to the actual value, which is approximately 37.7 µs.

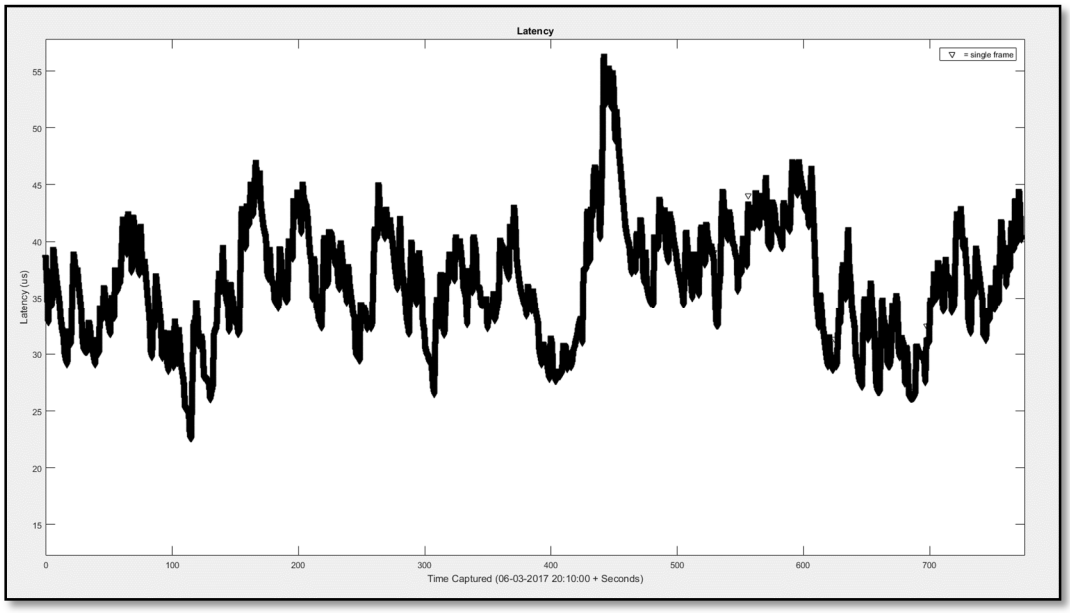

Figure.3.13. Measured delay for fronthaul traffic by using two in-line probes and with no contending traffic.

3.6 Conclusion

Different Ethernet queuing regimes in the switched fronthaul of the future C-RAN are presented and examined. The results show the performance of the different queuing regimes and the importance of using a suitable queuing regime in the fronthaul network based on the priority and the time sensitivity of each individual stream. SP can be used with sensitive delay/jitter services where the mean and STD of inter-arrival frame delay is slightly increased. However, this regime does not guarantee that the time-sensitive traffic will not encounter higher delays (due to lack of a pre-emptive mechanism). The WRR regime provides more capability for balancing and distributing the available trunk capacity between different streams in the fronthaul network. The results show that the background traffic rate and its Ethernet frame size affects the mean and STD values of frame inter-arrival delay of the LTE traffic. Using bigger frame sizes (jumbo frame regimes) increases the mean and STD of the inter-arrival frame delay with the WRR regime. The frequency of occurrence of the contention has an important role also in increasing the mean and STD of the inter-arrival frame delay of the LTE traffic with the SP regime. Two interesting special cases, which are the equal-weight WRR and the single queue (i.e. no-priority) regime are also compared. The equal-weight regime results show smaller mean frame inter-arrival delays than the no-priority case, but only when using small frame sizes. When using Jumbo frames the opposite behaviour is observed.

The main factors for choosing a queuing regime in the Ethernet fronthaul network is the latency and latency variation requirements of each stream. The need for queuing regimes that can eliminate the increase in the inter-arrival delay which is encountered by the LTE traffic in the previous results is clear. The queuing regime should as well guarantee STD and FDV within the proposed specifications for the high sensitivity traffic such as LTE (As discussed in section 2.2.1) and PTP traffic which are proposed alongside other traffic types to be transmitted in the future Ethernet fronthaul network.

4 Modelling and Performance Study for the Time Aware Shaper (TAS)

4.1 Introduction

As mentioned in Chapter 3, there is a need for a queuing regime that can minimize or absorb the effect of the contention on the frame delay and delay variation of time sensitive traffic such as PTP and the traffic resulting from the newly proposed C-RAN functional split (functional split traffic) in the Ethernet fronthaul network. As explained in section 2.4.1, the main objective of the TAS standard is to allow a timely aligned transmission for the different traffic types in the Ethernet network based on allocating time sections to each traffic stream in order to remove the FDV of the time sensitive traffic.

The focus of this chapter is the scheduling in an Ethernet fronthaul network and the modelling of TAS based on the 802.1Qbv standard in the Opnet/Riverbed simulation platform. The TAS modelling takes into account current trends in softwarization (hardware abstraction techniques such as network-function virtualization (NFV) and SDN), that are expected to have an impact on the timing and delay instability in the RAN and switching nodes in the fronthaul due to variations in the processing time. As mentioned in section 2.4.1, a limited implementation has been done for the TAS in the NS-3 simulation platform [65] by deploying gating in the Ethernet switches. This implementation does not fully comply with the standard and the simulated scenarios are limited to specific traffic types (CPRI, Background traffic) with specific rates and transmission patterns.

A range of simulation scenarios and results for PTPv2 and functional split traffic with different background traffic rates, frame sizes and burst sizes are presented and discussed in this chapter. The TAS performance is compared with the performance of the traditional queuing regimes, such as SP and WRR.

The importance of using global scheduling and SDN in the Ethernet fronthaul with TSN is also presented and discussed.

The choice to use a software-based platform such as Opnet/Riverbed to implement TAS is based on the scalability advantage that the simulation platforms have in terms of the network size and the ability to model different traffic types and transmission patterns in comparison to hardware platforms. In addition, TAS has not been deployed yet in any hardware platform. Implementing TAS in hardware requires the hardware to be programmable in the Ethernet layer level and has an efficient fabric response. Some implementation for scheduling techniques such as the one presented in [80] has been done by using Field Programmable Gate Arrays (FPGA) boards.

The servers and switches in this simulation platform are all perfectly synchronised, i.e. they have the same time reference. Thus, the potential synchronisation issue that was discussed in sub-section 2.1.5 does not exist here. However, the drifting and the timing instability in the Ethernet fronthaul is considered in the presented modelling and design.

4.2 Bridge Aware Time Aware Shaper Design

In this section, the TAS model design and its implementation in Opnet/Riverbed are presented. Bridge aware time aware shaper means that only the network bridges are aware of the time shaping and transmit the traffic according to specific time windows. The rest of the nodes in the network transmit the traffic according to their own timing or as soon as they receive the traffic.

Note, throughout the rest of the chapter, the term “packet” may be used instead of “frame”, with both terms used interchangeably to describe an Ethernet frame.

The duration of the windows should enable the accommodation of the generated traffic in every *TW*. The size of the *PS* (or *PSS*) (*TW* sections and subsections based on IEEE 802.1Qbv standard were described in section 2.3.3*)* in the switch is calculated according to :

$$W_{s_p} = \sum_{n=1}^{N-1} \left(\frac{P_n}{R} + I_n \right), \qquad (4)$$

where N is the total number of packets sent in the *PS, R* (bits/s) is the output interface link rate, P_n (bits) is the packet length and I_n (s) is the inter-frame gap. Note that the first term inside the parentheses represents the serialization delay of the frame.

Then, the best effort section duration W_{BE}, is given by:

$$W_{BE} = TW - W_{sp} - W_{GP}, \qquad (5)$$

where *TW* is the transmission window duration and W_{GP} is the duration of the guard period. The simulation setup in Opnet is shown in Fig. 4.1. Two traffic generators are used, one representing the HP traffic source (TG1) and the other representing the LP traffic source (TG2). The traffic from these sources are subsequently assigned to the PS and BES respectively by the TAS. The TAS is implemented in the input ports of the switch as shown in Fig. 4.1, through port gating.

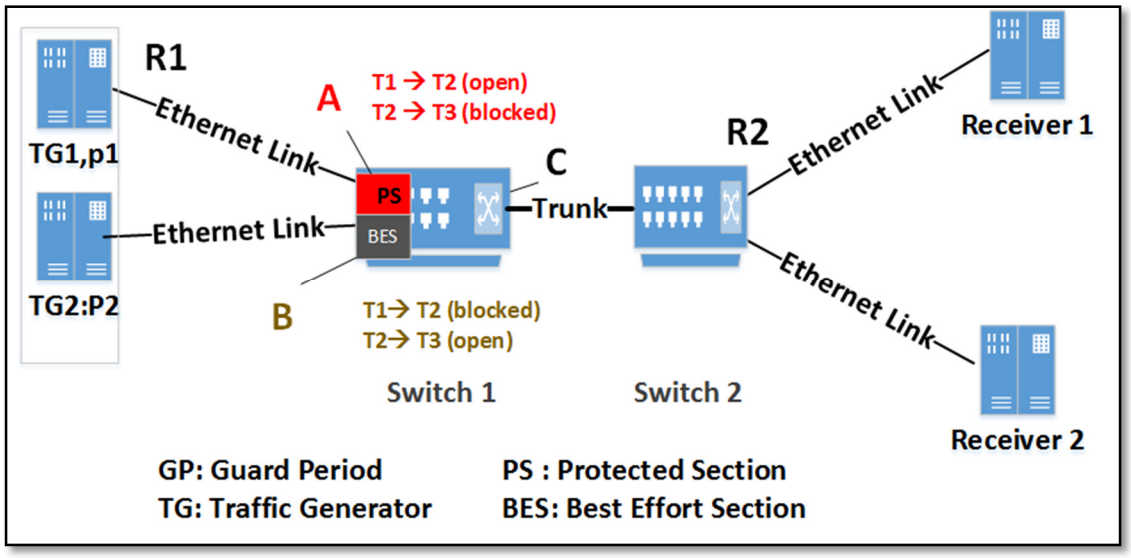

Figure.4.1. TAS implementation in Opnet. TG1 generates the HP traffic while TG2 the LP traffic.

If an HP packet is received in the input port A of the switch, the scheduler will allow the traffic to go through to output port C, only if it is received within the PS (given by the time limits T2 and T1) which has a length given by T2-T1. If the packet is received outside these time limits, it will be dropped. After time T2, port A will be blocked and port B will become unblocked for a duration given by T3-T2 (where T3 is the time limit for the best effort section) allowing the LP packets received in port B to be passed through to the output port C. After T3, a time section is allocated for the GP. Note that T1, T2 and T3

values are set according to (4) and (5) and has the same size for the whole transmission time in each scenario (no dynamic sizing for the windows).

The algorithm pseudocode in the switch is shown in Fig. 4.2. First, PS and BES boundaries for the current TW are initialized based on the window design parameters described by (4) and (5). Once the section boundaries are initialized, the switch medium access control (MAC) layer checks whether any received packet coming from the input port is received within the section that has been allocated to this source.

```
1    Initialize Protected Section time boundaries
       T1, T2, T3, .... Tn ; {Dp, Pk, D, In}
2    Initialize Best Effort Section time boundries
       {1 − [T1, T2, T3, .... Tn]} ; {Dp, Pk, D, In}
3    Rcv frame from the Physical Layer  RcvF(f);
4    if [ (current time < Tx)&& (current time > Tx − 1)]
       Send_To_Output_Queue(f);
5    if [ (current time > Tx )&& (current time < Tn]
       Drop_Frame(f);
6    Else
7    if [ (current time > Tx )&& (current time > Tn)
     Update Transmission Windows/subwindows time
       T1 = T0 + Tn.
       T2 = T1 + Tn.
       .
       .
       .
       Tx = Tx − 1 + Tn.
```

Figure.4.2. Implemented algorithm for the scheduler in the switch in Opnet.

If the packet is received within its allocated section, the switch will allow it to pass through to the output port, otherwise it will be dropped. Finally, the algorithm checks whether the current TW is expired; if it has, it updates the sections for the new TW. Note that the section boundaries for the new TW can be different, allowing the scheduler to accommodate changes in the traffic characteristics.

The latency, *Ln*, experienced by packet, *n*, within the network is measured between reference points R1 and R2 (see Fig. 4.1). The equivalent simulation-generated timestamps at these two points correspond to the time that a packet is fully serialized out of the traffic generator output port up to the time the same packet is fully serialized out of the switch 2 output port. The average frame delay variation ($\overline{FDV}$) is then given as:

$$\overline{\mathrm{FDV}} = \frac{\sum_{n=2}^{N} |L_n - L_{n-1}|,}{N-1} \qquad (6)$$

The initial result for operational verification and the simulated scenarios to compare the performance of the bridge aware time aware shaper with SP are shown in subsections 4.3 and 4.4 respectively.

4.3 Initial Results

An initial set of results is obtained to demonstrate the port-gating operation in the switch. Here, both traffic generators have the same transmission pattern (i.e. start and end their transmissions at the same time), frame size and data rate while both sources are constant-packet rate ones. The inter-repetition time for both is set to 800 µs while the TW is set to 1.6 ms with the PS section (allocated to TG1) occurring from 0-800 µs (T1→T2), followed by the BES section (allocated to TG2) occurring from 800-1600 µs (T2→T3).

Fig.4.3 shows the transmitted traffic originating from TG1 and the traffic that is sent by Switch 1 to the trunk. The results show that the packets that arrives outside the PS in the switch are dropped by the switch scheduler. The frames that reach the switch scheduler within the allocated time window are transmitted from the output port to the trunk toward the end station. A summary of the results is shown in Table. III. The TAS completely resolves any contention in the network thereby resulting in zero queuing delay variation. Note that there is no change in FDV as all sources produce traffic with constant parameters (i.e. there is no statistical variation and packets from both sources contend in the same way in every TW).

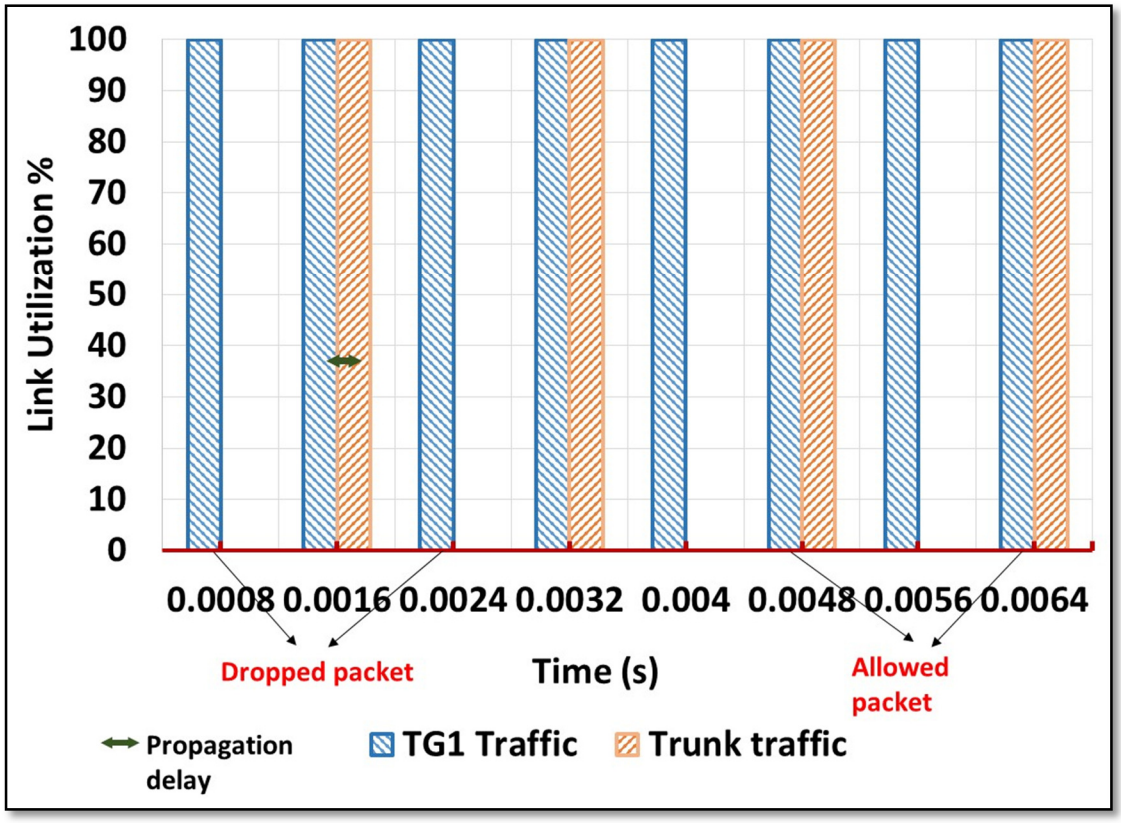

Figure.4.3. Transmitted traffic in the protected window by TG.

Table. III

Delay, FDV, Queuing Delay and Queuing Delay Variation for the Results of Figure.4.3

Applied Technique	Traffic Source	FDV (µs)	Delay (µs)	Queuing Delay (µs)	Queuing Delay Deviation (µs)
One Traffic at a time (Base line)	TG1	0	34.51	0	0
	TG2	0	34.42	0	0
With TAS	Protected (TG1)	0	34.51	0	0
	Best Effort (TG2)	0	34.42	0	
Without TAS	TG1	0	38.98	2.162	4.25

4.4 TSN and Traditional Queuing Regimes Comparison

To compare the queuing regimes, two different scenarios are implemented. In both scenarios, the PTP traffic (the HP traffic) and background traffic (the BE traffic) are transmitted over the same network segment (a trunk link), with the traffic stream emulating the PTPv2 traffic assigned to a higher priority setting. TG1 (PTP Transmitter) generates 32 timing messages per second per PTP slave. The number of slave stations is 50 (note that these are modelled through the amount of traffic generated and the corresponding utilization in the trunk and not as separate receivers) and each sync message is formed as a 68 octet frame. Note, that the amount of background traffic that shares the trunk link with the PTP traffic may not correspond to the same number of receiving stations. The HP time window section is designed to accommodate the high priority traffic.

4.4.1 Constant Background Frame Size Scenario

In this scenario, background traffic is generated as a burst of fifty frames, with an inter-frame gap of 20 μs and a frame size of 1000 octets. This traffic source may represent both CPRI-type traffic and C&M traffic. The PS duration is set to 50μs. The GP is allowed to vary from zero to the value of the serialization delay of a 1000-octet frame. Fig.4.4 shows the peak and average FDV results for SP and for TAS with different GPs.

The results show that the SP performance is equivalent to a TAS implementation with zero GP. Specifically, the peak and average FDV with TAS are upper-bounded to the peak and average FDV with SP. This makes sense as both schedulers cannot resolve cases where a background traffic transmission is ongoing, i.e. there is no pre-emption being employed in the network.

As the GP is increased, both the average and maximum FDV with TAS reduce steadily until they reach zero at a GP of 6 μs. This value corresponds to a serialization of a large part (75%) of a background traffic frame. Note that the worst case would be a full serialization (i.e. 8 μs) but as the background source is constant frame-rate and frame size, this worst case is not observed in these results due to the relative timings of the background and PTP traffic generators in the simulation. Note also that the peak-to-

average ratio of FDV can be very large and obviously, this ratio will depend on the transmission pattern of the sources.

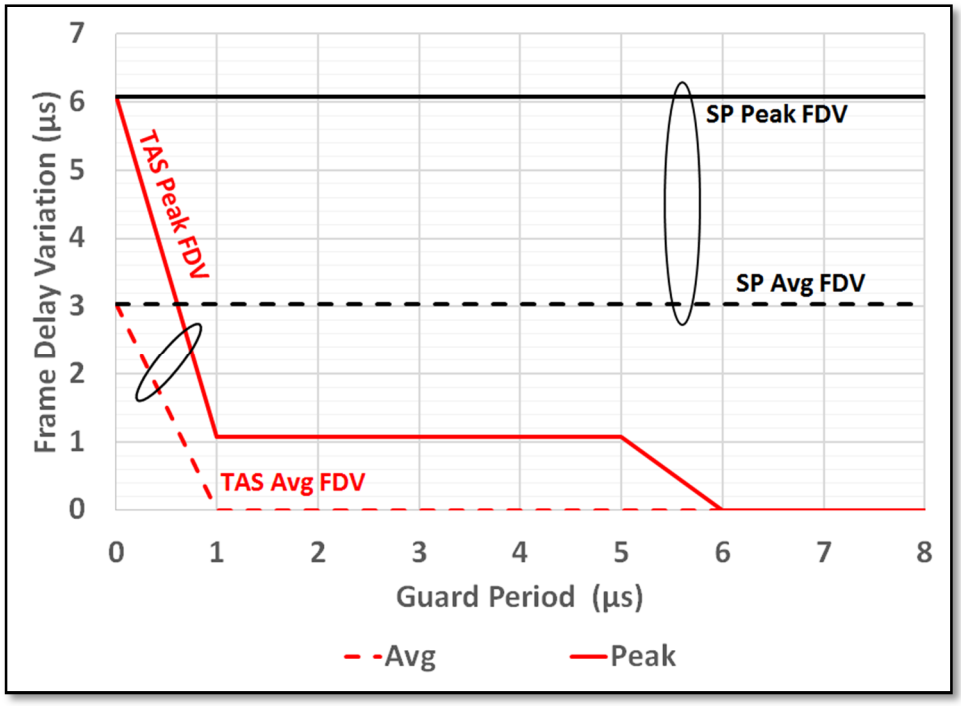

Figure.4.4. Average and peak FDV for the PTP traffic with SP and TAS with different GPs. The background traffic source is constant frame-rate and constant frame size.

4.4.2 Variable Frame Size Scenario

This scenario is similar to the previous scenario but with a varying frame size for the background traffic. The traffic source is meant to represent functional split traffic, for e.g. fifty user allocations per LTE subframe (i.e. 50 frames every 1 ms), in a MAC/PHY split (3GPP option 6 [16]). Two different settings are used: The first follows a normal distribution with a mean value of 1000 octets and variance of 200 octets (results are presented in Fig. 4.5).

The second setting is similar, albeit with an increased variance of 500 octets (results are presented in Fig. 4.6). The results show that the peak and average FDV is increased (compared to the first scenario) for both SP and TAS with zero GP and approaches the serialization delay of a full background traffic frame. Furthermore, the peak FDV for the results of Fig. 4.6 reaches zero at a GP that is equivalent to the serialization delay of a full background traffic frame. This is indicative of the dependence of the scheduler performance, with regards to FDV, on the transmission pattern characteristics of the

traffic sources. The larger variance in the traffic pattern in this case results in the occurrence of the worst case scenario of a background traffic frame serialized right at the end of its BES allocation. Fig. 4.7 is a zoom-in of Fig. 4.6 in the x-axis range from 0 to 1 µs. The large peak-to-average ratio of FDV is clear in these results. The small inset shows the resulting worst-case timestamping error with PTP for the peak FDV values shown in Fig. 4.7. The worst-case assumption is that this peak FDV is encountered in one direction of traffic (either downlink or uplink) while there is zero FDV in the opposite direction. The results in Fig. 4.7 show that SP can cause a large time stamping error due to the Peak FDV while TAS is capable in absorbing the FDV and achieving low or even removing the timestamping error (when the GP is sufficient).

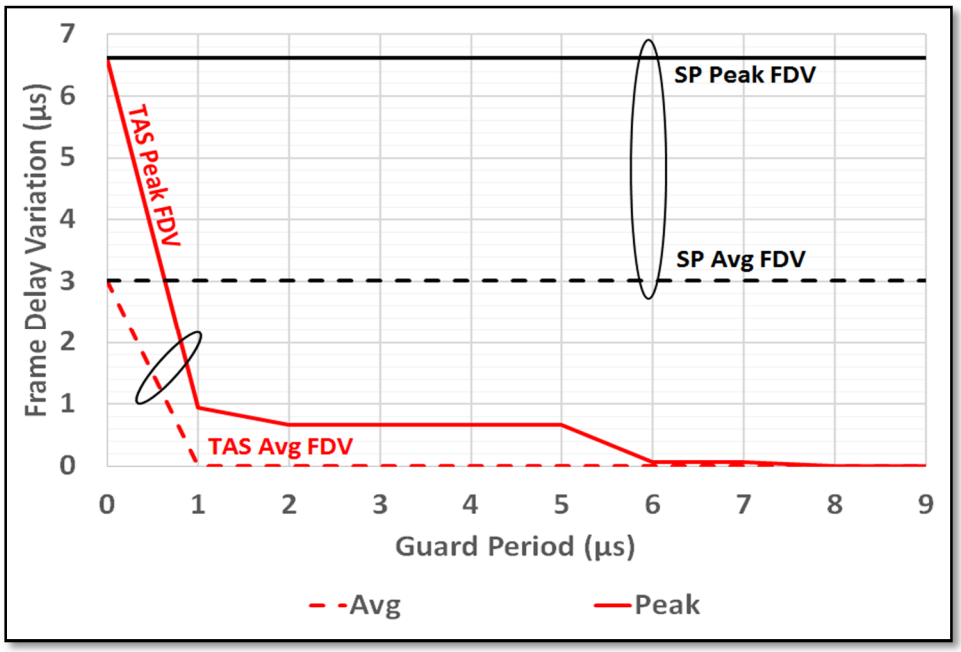

Figure.4.5. Average and peak FDV for the PTP traffic with SP and TAS with different GPs. The background traffic source is constant frame-rate with a varying frame size following a normal distribution with mean of 1000 octets and variance of 200 octets.

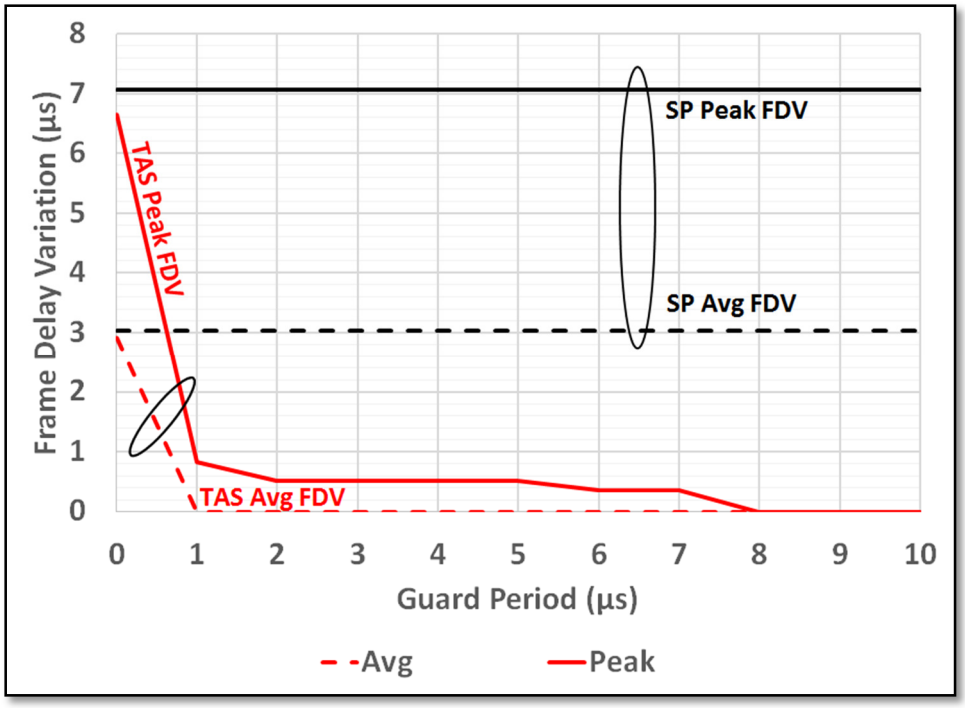

Figure.4.6. Average and peak FDV for the PTP traffic with SP and TAS with different GPs. The background traffic source is constant frame-rate with a varying frame size following a normal distribution with mean of 1000 octets and variance of 500 octets.

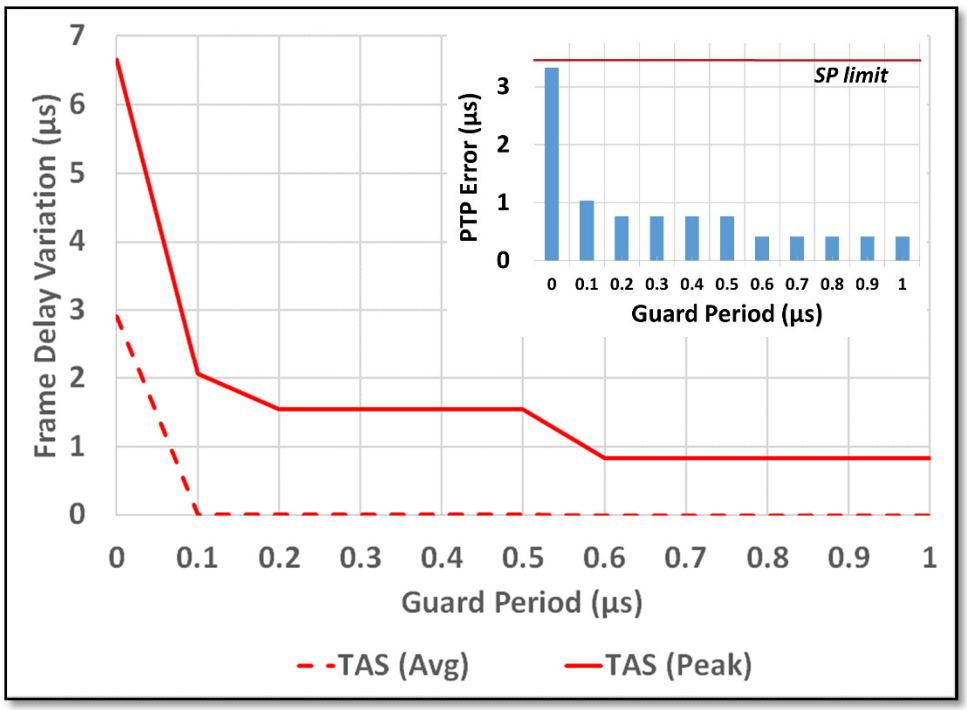

Figure.4.7. Zoom-in in the region of GPs from 0 to 1 µs for the results of Fig. 4.6. The inset shows worse- case PTP timestamping error that would result from the peak FDV values.

To summarize, the results in Fig. 4.4, Fig.4.5 and Fig.4.6 have shown that TAS is capable of removing the FDV of the PTP traffic (in case the GP is sufficient) when contending with background traffic with different and varied frame sizes. The GP size depends on the traffic characteristics where larger variance in the transmission pattern in this case results in the occurrence of the worst case scenario of a background traffic frame serialized right at the end of its BES allocation which in order to be absorbed, a larger GP Size is required. The results in Fig.4.7 have shown the main limitation of SP for which the peak FDV remains constant and can potentially result in large PTP timestamping errors (depending on the size of the background traffic frame). TAS on the other hand looks promising in its ability to reduce FDV (and thus timestamping errors) as the GP is increased, or eliminate FDV entirely when the GP is sufficient to eliminate contention. The drawback of TAS can be the increased end-to-end latency especially if the number of aggregation nodes becomes large.

4.5 Network Aware Time Aware Shaper Design

In this section, the TAS model design and its implementation in the traffic sources and the Ethernet switches in Opnet/Riverbed are presented, with verification of the performance in different scenarios. Network aware time aware shaper means that all network nodes are aware of the time shaping and transmit the traffic according to specific time windows. The duration of the windows should enable the accommodation of the generated traffic in every TW. The size of the *PS* (or *PSS*) in the switch, W_{s_p}, and in the end stations W_{e_p} can be calculated according to:

$$W_{s\_p} = \sum_{n=1}^{N-1} \left(\frac{P_n}{R} + I_n \right) + D_p + 2D, \qquad (7)$$

$$W_{e\_p} = \sum_{n=1}^{N-1} \left(\frac{P_n}{R} + I_n \right) + 2D, \qquad (8)$$

where *N* is the total number of packets sent in the *PS*, *R* (bits/s) is the output interface link rate, *Pn* (bits) is the packet length, *Dp* (s) is the propagation delay, *In* (s) is the inter-frame gap and D (S) is a factor that takes into account the time drifting (or timing instability) in the section boundaries and/or packet generation times in the application within the end-station. Note that the first term inside the parentheses represents the

serialization delay of the frame. Fig. 4.8 shows how the PS duration in the switch and end-station is set-up according to (7) and (8); the only difference is the inclusion of the propagation delay from the end-station to the switch. The inclusion of the propagation delay here is due to the way in which the windows are designed, where the time windows are started at the same time in both the end station and switch. Ideally, the start of the window in the switch will be shifted by amount of time equivalent to *Dp* while the window size will be the same at the end stations and switch. Then, the best effort section duration W_{BE}, is given by:

$$W_{BE} = TW - W_{protected} - W_{GP}, \qquad (9)$$

where TW is the transmission window duration and W_{GP} is the duration of the guard period. The simulation setup in Opnet/Riverbed is shown in Fig. 4.9. Two traffic generators are used, one representing the HP traffic source (TG1) and the other representing the LP traffic source (TG2). These are then assigned to the PS and BES respectively by the TAS. The TAS is implemented in the output ports of the end-stations and the input ports of the switch as shown in Fig. 4.9, through port gating.

Similarly to the Initial implementation, the latency, *Ln*, experienced by packet, *n*, within the network is measured between reference points R1 and R2 (see Fig. 4.9).

The difference between this implementation and the bridge aware TAS implementation is that TAS applied at the end-stations and Ln in this implementation includes as well the amount of time the frame waited at the end station before being transmitted in its time section. The TAS with the queuing feature is implemented at the end stations to prevent the traffic that received outside the allocated time section from being dropped and avoid excessive queuing at the network bridges.

The latency, Ln, experienced by packet, n, within the network is measured between reference points R1 and R2. The equivalent simulation-generated timestamps at these two points correspond to the time that a packet is fully serialized out of the traffic generator output port up to the time the same packet is fully serialized out of the switch 2 output port. The average frame delay variation ($\overline{FDV}$) is then given as:

$$\overline{\mathrm{FDV}} = \frac{\sum_{\mathrm{n}=2}^{\mathrm{N}} |\mathrm{L_n} - \mathrm{L_{n-1}}|,}{\mathrm{N}-1} \qquad (10)$$

The TAS is implemented in the input ports of the switch as shown in Fig. 4.9, through port gating. The algorithm at the end-stations is shown in Fig. 4.10, and it is similar to that in the switch with one important difference: LP packets received in the MAC layer from the upper layers will be queued and sent as soon as the BES occurs. Thus, the algorithm bases the TW design on the requirements of the HP traffic source(s); i.e., section boundaries in the end-stations and switch are set according to HP traffic characteristics.

The initial results and the simulated scenarios to compare the performance of the network aware time aware shaper with the traditional queuing regimes (SP, WRR) are shown in subsections 4.6 and 4.7 respectively.

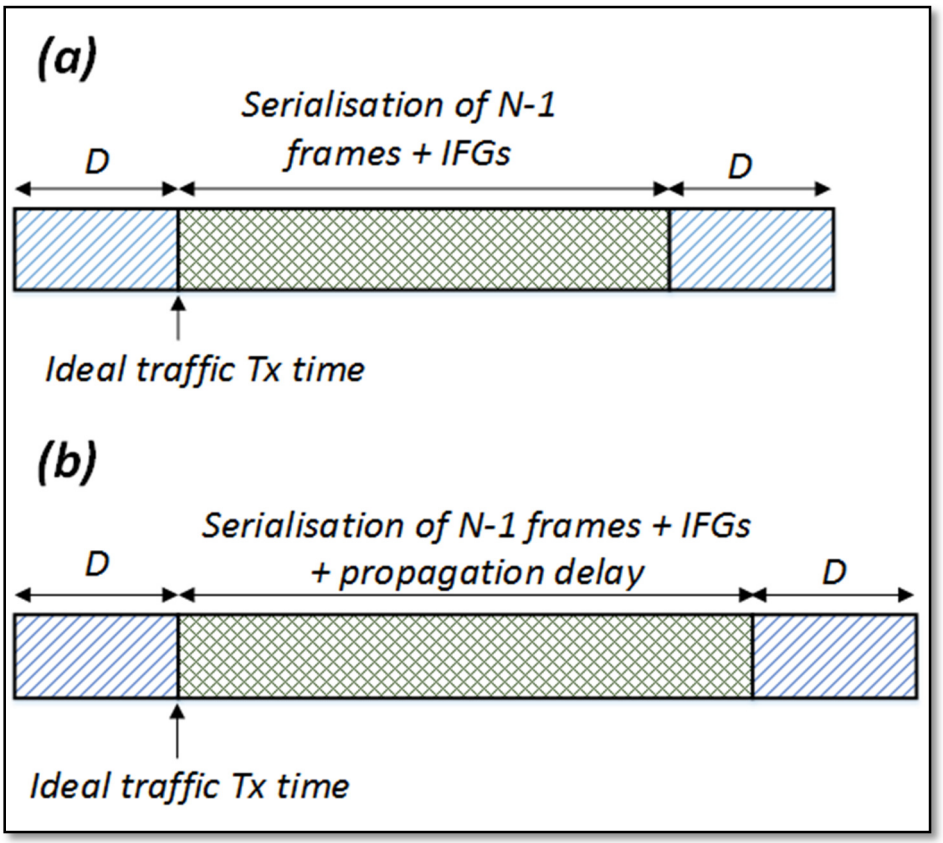

Figure.4.8. Durations of the HP sections in (a) the end-station and (b) the switch.

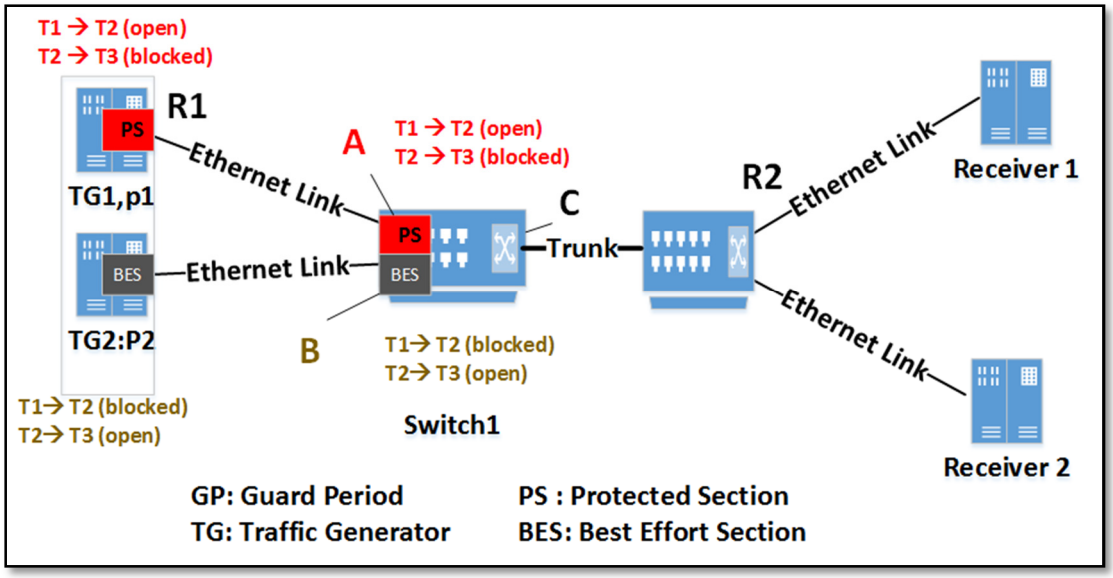

Figure.4.9. TAS implementation in Opnet. TG1 generates the HP traffic while TG2 the LP traffic.

```
1    Initialize Protected Section time boundaries
        T1, T2, T3, .... Tn ; {Dp, Pk, D, In}
2    Initialize Best Effort Section time boundries
        {1 − [T1, T2, T3, .... Tn]} ; {Dp, Pk, D, In}
3    Rcv frame from the Upper Layer  RcvU(f);
4    While [ (current time < Tx)&& (Input_Queue
        = = ! null)&& (current time > Tx − 1)]
           Send_To_Output_Queue(f);
5  if [ (current time > Tx )&& (current time < Tn]
        Insert_Frame_In_Input_Queue(f);6
                  Else
7  if [ (current time > Tx )&& (current time > Tn)
   Update Transmission Windows/subwindows time
                  T1 = T0 + Tn.
                  T2 = T1 + Tn.
                     .
                     .
                     .
                  Tx = Tx − 1 + Tn.
```

Figure.4.10. Implemented algorithm for the scheduler in the end-station in Opnet.

4.6 Initial Results

Fig. 4.11 shows the transmitted traffic originating from TG1 and the traffic that is sent by Switch 1 to the trunk. The transmitted traffic from the end stations are transmitted through the Trunk and the network is designed to not drop any traffic. TAS at the end station queues the traffic that is transmitted outside of the window time and minimizes the dropped frames by TAS to zero. To confirm the behaviour, the transmitted traffic from TG2 has been shown as well in Fig. 4.12. The figure is zoomed in to show the queuing in the station when the traffic is received from the upper layer outside its transmission window and how it is transmitted in the trunk link.

As there is an arbitrary defined propagation delay from end-station to switch, frames that are transmitted at the end of their section in the end-station are dropped by the switch scheduler. For the previous reason, the propagation delay has been considered in the allocated time section in the switch. Similarly to the previous design, the TAS completely resolves any contention in the network thereby resulting in zero queuing delay variation.

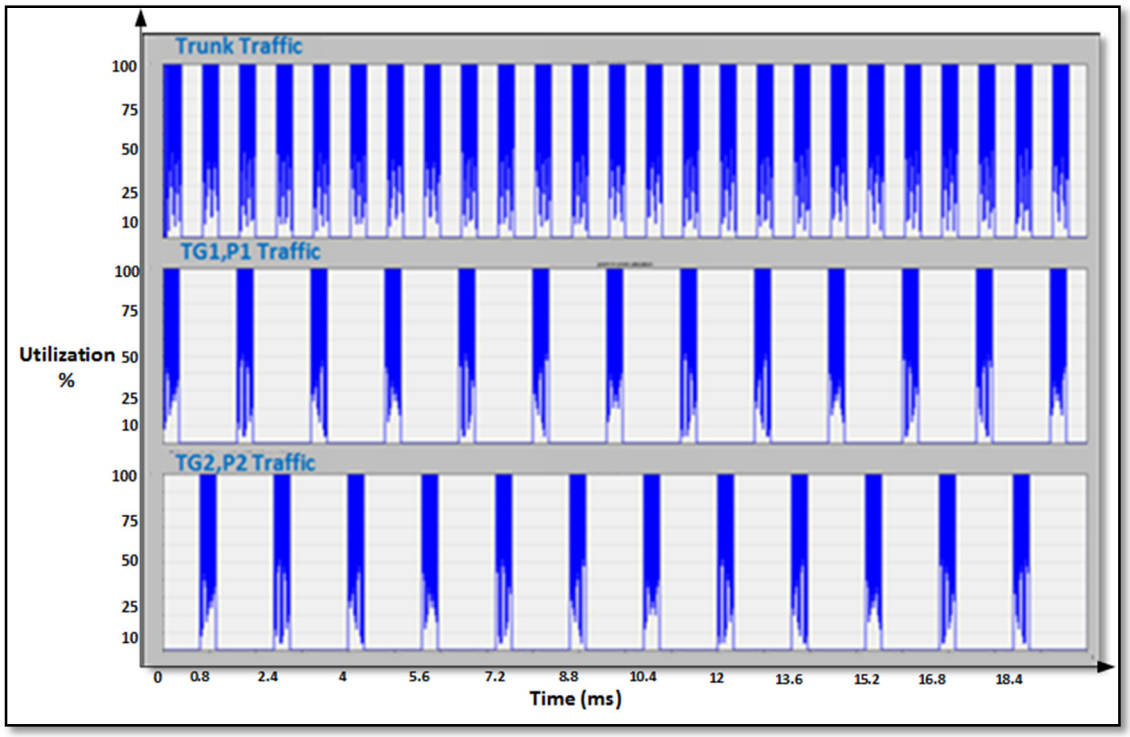

Figure.4.11. Traffic in the network with TAS (taken from the utilization statistic in Opnet).

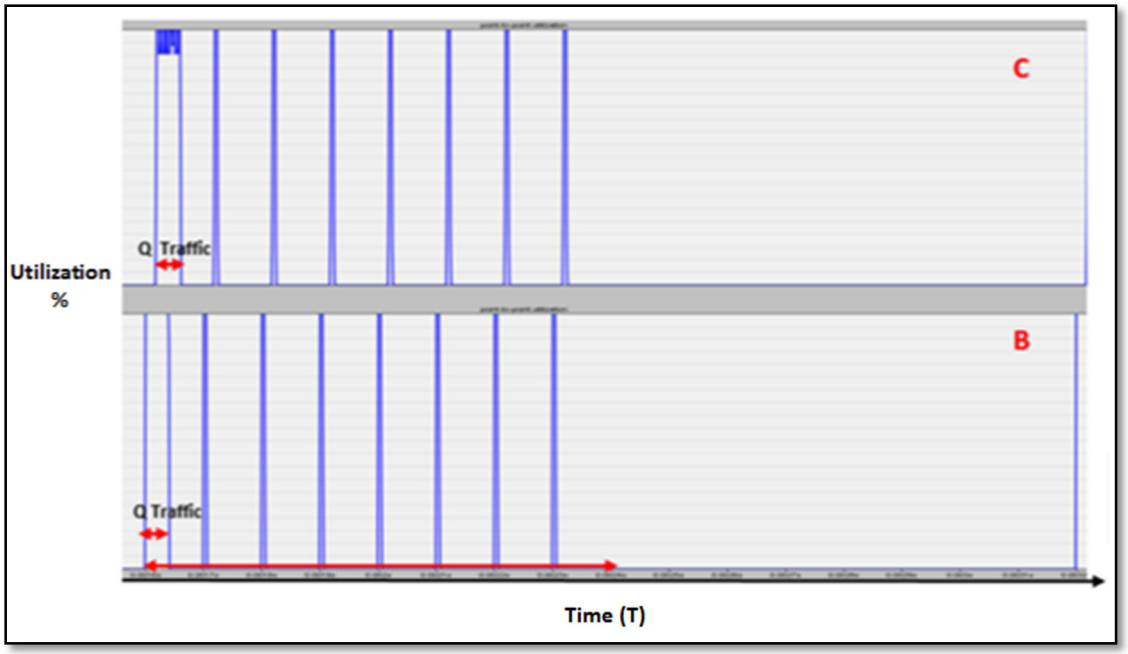

Figure.4.12. TG2 Traffic in the network with the queuing (taken from the utilization statistic in Opnet).

4.7 TSN and Traditional Queuing Regimes Comparison

For the results presented in this sub-section, the high priority traffic is a stream emulating PTPv2 packets generated by traffic generator TG1 and is composed of 32 timing messages per second per PTP slave (Receiver 1). The number of slave stations is 50 (these are modelled through the amount of traffic generated and the corresponding utilization in the trunk and not as separate receivers) while each PTP 'sync' message is formed as a 68 octet frame. Note that the amount of background traffic that shares the trunk link with the PTP traffic may not correspond to the same number of receiving stations. The background traffic is meant to represent the traffic produced by a functional split at the LTE MAC/PHY interface. In such a split, transport blocks, each corresponding to a different user, are produced at the beginning of each LTE subframe (every 1 ms, corresponding to the scheduling resolution of LTE).

The background traffic is generated in bursts with specific inter-frame gaps between each individual frame. The background traffic generation implementation flowchart with TAS is shown in Fig. 4.13. Any frame generated outside the transmission window and after achieving the number of frames corresponding to the targeted bandwidth will

be dropped. If the targeted number of frames is not achieved within the window, the rest of the targeted frames will be queued.

The weights used for WRR are 8:1, 8:4, 8:6 and 8:8 with the higher weight corresponding to the high priority traffic. The performance comparisons presented here are based on the FDV experienced by the PTP traffic. FDV can have detrimental effects in the PTP timestamping accuracy. Three different sets of scenarios are presented to show the effect of different types of traffic on the PTP traffic in the Ethernet fronthaul and the performance of TAS in these scenarios.

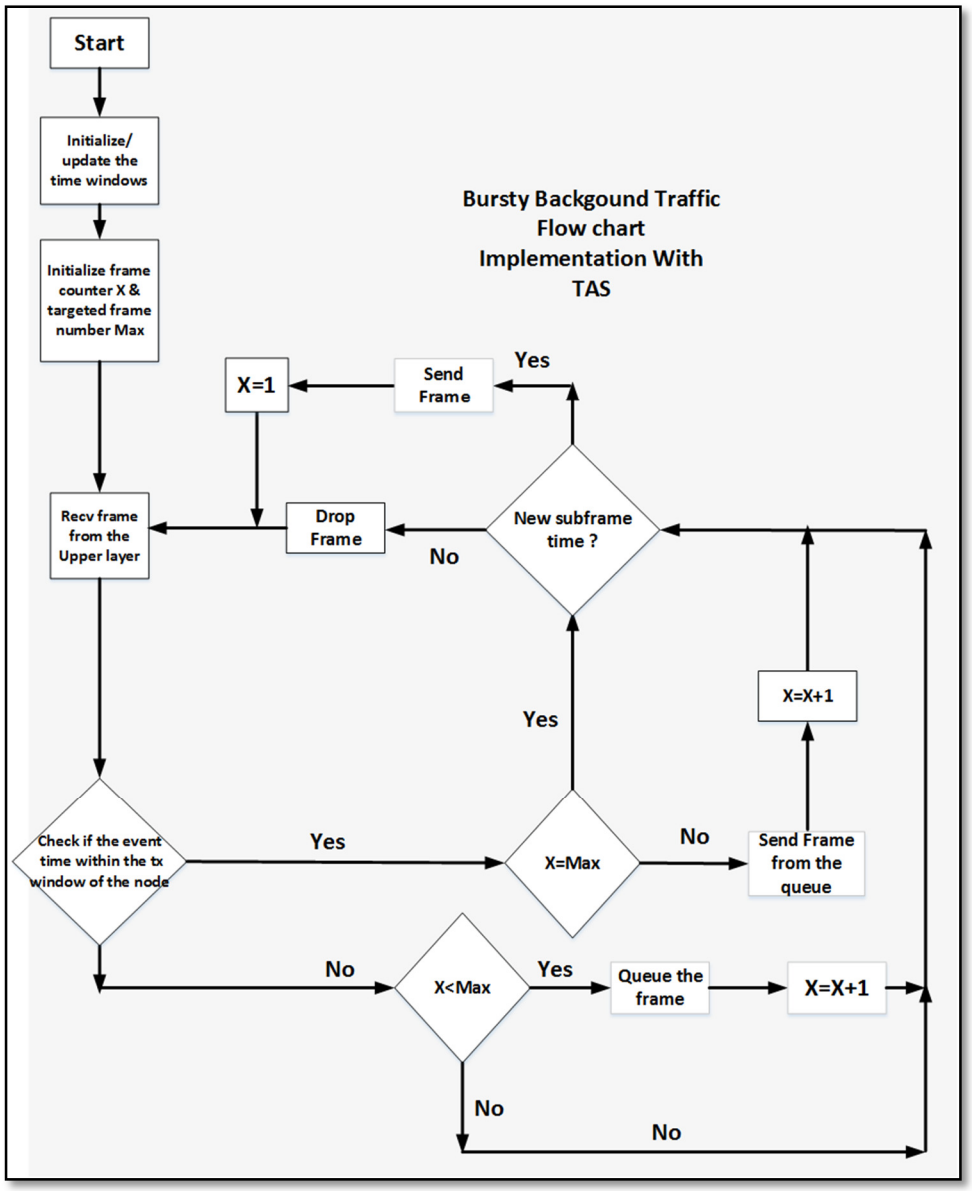

Figure.4.13. Implementation flow chart of the Bursty background traffic.

4.7.1 Variable Frame Size Scenario (SP and TAS comparison)

In this case, the frame size is allowed to vary between 100 and 1500 octets within the burst, following a uniform distribution, while the burst size is constant (10 frames). The results for this scenario are shown in Fig. 4.14. It can be seen that even with a variable frame size for the LP flow, the TAS can eliminate the FDV. For these results specifically, zero FDV for the HP packets is achieved with a GP of approximately 85% of the maximum LP frame serialization delay.

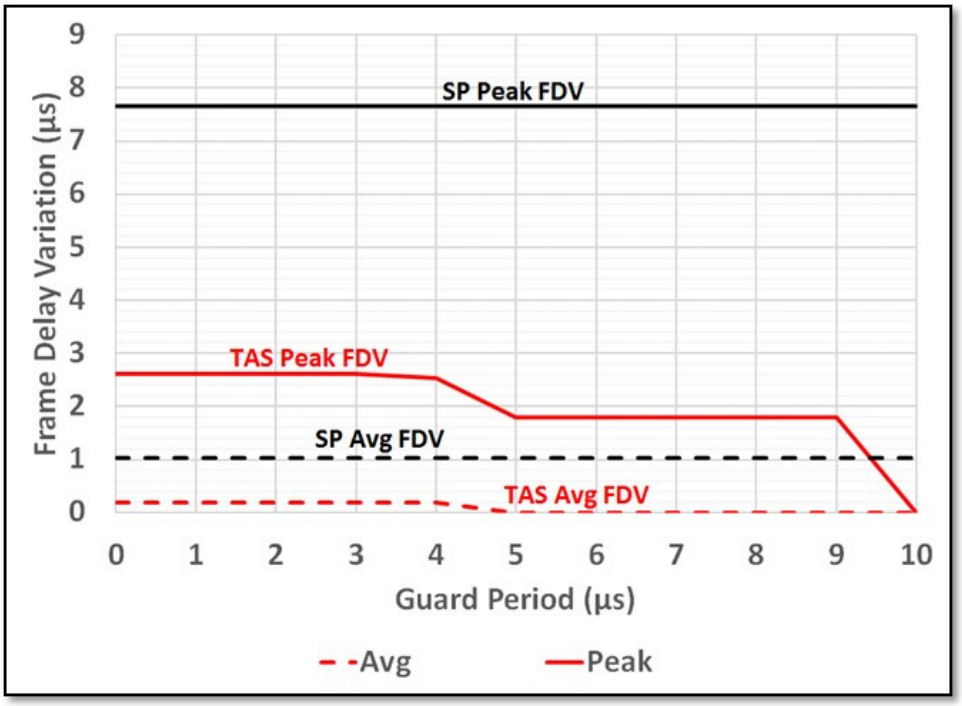

Figure.4.14. Average and peak FDV for the PTP traffic with SP and TAS with different GPs. The background traffic source is bursty with variable frame size.

4.7.2 Variable Burst Size Scenario (SP and TAS comparison)

The LP traffic for this scenario will be bursty with a varied burst size and constant frame size. The variation in the burst size in this case emulates a traffic stream that would be produced from the implementation of a MAC/PHY split where the number of users serviced in a cell (i.e. the cell load) varies from one LTE transmission time interval (TTI, 1 ms) to the next. Thus, the packets here represent LTE MAC transport blocks (TBs) encapsulated by Ethernet. The TG2 traffic burst size varies between 1 and 10 frames, following a uniform distribution. The frame size in each burst is 1000 octets (excluding headers) and the inter-frame gap is 2,000 bits, corresponding to a duration of 2 µs.

Based on (7), and assuming a timing drifting factor D, equivalent to 4% of the TW, the PS is set to 50 µs. The GP is allowed to vary from zero to the value of the serialization delay of a LP frame. Fig. 4.15 shows the peak and average FDV results for TAS with different GPs and for SP. The worst-case performance for TAS, i.e. with zero GP, is equivalent to the SP performance. This is expected, as any ongoing transmission would force an HP packet to wait until the end of transmission in both cases.

The step-like behaviour is attributed to the constant TW duration, which means that every time the GP is increased the BES duration is reduced. As a result, a change in the FDV will not occur until the BES section is reduced by an amount that results in a packet being excluded by the window section. This can also be seen by the fact that the sum of the peak FDV value and the guard period, whenever a step change occurs, is approximately equal to a full serialization of an LP frame. As the GP is increased, both the average and maximum FDV with TAS reduce steadily until they reach zero at a GP of 8 µs. This value corresponds to a full serialization of a LP packet.

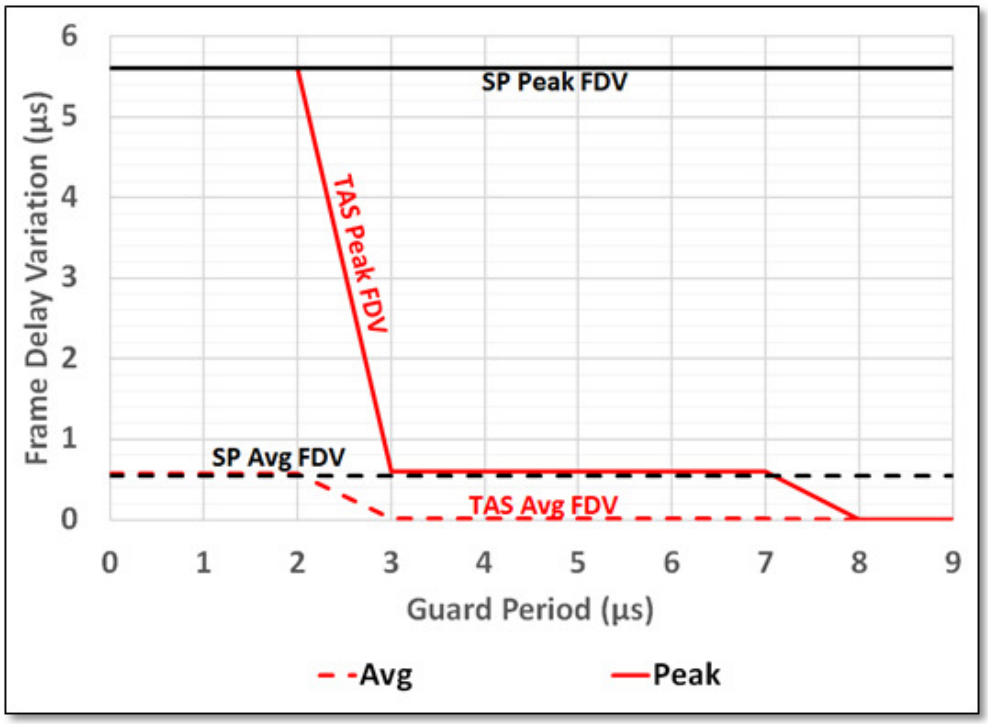

Figure.4.15. High priority traffic emulating PTP transmissions and background traffic with constant frame size and variable burst size.

4.7.3 Variable and Constant Burst Size Scenario (SP, WRR and TAS comparison)

Fig. 4.16 shows the results for the background traffic configured with a constant frame size (1000 octets), constant burst size (10 frames per burst) and an inter-frame gap of 30 µs. While for the results of Fig. 4.17, the background traffic is configured with a variable burst and frame size following a uniform distribution (1-10 frames) and (700-1500 bytes) respectively. It can be seen that both WRR and SP schemes result in the same performance irrespective of the weights used for WRR. (Note that only one WRR trace is shown here as the traces for all weights overlap). This is a result of a combination of two factors:

The first is that the aggregate traffic data rate (trunk utilisation) is low which leads to low probability of contention in the output port of the switch

The second is the large size of the inter-frame gap between the frames in each burst which allows the PTP frames to be transmitted within the inter-frame gap.

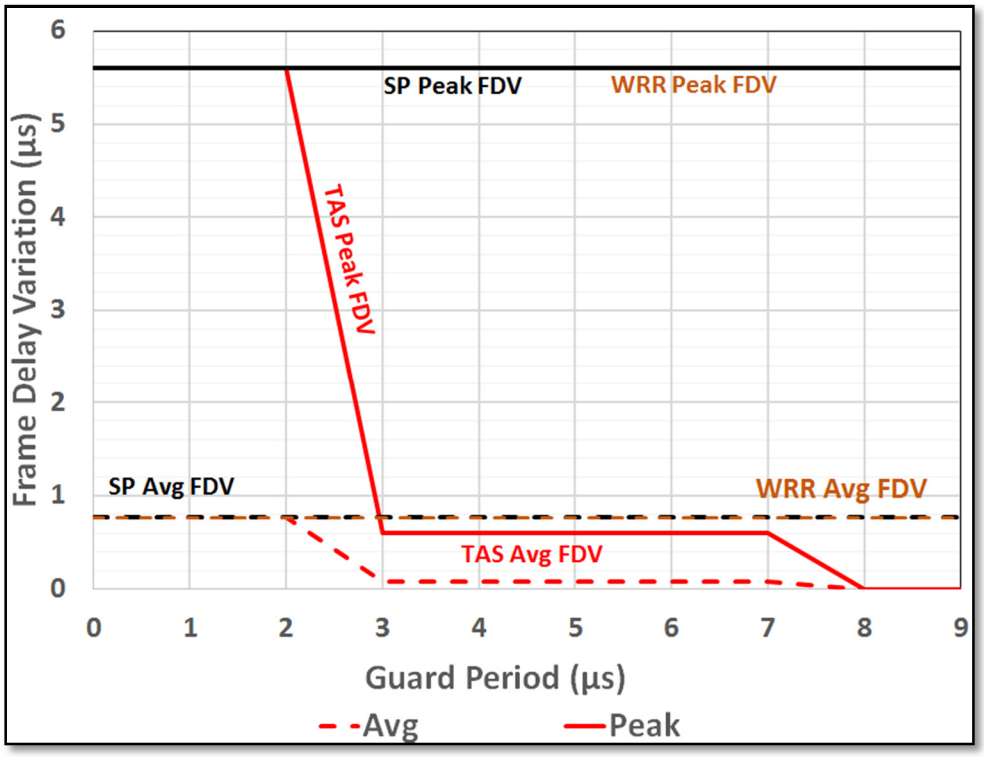

Figure.4.16. High priority traffic emulating PTP transmissions and background traffic with constant frame size and constant burst size.

Furthermore, the worst-case performance for TAS in terms of both an average and peak FDV, is equivalent to the SP and WRR performance. However, as the GP is increased, the peak and average FDV reduce consistently. Zero FDV is achieved for a GP that is equivalent to a full background frame serialisation delay (8 µs).

The step-like behaviour for the TAS results is an effect of the resizing of the BES in order to accommodate the GP (i.e. the TW remains constant). As the GP is increased, there is no change in FDV until the GP "eliminates" the frame from the burst that is closer (in time) to the GP boundary. This can be seen in Fig. 4.16 where both the burst and frame sizes are kept constant, by observing that the step changes for the peak FDV occur at GP values that when added to the corresponding FDVs are approximately equal to one background frame serialisation. The same relation is observed in Fig. 4.17 where the burst and frame size are random.

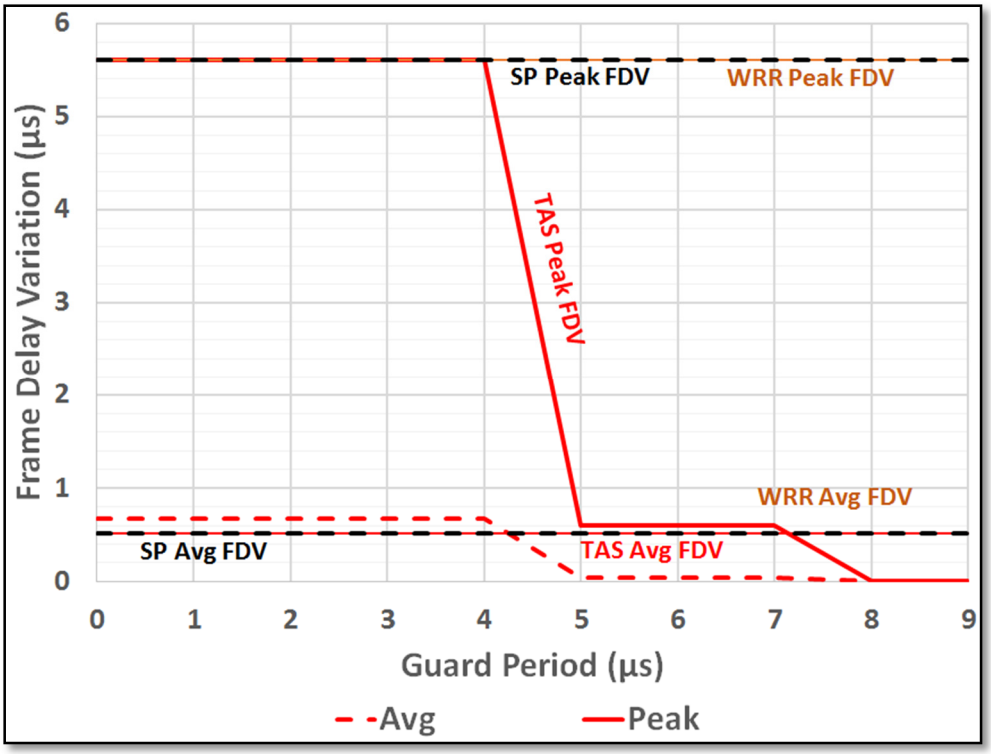

Figure.4.17. High priority traffic emulating PTP transmissions and background traffic with variable frame and burst size.

4.8 Buffering Protection

It is conceivable that in certain cases the time drifting factor D, will be exceeded. This can be a result of limited provisioning in order to reduce the end-to-end latency of the fronthaul. There are two solutions for this. The first is to drop the frame. This can work for PTP traffic but other HP streams such as MAC/PHY or Upper-PHY split primitives for example, should not be dropped. These primitives can consist of downlink control information and user-specific configurations for the LTE PHY layer in the RU. Dropping a frame then, may result in the user allocations for a whole LTE subframe (1 ms TTI) being lost. Another option is to enable buffering protection and thus buffer the frame(s) that are received outside the HP section and transmit them in the next TW. To allow the transmission of all traffic in the buffer and prevent any continuous buffering in the end stations queues or dropping the traffic in the switch port due to the limited TAS time section, the PS duration, $W_{s\_buf,}$ in the switch has to be modified to accommodate the buffered frames and will be given as:

$$\mathrm{W_{s\_buf}} = \sum_{\mathrm{n=1}}^{\mathrm{N-1}} \left(\frac{\mathrm{P_n}}{\mathrm{R}} + \mathrm{I_n}\right) + \mathrm{D_p} + \mathrm{D} + \max(\mathrm{D}, \mathrm{S_K}), \qquad (11)$$

The PS duration in the end stations, W_{e_buf}, has to be modified to accommodate the buffered frames and will be given as:

$$\mathrm{W_{e\_buf}} = \sum_{\mathrm{n=1}}^{\mathrm{N-1}} \left(\frac{\mathrm{P_n}}{\mathrm{R}} + \mathrm{I_n}\right) + \mathrm{D} + \max(\mathrm{D}, \mathrm{S_K}), \qquad (12)$$

where S_K is the serialization of up to K frames that have been buffered from the previous TW. Note that the change in the PS duration will depend on the size of the buffered frames. For very small frames, the variability factor D might be large enough to accommodate the transmission of the buffered frames (this is taken into account by the *max* term in (12)).

Fig. 4.18 shows the changes in the PS design with buffering protection in the switch (a) and end stations (b). The modified PS duration is applied only for the TWs for which buffering has occurred. The local scheduler will check its buffer and determine whether it needs to modify the PS boundaries for the next TW (and to communicate the modifications to the switch through the global scheduler).

Otherwise, if buffering has not occurred, the normal PS configuration is applied. Fig. 4.19 shows the result of not provisioning the PS duration to take into account buffered frames. For this result, the encountered time drifting exceeds *D* and is such that a single frame is buffered. If the PS duration is not modified according to (12), then for every subsequent TW a new frame (or more than one frame) will be buffered.

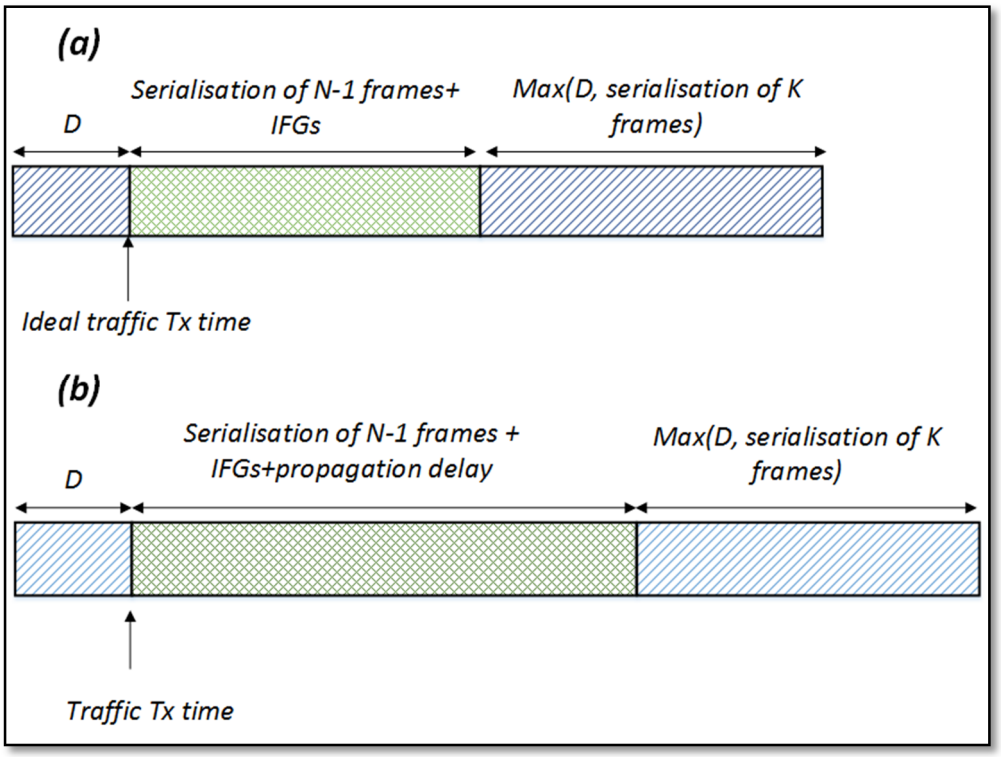

Figure.4.18. PS duration definition with buffering protection in a) the end station b) the bridge (switch).

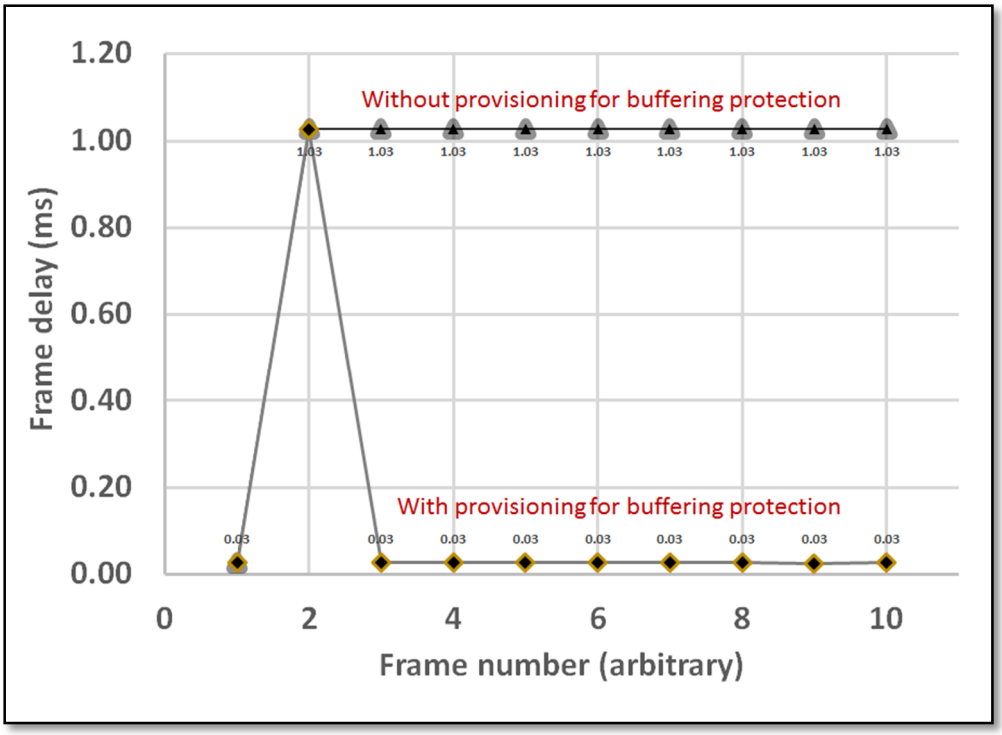

Figure.4.19. Comparison of frame delay results with buffering protection, with and without the modified PS design shown in Fig.4.18.

4.9 Global Scheduler with TAS

While increasing the time section as discussed in sub-section 4.8 allows the queued traffic to be transmitted without causing continuous buffering in the end stations or dropping the traffic in the switch, the utilization efficiency can be affected, since part of the time section window is not used in all the transmission time.

To improve the use of the available transmission time, a global scheduler (GS) can be deployed in the TAS application area (part of the network where TAS is applied) as shown in Fig. 4.20. The GS can manage the time section based on the buffering status and shrink or extend the time section window of the targeted traffic accordingly.

The GS communicates with local schedulers in the DU and RU and with the SDN.

Fig. 4.21 shows the number of 1000 byte frames that can be possibly sent (Y axis) if the GS is deployed in an Ethernet fronthaul network and the bandwidth is used efficiently. The event of queuing occurring in the switch port for different number of times (X axis)

during the transmission time (1s) (1s has been selected here as transmission time for simplicity as the data rate measured by bit per second). The maximum number of frames in the queue in each queuing event is four 1000 bytes frames.

The GS has more importance with scenarios with different functional split, control and synchronization and backhaul traffic sources where assigning the time section and sub-section to each stream (traffic type) and ensuring no section or sub-section overlap (inter-section interference) is occurring in any point during the transmission. Furthermore, the time allocation to each traffic stream should be managed very efficiently to accommodate the received and queued traffic.

The GS can also control the queuing based on obtained or received information from the SDN about the experienced delay and FDV by each traffic frame and compare it with its specifications and take the action accordingly. Or, SDN can perform the comparison with the specification and instruct the GS to take the action accordingly. SDN and GS can be one entity or separated entities as shown in Fig. 4.20 and the assigned functionality to each of them depends on the implementation approach.

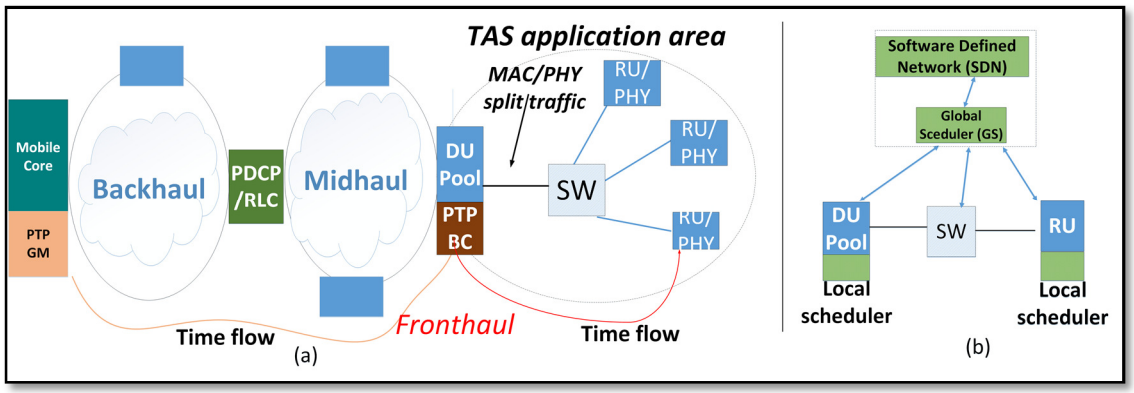

Figure.4.20. Scheduling design concept. SDN: Software-defined networking; GS:, Global Scheduler; SW: Ethernet switch; PTP: Precision-time protocol; BC: Boundary clock; GM: Grand master; PDCP: Packet data convergence protocol; RLC: Radio link control; MAC: Media-access control; PHY: Physical layer.

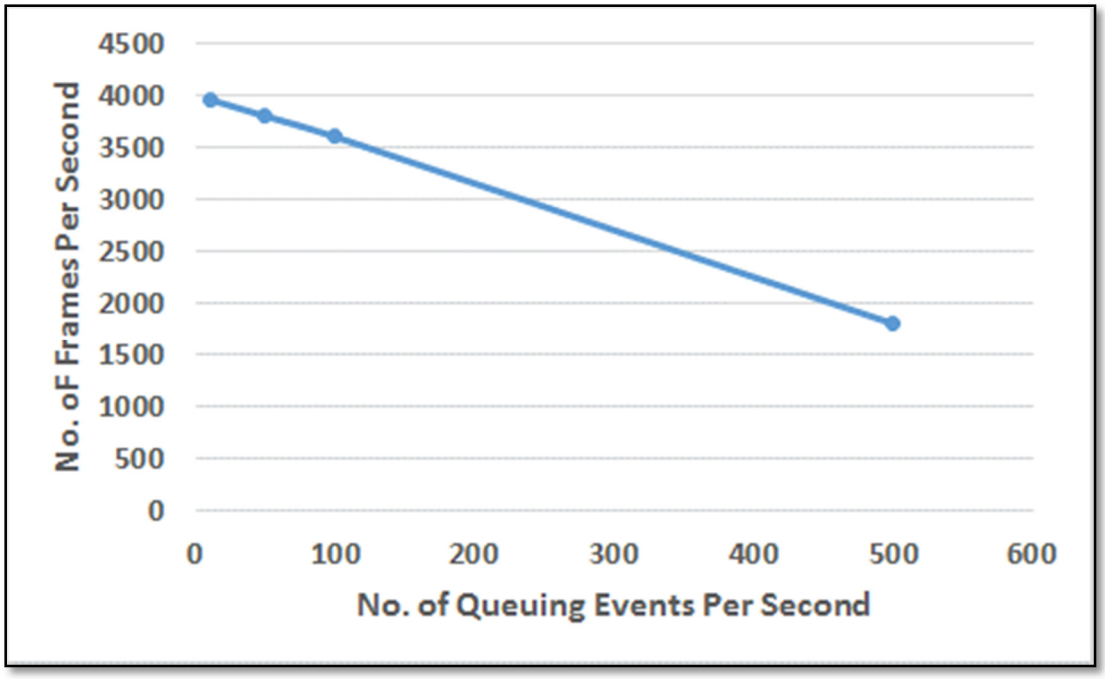

Figure.4.21. Number of transmitted frames in case of GS deployment in the network.

4.10 Conclusion

An Opnet model design and implementation for the TAS based on the IEEE 802.1Qbv standard was presented. The Bridge aware and network aware design of TAS in the Ethernet fronthaul network has been explained. The bridge aware TAS design considers the implementation of TAS in the Ethernet bridge ports. This design and implementation has the advantage of the simplicity since it just considers applying the TAS in the bridge ports and does not take under consideration any possible variation in the network timing due to the possible factors such as synchronization. On the other hand, this design has many limitations such as dropping the frames that are transmitted outside the allocated time window and the low immunity to the possible time variation in the network

The network aware TAS design considers implementing TAS in the end stations and Ethernet bridges ports. This design takes into account the time instability in the network and the frames that are received outside the allocated time window section. These frames will be queued in the end stations port and sent in the next time window.

While the network aware TAS has more implementation and deployment complexity, it is more feasible to be used as it has low frame loss and considers the timing variation and drifting in the network which is one of the main concerns in the Ethernet fronthaul.

A number of use cases with both design and implementation approaches were used to show the performance of the implemented TAS and compare it with the performance of the built in SP and WRR regimes in the Opnet/Riverbed simulation platform. The comparison focuses on the performance of a precision time protocol (PTP) stream, in terms of FDV, when contention with background traffic takes place in an Ethernet fronthaul.

The simulation results show that the TAS is capable of minimising the contention-induced frame-delay variation for the high-priority traffic, while provisioning a guard period based on the maximum serialisation delay of a low-priority frame can lead to a complete removal of FDV.

The results show as well that the average and peak FDV of TAS are upper-bounded to the average and peak FDV of SP. This worst-case occurs when the GP in TAS is set to zero, but as the GP is increased both average and peak FDV reduce steadily, until FDV is completely eliminated. The GP that is required to eliminate FDV has a strong dependence on the statistical variations of the traffic sources. The stronger the variation, the closer the required GP needs to be to a full background traffic frame serialization delay. The obtained peak FDV results are extrapolated to worst-case PTP time stamping errors and it is shown how these errors reduce as the GP in TAS is increased. Allowing the buffering with TAS is fundamentally important to prevent dropping any high priority traffic frames and to be sent in the next time window. The buffering protection is important to prevent any continuous buffering in the end stations due to the limited time section. Even though the queuing here prevents any frame loss in the network, some traffic with very tight delay and FDV requirements such as CPRI (section 2.2.1) might drop the frame due to a long queuing time.

The need for global scheduling to improve the use of the network bandwidth with the buffering protection and manage the overall time section and sub-section allocation has been discussed.

It should be noted (even it has not been shown) that TAS allows the traffic to be received with less delay than SP in case all traffic transmitted within the allocated time section and no queuing occur at the end station. In case of queuing at the end station with TAS, SP can have a better performance in terms of the traffic delay than TAS (considering the queuing delay is bigger than the effect of lack of pre-emption in the SP).

Proper operation for the high priority and time sensitive traffic such as PTP and functional split and the required scheduling to guarantee it will be of fundamental importance in the future C-RAN fronthaul that employs Ethernet transport.

5 Upper-PHY Split Modelling in Opnet/Riverbed with Different Traffic and Transport Use Cases in the Ethernet Fronthaul

5.1 Introduction

As mentioned in section 2.1.7, different functional splitting options have been introduced in the proposed C-RAN in order to overcome the limitations of the CPRI protocol bandwidth and achieve a reduction in the data rate, allow the use of the statistical multiplexing in the fronthaul and implement the different radio techniques such as, CoMP and massive MIMO [22]. UPS, equivalent to 3GPP option 7.2, is interesting as it is the closest split point to the antenna which can lead to statistical multiplexing gains [24]. It also readily allows for joint processing techniques in both downlink and uplink and offers centralized aggregation for the transmission of 4G and 5G New Radio interface (NR) signals. In addition, a little investigation has been done around this split point and on the effect of the time sensitive networking on its performance in the Ethernet fronthaul network [22]. According to Table. II in section 2.2.1, the proposed delay and FDV requirements for the UPS are very tight. With such requirements, the effect of the contention between UPS traffic and other traffic types with different transmission patterns, rates and regularities in the Ethernet fronthaul bridges on the delay and FDV of the UPS traffic is important to be investigated and analysed.

In [44] and [45], a software-emulated Option-6 split was presented, focusing on the latency performance [45], and the contribution of different transport channels in the Ethernet data rate [44]. In [16], a Mac/PHY split was evaluated specifically for CoMP and at 4G data rates. In [41], a PDCP-RLC split has been implemented in Open Air Interface (OAI) and the increase in the throughput with different MCS has been shown.

In [81], a specific Ethernet frame size has been proposed to be used with the UPS (around 4300 bytes) considering the delay in the fronthaul network. The

implementation in this chapter uses frame sizes based on the received data from the upper layers. Using jumbo frames can cause significant FDV especially with a high data rate as was shown in subsection 3.4.2. In this work, the Ethernet frame size depends on the received data from the upper layer and the jumbo frames are not used (maximum frame size is 1518 bytes).

In this chapter, an implementation of the UPS in Opnet/Riverbed is presented. This implementation considers the Radio over Ethernet standard (RoE) [32](explained in detail in section 2.1.6). Furthermore, a TAS model is used to investigate how such a scheduling mechanism can efficiently remove most of (or even fully eliminate) any contention-induced FDV. The performance and limitations of TAS in the Ethernet fronthaul with different contention cases are investigated; taking into account different traffic types and their transmission patterns (bursty or random) and the use of buffering to eliminate FDV. Different UPS traffic allocations in TAS are investigated and using buffering in the fronthaul to absorb any residual FDV is thoroughly discussed.

Implementing UPS in the hardware would require long term development in an open source software defined eNodeB platform which allows access to the LTE stack and modify the targeted LTE layers. The platform should introduce low processing delay as well. In simulation platforms, different traffic types can be modelled alongside UPS traffic and different use cases with different network sizes and scales can be tested. This is costly and very challenging in the hardware platforms.

5.2 Upper-PHY Split Modelling in Riverbed

As has been stated in section 2.5, Opnet/Riverbed is an event-based simulation platform that provides model suites for different network technologies, with LTE being one. The eNodeB model, a node model within the LTE suite, is made up by three main modules associated with LTE functionality. The distribution of the standard LTE functionality in Riverbed's eNodeB model and the implementation of the UPS are shown in Fig. 5.1.

The PHY module performs Physical layer functionality such as power control. The LTE_AS module performs the functionality of the LTE Medium Access Protocol (MAC), Radio Link Control (RLC) and some Packet Data Convergence Packet (PDCP) functions. The

remaining PDCP functions and handover are in the LTE_S1 module. The LTE_S1 receives the traffic from the EPC through the backhaul.

In the implementation of the UPS, all the functionalities after the layer and antenna processing in the LTE Physical layer are moved to a newly implemented DU, while the remaining LTE functionalities are handled by the CU. Physical channel data are first encapsulated in a newly implemented Radio over Ethernet (RoE) sub-layer. The headers are based on the RoE standard (section 2.1.6 for more explanation) and include headers for sequence numbers, packet type etc. The resulting RoE frames are encapsulated in standard Ethernet frames and sent over the Ethernet fronthaul. It should be noted that the physical channel data are copied from the original stream and sent to the DU. However, as the DU is not a full implementation, the UEs remain connected to the original eNodeB for the duration of the simulation. This process guarantees generation of new traffic while allowing for performance monitoring of the copied traffic that flows through the newly developed fronthaul model. The main modules in this implementation, as shown in Fig. 5.1 and Fig. 5.2 are the LTE_AS and UPS Module. This implementation considers the downlink and the transmitted traffic from the CU follows the timing of the air interface. The LTE_AS module is modified in order to copy the physical channel data and transmit it to the UPS Module. While one or more Physical Downlink Shared Channel (PDSCH) messages are sent every LTE subframe based on the data rate, three different control messages are sent: Primary and Secondary Synchronization Signals (PSS & SSS) Master Information Block (MIB) and Physical Downlink Control Channel (PDCCH).

5.2.1 LTE-AS Module

This module is modified in order to copy the physical channel data and transmit it to the UPS Module. As this split point is before the resource mapper, one or more (depending on number of connected users) PDSCH messages are sent every LTE subframe (1 ms duration). In addition a number of physical control channels are sent. These include, PSS & SSS which are sent approximately every 0.5 ms (a slot duration), MIB which is sent once every 10 ms (a radio frame duration) and PDCCH. The latter is sent only in subframes that include System Information (SI) and/or PDSCH messages. Additional control information, which has negligible effect on the overall data rate (e.g. format

indicator channel), is either aggregated within the aforementioned control messages or sent directly to the UE (through direct memory exchanges, i.e. not modelled as a message exchange).

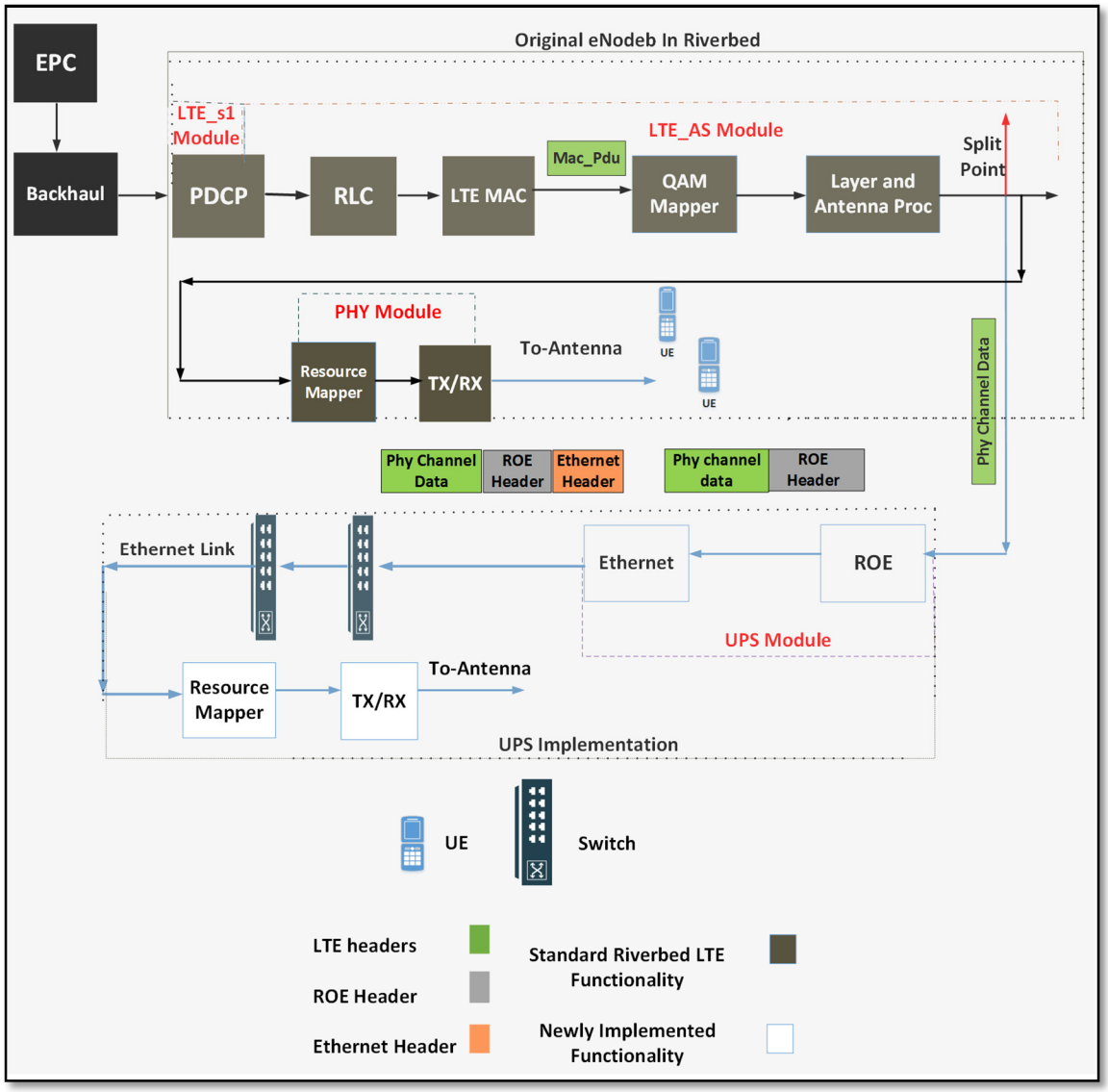

Figure.5.1. Implementation of the UPS in the Ethernet fronthaul network (Block diagram).

5.2.2 UPS Module

This module handles two main functions for the evolved Ethernet fronthaul: The first is encapsulating the physical channel data into the implemented RoE frame, and setting some of the RoE header fields such as the packet type and flow identification (ID). The pseudocode of this functionality is shown in Fig. 5.3 and the RoE frame structure in Opnet/Riverbed is shown in Fig. 5.4. In Fig. 5.3, the RoE frame created first and then

some of the fields are set before being encapsulated in the Ethernet frame and sent over Ethernet fronthaul network. The only used fields in the RoE frame are the packet type and flow_id while the rest of the fields are just reserved.

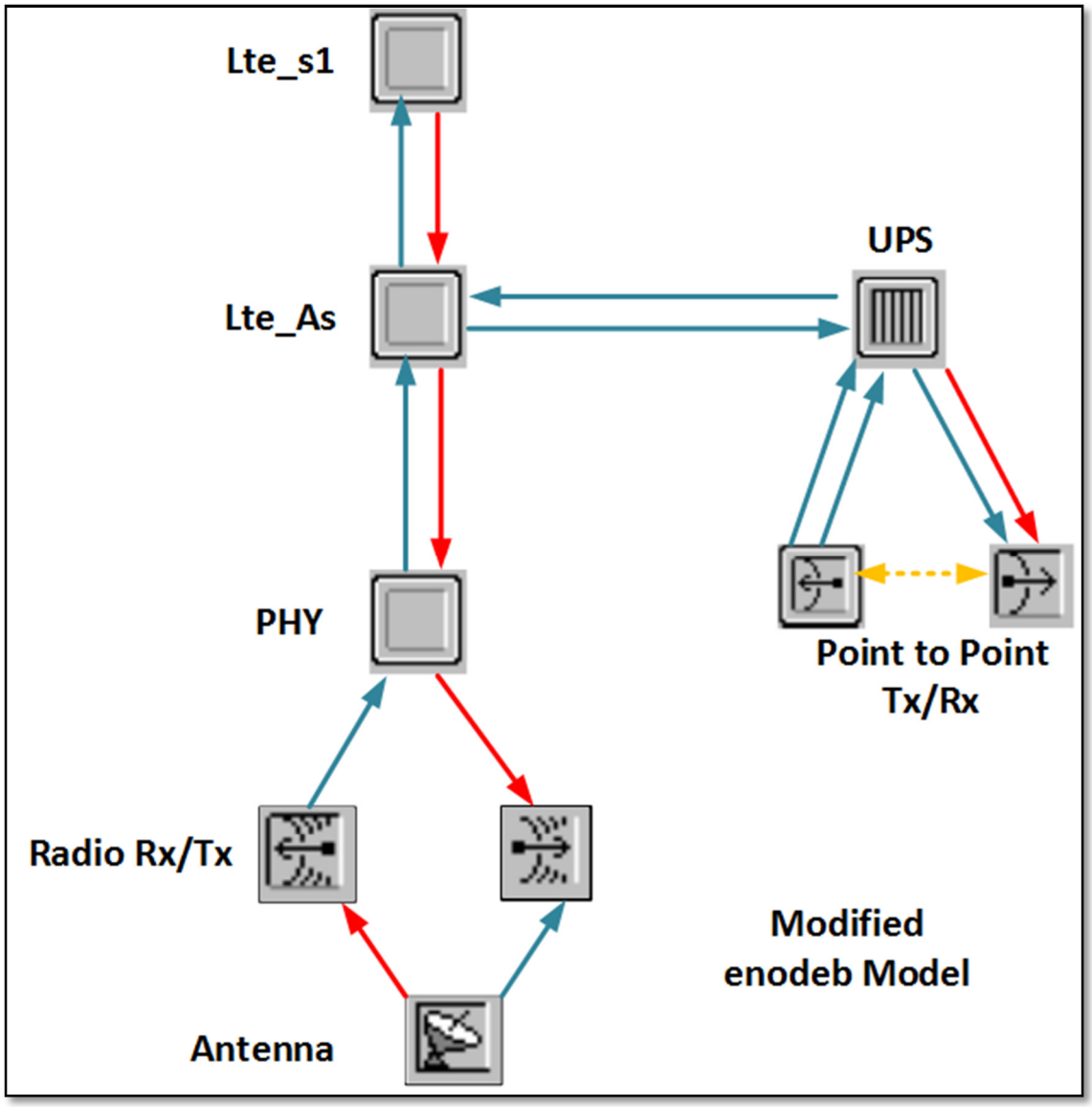

Figure.5.2. Implementation of the UPS in Opnet/Riverbed.

The second function is the transport over standard Ethernet links as used in the modelled fronthaul. A modification was necessary to the existing Ethernet module functions to allow transmission of the encapsulated UPS traffic in Ethernet frames. In the original Riverbed Modeler module implementation, higher layer modules set fields of the Ethernet header. In this implementation, with a purely layer-2 fronthaul, the Ethernet frame parameters are set in the modified Ethernet module and the Ethernet

frames sent over the Ethernet fronthaul. The Ethernet frame structure in Opnet/Riverbed is shown in Fig. 5.5. The fields include the source and destination Media Access Control (MAC) addresses, Ethernet frame Length & Cyclic Redundancy check (CRC). The Tag field is reserved for the Virtual Local Area Network (VLAN) associated information.

```
ROE_ptr = op_pk_create_fmt ("REO"); //creating ROE frame.
op_pk_nfd_set (ROE_ptr,"Ordering-Info", FrameID);// set the Frem_ID in the ordering info field.
op_pk_nfd_set (ROE_ptr, "Frame_type", pk_type); // set the Frame_type in the pkt_type field.
op_pk_nfd_set (eth_pktr, "Data", ROE_ptr); // encapsulate the frame ROE frame in Ethernet frame.
op_pk_send (eth_ptr, ethernet_state_info_ptr->strm_to_lower_layer); //sending the Ethernet frame.
```

Figure.5.3. UPS Module pseudocode.

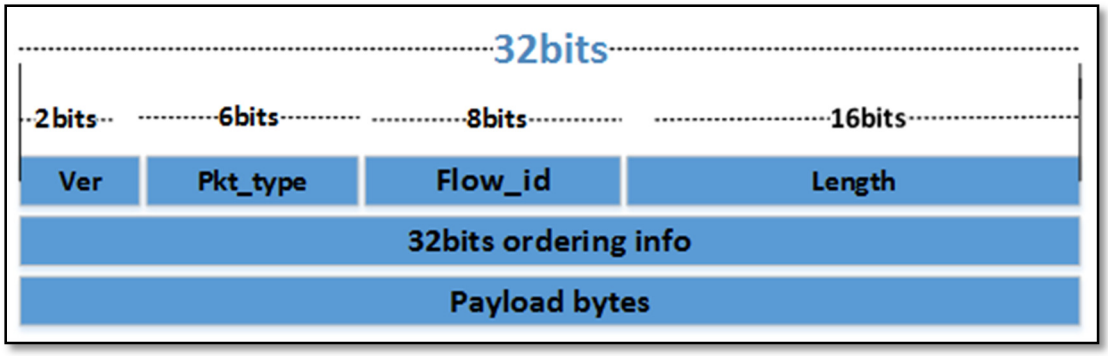

Figure.5.4. ROE Frame Structure in Opnet/Riverbed.

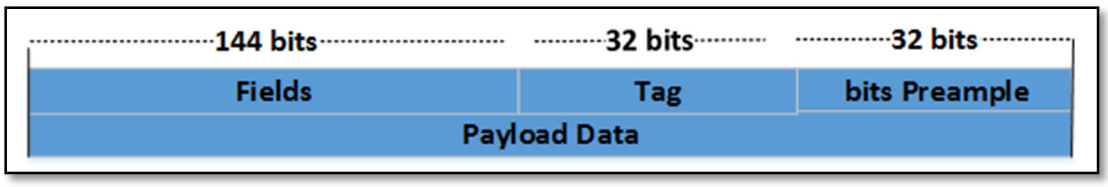

Figure.5.5. Ethernet Frame Structure in Opnet/Riverbed.

5.2.3 Statistics Implementation in Opnet/Riverbed

In order to measure Key Performance Indicator (KPI) values of the Ethernet fronthaul network, new statistics have been defined and built into the CU and DU models. These statistics allow extraction of the UPS traffic frame size and frame ID number. The ID number statistic allows the simulator to keep track of the transmitted frames from the

CU and identify any lost or out of order frames at the DU. In addition, associated time stamps are used to calculate the delay and FDV of the transmitted UPS frames. Fig. 5.6 shows the pseudocode of the implemented statistics in Opnet/Riverbed. The statistics are registered first and then the size or ID number of every transmitted Ethernet frame is written in the memory to be extracted and used later.

```
ethernet_state_info_ptr->frame_size    = op_stat_reg ("Ethernet.framesize (bits)",
OPC_STAT_INDEX_NONE, OPC_STAT_LOCAL); // Registering the statistic.

ethernet_state_info_ptr->frame_id    = op_stat_reg ("Ethernet.frameid (no)",
OPC_STAT_INDEX_NONE, OPC_STAT_LOCAL); // Registering the statistic.

op_stat_write (ethernet_state_info_ptr->frame_size, Frame-size); // writing the statistic

op_stat_write (ethernet_state_info_ptr-> frame_id    , frame-id); // writing the statistic
```

Figure.5.6. Statistics Implementation in Opnet.

5.3 Fronthaul Scenarios

In this section, a number of scenarios are implemented to show the effect of different combinations of traffic types on the performance of the UPS and CPRI-type traffic. An overview of the simulation set-up including the different nodes (traffic transmitters and receivers) that will be used in the following scenarios is shown in Fig. 5.7. Precisely which nodes are used in each scenario will be specified in each scenario.

LTE traffic is generated at the LTE application server, which sends traffic over the backhaul to the CU pool. The CU generates the UPS traffic after encapsulating the received data with the RoE and Ethernet headers (as described in Fig. 5.1) and transmits the resulting Ethernet frames to the DU through the Ethernet network. Twenty UEs are attached to the eNodeB (unless otherwise specified) with 0.84 Mbps data rate for each UE. The MCS index in the eNodeB is set to 20. CPRI-type traffic is generated in bursts, with the burst size equivalent to the amount of traffic that is transmitted in one subframe (1 ms), based on bandwidth. Fig. 5.8 shows the implementation flow chart of the CPRI-type traffic in Opnet/Riverbed. The burst is sent at the start of every 1ms, with the number of frames calculated based on the targeted data rate per second. In the

following scenarios, the CPRI –type traffic data rate is 200 Mbps (which corresponds to 20% of the link capacity) with an average frame size of 1000 bytes. There are up to five background traffic servers in the following scenarios (how many are used will be specified according to scenario). The background traffic from each is configured to follow a uniform distribution, set to vary between +/- 50% of the average data rate, and with a frame size of 1000 bytes. The Ethernet network comprises of two GbE (Gigabit-Ethernet) switches connected by a trunk, where contention takes place. Gigabit Ethernet has been used here as this is the maximum data rate that modelled in the simulation environment. Traffic sources flows are logically separated with Virtual-Local Area Network Identifiers (VLAN IDs). Each network segment has a link length of 200m and a link rate of 1 Gbps.

The queuing delay and delay variation at the end station and switch are the focus of this work as other delays are not variable, or can have small delay variation (ex. fabric delay could very base on the load).

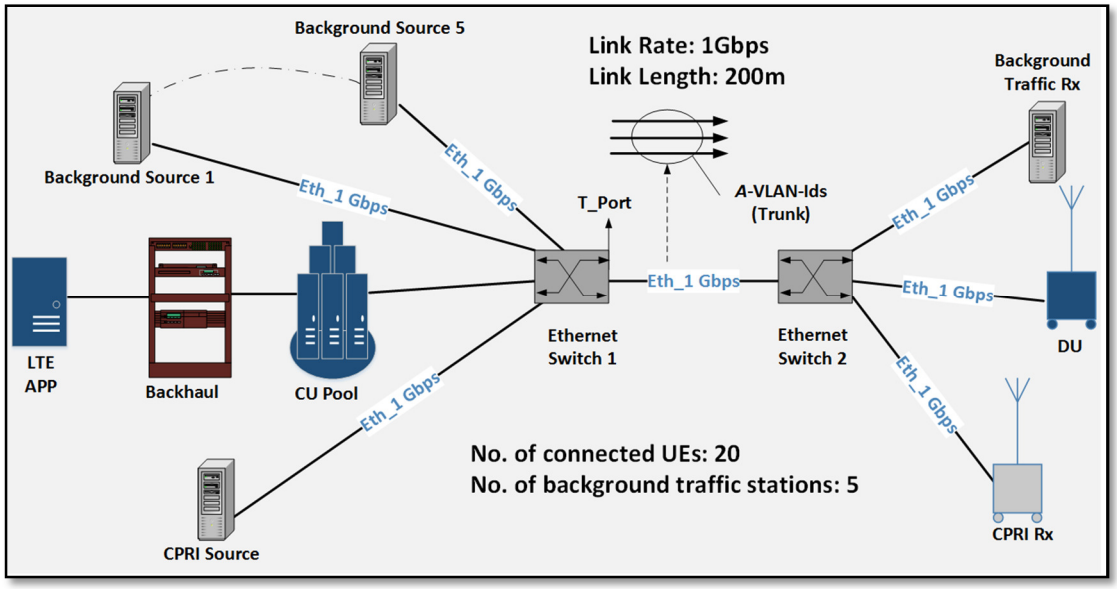

Figure.5.7. the simulation set-up of the Ethernet fronthaul.

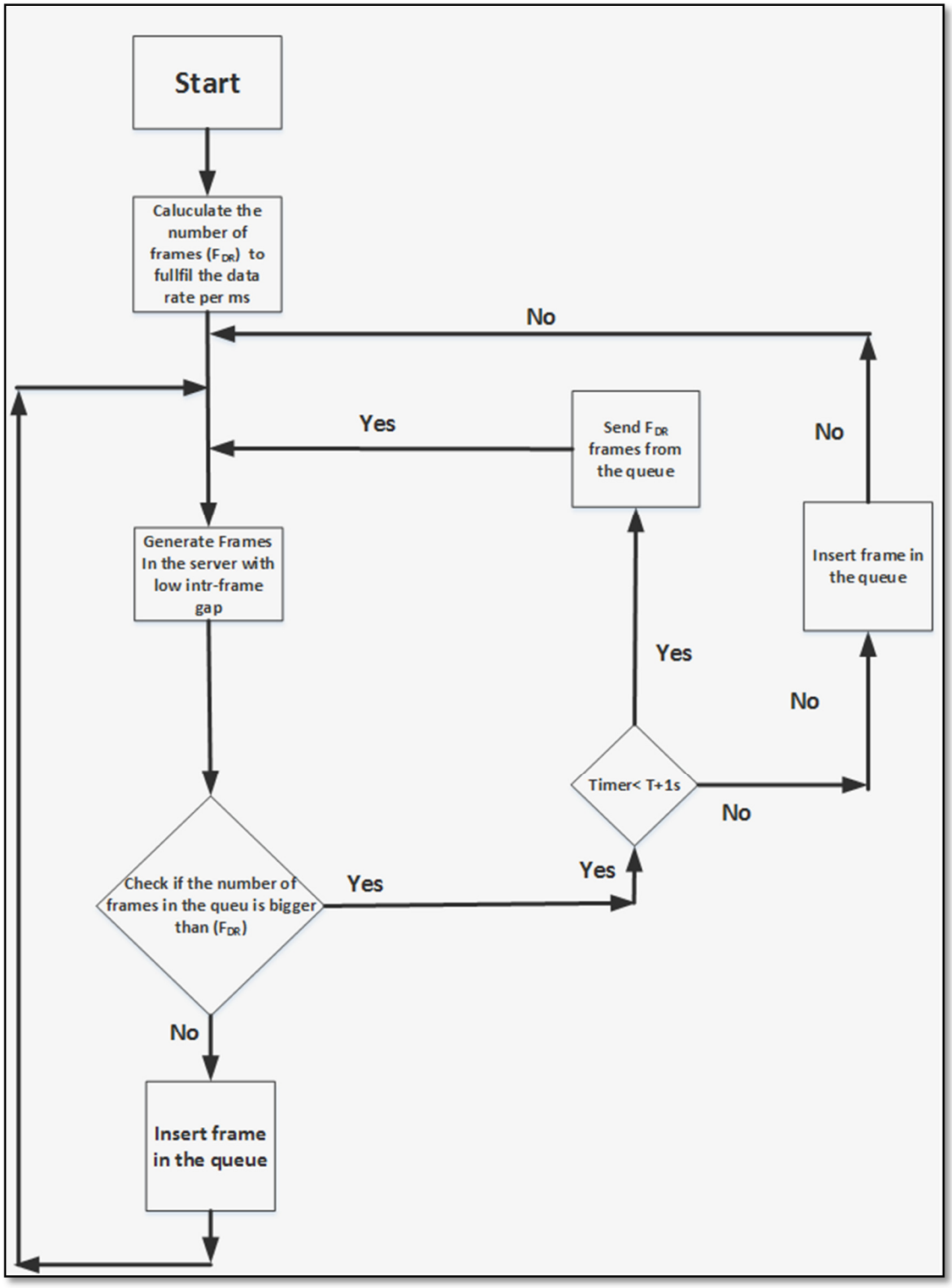

Figure.5.8. Cpri-type traffic implementation flow chart in Opnet.

5.3.1 Initial Results

This scenario targets showing frame delay and FDV of the UPS and CPRI-type traffic in a baseline case, when there is no other traffic in the Ethernet fronthaul network. For this scenario, the CPRI and UPS traffic are not transmitted at the same time while the background traffic nodes are disabled.

For the UPS baseline, two UEs are connected with a total application data rate of 1.68 Mbps. The resulting data rate over the fronthaul for UPS is 2.08 Mbps. Due to the overheads of the LTE, Ethernet and RoE standards, the fronthaul traffic is 23% more than the backhaul traffic. The size of the Transport Block (TB) which depends on the LTE bandwidth and the MCS can affect the percentage of the control overheads to the data.

In [44], an experimental implementation of a MAC/PHY split showed higher overheads of approximately 35%, attributed to a fixed TB size. Here the TB size can be more than twice as large, leading to a lower overhead for the transmitted traffic. The calculated overheads based on the LTE [34]. In [44], an experimental implementation of a MAC/PHY split showed higher overheads of approximately 35%, attributed to a fixed Transport Block (TB) size. Here the TB size can be more than twice as large, leading to a lower overhead for the transmitted traffic. The calculated overheads based on the LTE [82], RoE [32]and Ethernet [75] standards is close to what has been measured with UPS (approx... 20% overheads).

The average frame delay (D_a) in the baseline scenario can be given by:

$$D_a = 2(D_s + D_P + D_F), \qquad (13)$$

where D_S is the serialization delay, D_P is the propagation delay and D_F is the processing (fabric) delay in the switch. The propagation delay in each section of the network is constant at 1 µs (200 m link length). Based on the average frame size, the serialization delay is approximately 2 µs. The fabric delay in both Ethernet Switches is 5 µs.

Fig. 5.9 shows the delay and FDV of the UPS and CPRI-type traffic. Note that the results of the UPS and CPRI-type traffic are normalized to the serialization delay of 1000 bytes over a 1 Gbps link. The baseline FDV of the UPS traffic in this scenario is 1. 6 µs and the delay is 11.04 µs. The FDV value can be explained by the fact that the transmitted

Ethernet frames from the CU have different sizes which can lead to this amount of FDV. The minimum Ethernet frame size that captured by the Ethernet frame size statistic is 74 bytes while the maximum Ethernet frame size is 1470 bytes. The average frame size that transmitted from the CU is 255 Bytes. The average UPS baseline delay here is associated as well with the average frame size of the transmitted UPS frame.

Similarly, the baseline delay and FDV for CPRI-type traffic has been measured. The CPRI delay is 23.04 µs while the FDV is zero as the frame size is constant (1000 bytes).

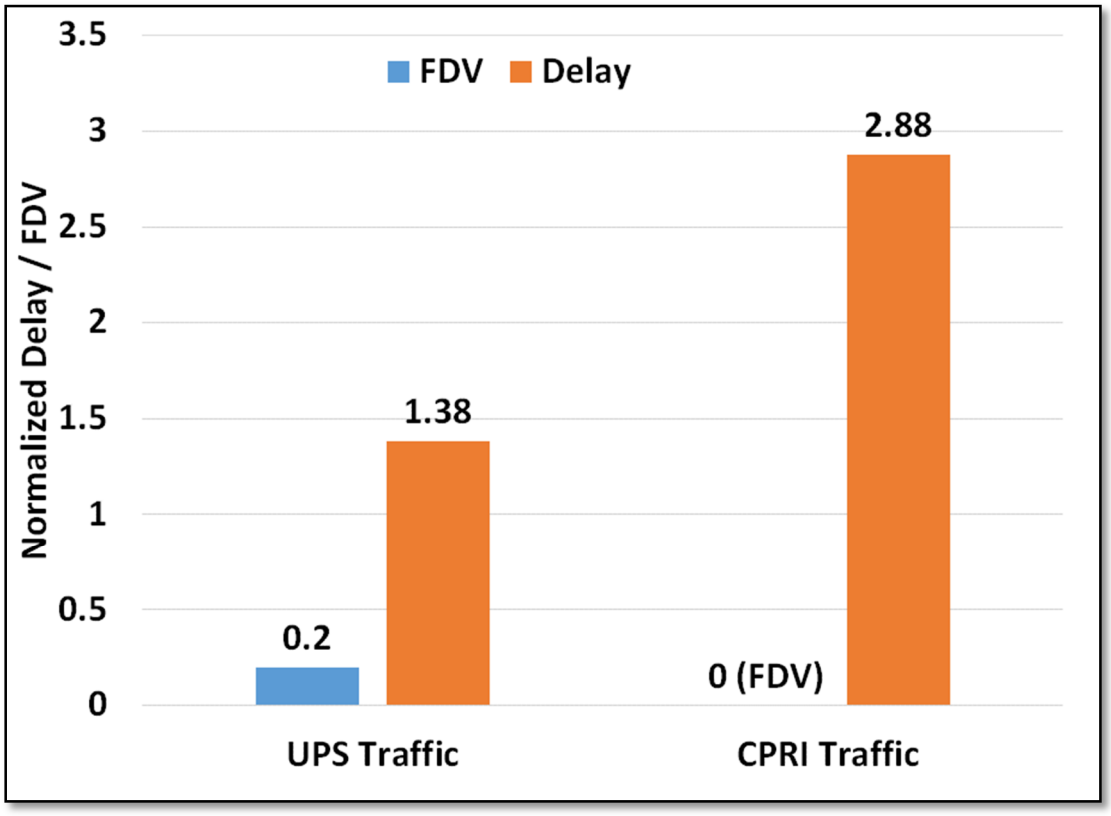

Figure.5.9. Baseline delay and FDV of the UPS and CPRI traffic.

5.3.2 Upper-PHY Split Traffic with Statistically Distributed Background Traffic

This scenario is used to show the effect on the frame delay and FDV of the UPS traffic when there is contention with statistically distributed background traffic. In this scenario, five background traffic servers are enabled and are configured with average background traffic rates ranging between 100 Mbps and 600 Mbps. traffic. The results in Fig. 5.10 show an increase in the delay and FDV of the UPS traffic due to contention in the Ethernet switch`s trunk port (shown as T_port in Fig. 5.7).

The maximum increase in UPS average delay is equivalent to the serialization of less than two frames of the background traffic while the maximum extra delay is equivalent to the serialization of approximately four background traffic frames. The increase in FDV is less than the serialization of one background traffic on average, while the maximum increase in FDV due to contention is equivalent to the serialization of approximately four frames. The results can be explained by considering that the extra delay and FDV that can be encountered by the UPS frames in the worst contention scenario is the serialization of five background traffic frames from each of the five background traffic stations.

The average delay of the UPS traffic is significantly lower than this maximum since its data rate is low in comparison to the background traffic. In addition, the switch scheduler attempts to balance the number of transmitted frames from each input queue based on the total number of transmitted bytes per time unit (i.e. byte-based scheduling).

As a special case, Fig. 5.10 shows the FDV and delay results for the UPS with bursty background traffic. Each of the five servers generates a burst by buffering (in each server) the generated frames for 700 µs. The results show that bursty traffic does not cause more delay and FDV for the UPS traffic than that measured with non-bursty traffic.

This is a result of the aforementioned byte-based scheduling of the switch. If the switch scheduler did not balance the output data rate from the input queues based on the number of bytes transmitted, the average delay would be significantly higher since a UPS frame would have to wait for a full burst to be serialized out of the trunk port.

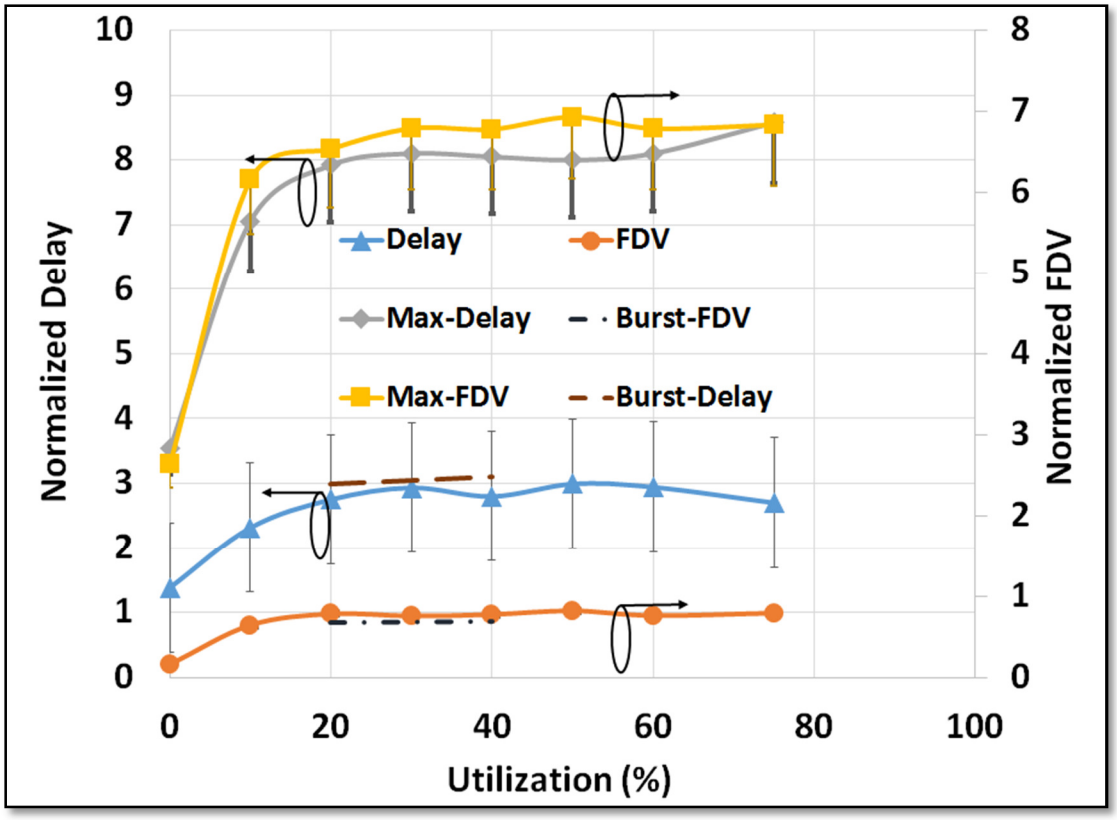

Figure.5.10. UPS traffic delay and FDV for scenario described in 5.3.2.

5.3.3 Mixed Ethernet Fronthaul Traffic Scenario

This scenario is used to show the effects that background traffic, CPRI-type traffic and UPS traffic have on each other due to contention in the Ethernet fronthaul. Table. IV shows the data rate and the frame size of each traffic type in this scenario. These data rates are selected to represent a clear contention case with average utilization of 40%, similarly to what was shown previously in Fig. 5.10. The results in Fig. 5.11 show the effect of contention on the delay and FDV of the UPS and CPRI traffic. The delay compared to the baseline case has increased by 8% on average for CPRI and by approximately 98% for the UPS, due to contention in the trunk port. The FDV is increased ten times for CPRI traffic while it has increased four times for the UPS. The increase in delay of the UPS is equivalent to the serialization of less than two background or CPRI traffic frames while the increase in CPRI traffic delay is equivalent to the serialization of less than one background or CPRI frame.

The increase in the delay and FDV of the UPS traffic is higher than the increase with CPRI-type traffic since the UPS traffic contends with high-rate CPRI and background traffic. In

addition, the CPRI and background traffic frame size is four times that of the UPS traffic (on average). The UPS delay and FDV are less than the serialization delay of six frames (there are five background traffic servers and one CPRI server) which is the maximum possible delay and FDV in the worst case contention. The increase in the delay is significant for both traffic types but it is not significant enough to violate CPRI delay specifications and requirements. The increase in FDV is high enough to be considered a problem for the transmission of both traffic types since it violates FDV specifications.

Table. IV

Background Traffic Settings for Scenario 5.3.3

Traffic Type	Average Data Rate (Mbps)	Average Frame Size (Bytes)
UPS	16	276
Background	Dist (100,300)	1000
CPRI	200	1000

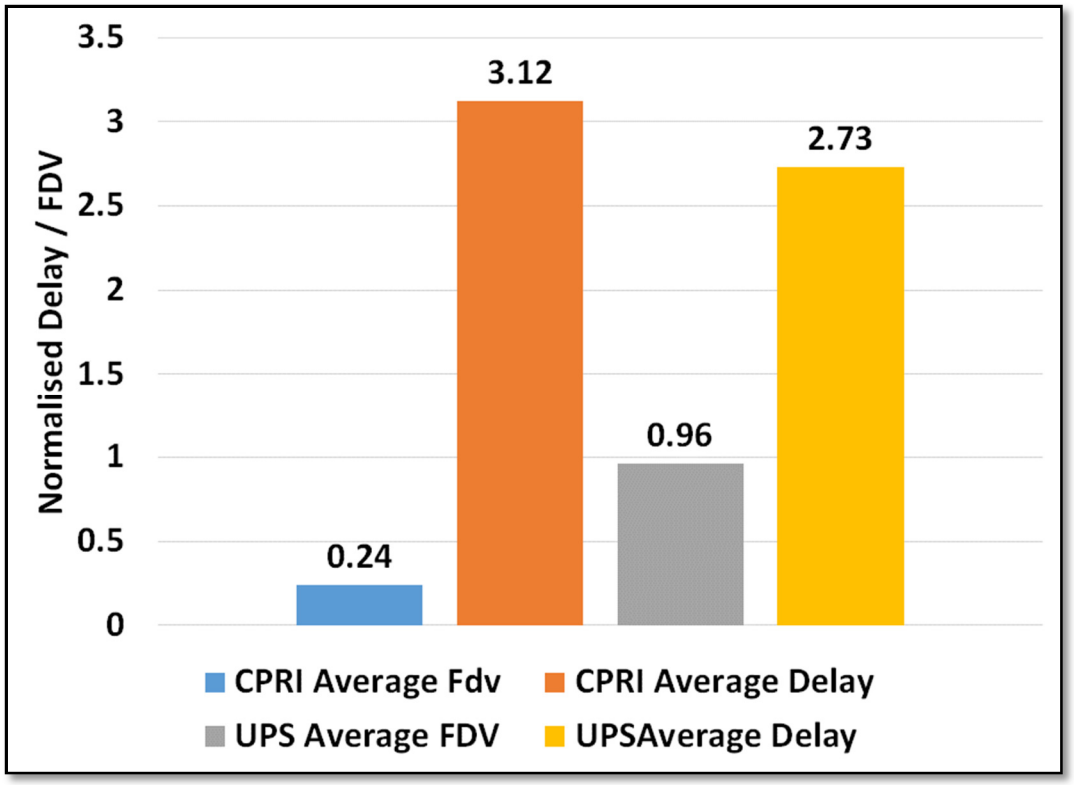

Figure.5.11. UPS & CPRI traffic delay and FDV with the existence of background traffic for scenario described in 5.3.3.

5.4 Time Aware Shaper in the Fronthaul Network

As explained in sub-section 2.4.1, the TAS divides the transmission time into sequential transmission windows (TWs) and each TW into sections and sub-sections. The Protected Section (PS) is reserved for high priority streams while the Best Effort Section (BES) is used for lower priority streams. A Guard Period (GP) is inserted to prevent lower priority, best effort frames, from overrunning into the PS. Traffic generated outside its allocated section must be queued and transmitted in the next TW.

The implementation of TAS in Ethernet switch and transmission servers models is described in section 4.3, the points in the network where TAS takes effect are shown in Fig. 5.12.

The focus here is on the delay and FDV of the UPS and CPRI-type traffic. Fig. 5.13 shows the different TAS section allocations for the traffic types in the following scenarios. The TW of the TAS for all scenarios is made equal to the LTE subframe duration (1ms).

The results show that TAS removes the FDV of the UPS traffic. The delay in average with the different background traffic rates (the same used rates in scenario B) is 11.3 µs while the FDV is 1.82 µs.

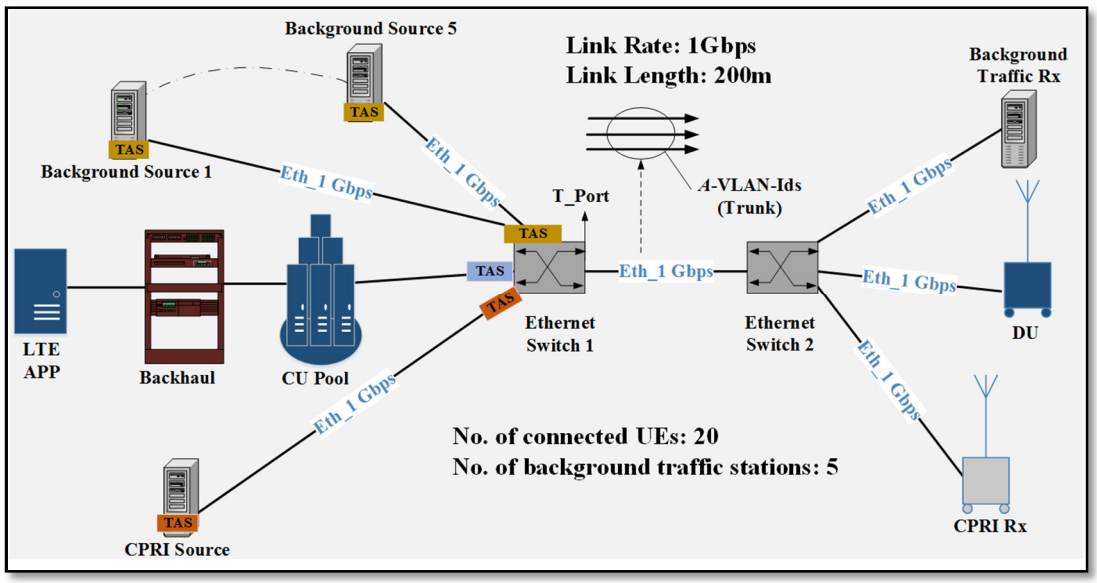

Figure.5.12. Simulation set-up of the Ethernet fronthaul with TAS.

5.4.1 UPS and Uniformly Distributed Background Traffic

As shown in Fig. 5.13.A, the UPS traffic is allocated 30% of the TW, GP is allocated 8% and the background traffic is allocated the rest of the TW (62%). This allows the UPS traffic to be transmitted within the window (the traffic is still transmitted according to the air interface timing but the window is aligned to accommodate the UPS traffic). In this and the following scenarios, GP is allocated 8% in order to prevent traffic in the best effort section from overrunning into the protected section and to accommodate low rate and high priority traffic such as PTP and control primitives for transmission without any contention (such traffic is considered, but not modelled here). The results in Fig. 5.14 show that TAS removes most of the FDV of the UPS traffic for a percentage of the frames (the frames that do get transmitted through the 300 µs section). There is an overrun of frames with respect to the section time allocation and these frames are queued for transmission to the next TW. This issue will be discussed in more detail in the following sub-sections. For the frames that are transmitted through the allocated time section, the delay on average with the different background traffic rates (same rates as in section 5.3.2) is 11.3 µs while the FDV is 1.82 µs.

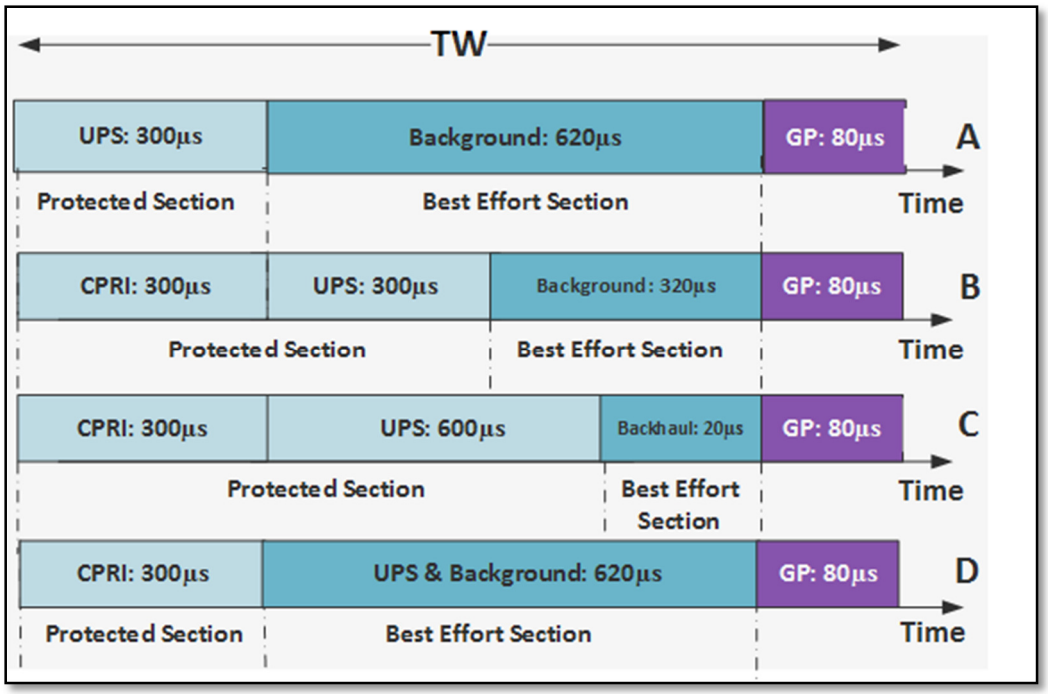

Figure.5.13. TAS section allocations in: (A) UPS and background traffic scenario; (B) Mixed traffic scenario (case 1); (C) Mixed traffic scenario (case 2); (D) Mixed traffic with different time sections allocation scenario.

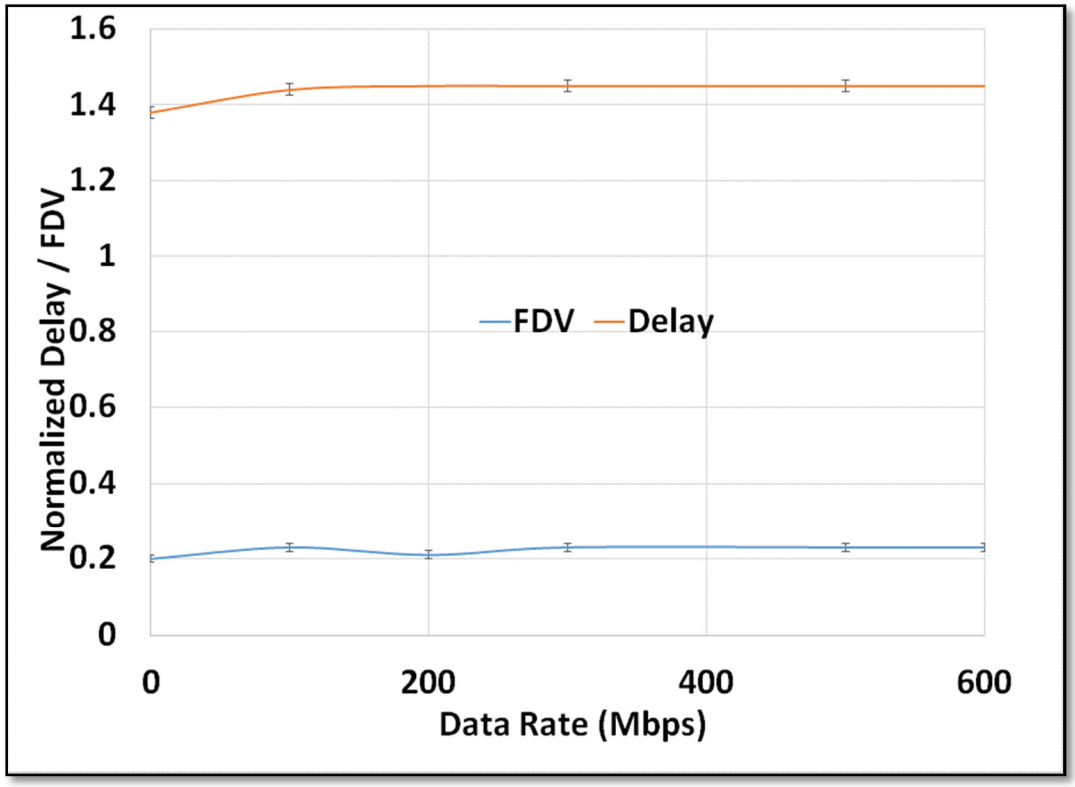

Figure.5.14. Frame delay & FDV of UPS traffic for scenario described in 5.4.1.

5.4.2 Mixed Traffic Scenario

In this scenario, UPS, CPRI-type and background traffic are transmitted over the Ethernet fronthaul network. Two section allocation cases are presented.

These values are similar to those obtained in Section 5.3.1 (small differences are due to using different seed values and numbers of UEs for these simulation runs) and will be used as the baseline case for comparison in the following sub-sections.

The first case is shown in Fig. 5.13.B where UPS and CPRI-type traffic are each allocated 30% of the TW, the GP is allocated 8% and background traffic allocated the remaining part of the TW (32%). CPRI Traffic is allocated this window size in order accommodate the burst of thirty frames that are required to transmit CPRI traffic for a bandwidth of 5 MHz within a subframe duration. UPS is allocated 30% of the TW considering the characteristic of the UPS traffic (transmitted based on the air interface timings).

The second case is presented in Fig. 5.13.C where the UPS traffic is allocated 60% of the transmission time, CPRI traffic is allocated 30%, background traffic is allocated 2% of the transmission time and the GP allocated the remaining 8%. UPS traffic is allocated a larger

time section to allow more UPS traffic to be transmitted within its allocated window and reduce the percentage of frames queued to the next TW.

The results of the delay and FDV of the UPS and CPRI traffic with TAS section allocations according to Fig. 5.13.B and Fig. 5.13.C are shown in Fig. 5.15. The results show that TAS reduces the FDV for UPS and CPRI traffic to the baseline level in both cases (although it is not shown in Fig. 5.15). While the UPS FDV problem is solved, the average delay of the UPS traffic is significantly increased with the smaller allocated time section (Case 1) since a number of frames are generated outside this section and are therefore queued for transmission in the next TW.

The results show that the average delay of the UPS traffic is ten times higher than the baseline delay. CPRI traffic bursts are transmitted within the allocated section and no frame is delayed to the next TW. With the allocation in Fig. 5.13.C, the UPS traffic is allocated a time window corresponding to a much larger capacity than that required for its data rate, in order to allow nearly all UPS traffic frames to be transmitted within the section.

The results show that the delay and FDV of UPS traffic are close to the baseline values. While this solution achieves FDV and delay close to the baseline values (for the percentage of frames that transmitted through the allocated time window) for the UPS traffic, using such a large window section is not an efficient use of available network capacity (only 3.3% of the UPS window is utilised in this case). The presented delay and FDV of the UPS traffic in Fig. 5.15 consider the queued frames. The delay and FDV of the UPS traffic without considering the queued frames are equivalent to the baseline values.

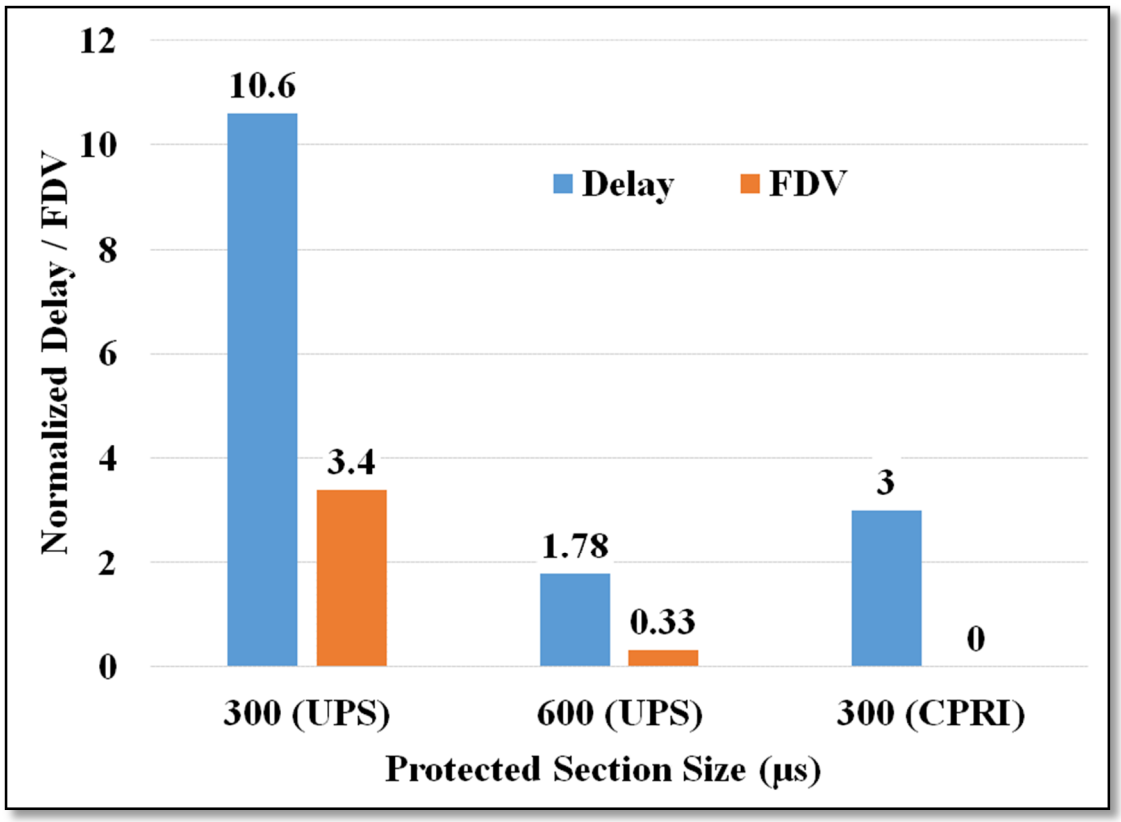

Figure.5.15. Frame delay & FDV of UPS traffic for scenario B with TAS.

5.4.3 Mixed Traffic with Different Time Section Allocation Scenario

To avoid allocating a larger time section for the UPS traffic and to solve the delay problem, in this scenario, the UPS traffic is moved to the BES, albeit over a longer section window, as shown in Fig. 5.13.D. Fig. 5.16 shows the delay and FDV with different background traffic utilization. The results show that contention results in an FDV for the UPS traffic that violates the specification, for all background traffic rates, while the delay remains within an acceptable level. The bursty traffic parameters used here are similar to the ones used for the bursty results in Fig. 5.10, to allow a direct comparison. The burst here is created as a result of the TAS buffering (which allows transmission only during the allocated time section). As it was also shown in Fig. 5.10, the effect of bursty background traffic on the UPS traffic is similar to that of non-bursty traffic.

The maximum increase in the delay with 64% utilization (note that now, this corresponds to the utilization of the TW and not of the link rate as was the case for the results of Fig. 5.10) is less than the serialization of two background traffic frames while the increase in the average FDV is less than the serialization of one background traffic frame. In order

to achieve FDV less than the proposed requirements of Table. I or even eliminate the FDV, a buffering mechanism can be applied at the end node (DU). This requires such a node to playout the buffered frames according to the air interface timings (since the UPS traffic is sent to the DU based on the air interface timings) and these timings need to be maintained. To this end, the buffer needs to be designed so that contention-induced FDV is "absorbed". In addition, such an implementation would require accurate time information (for example, provided through PTP) in addition to future buffer play-out timestamps (such as those included in the RoE specification).

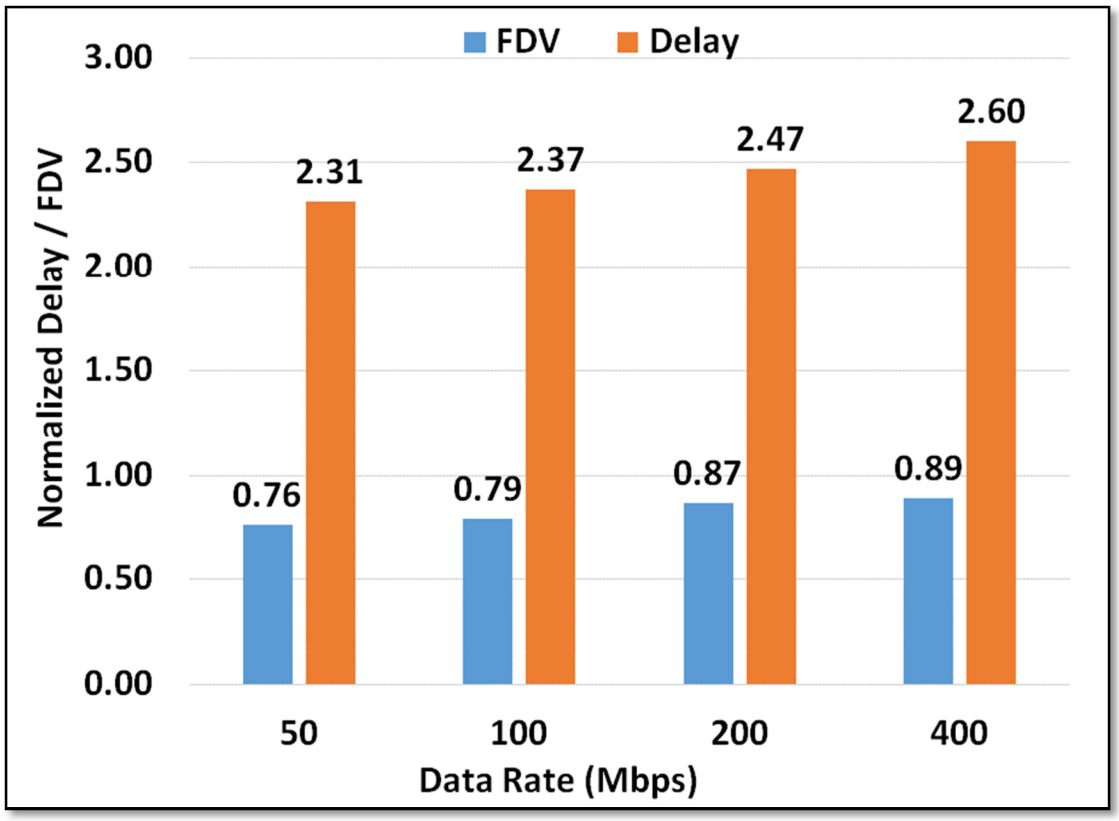

Figure.5.16. Frame delay and FDV of UPS traffic for scenario described in 5.4.2.

5.4.4 Buffering in the Ethernet Fronthaul

The size of the buffer to absorb the FDV *Bs*, is given by

$$B_s = 2B_D L_r, \qquad (14)$$

where B_D is the average buffer delay, given by:

$$B_D = 2\,\sigma_f, \qquad (15)$$

and L_r is the link rate and σ_f is the FDV.

The factor of two in (14) is due to the fact that for the buffer size, the delay variations of the first and last frame of the UPS traffic are being considered. This approach is sensible provided that frames are received in-order in the DU. The overall average delay DT, in the network can be given by:

$$D_T = B_D + \overline{D}, \qquad (16)$$

Where $\overline{D}$ is the average delay in the network without buffering .

In Fig. 5.17, the Cumulative Distribution Function (CDF) of the UPS FDV has been plotted for the scenario in sub-section 5.4.2 (Mixed traffic with different time sections allocation scenario). In addition, the FDV of the baseline case is also plotted in Fig. 5.17. In this scenario (scenario in sub-section 5.4.2), the maximum FDV with 32% utilization was 43 µs for a link rate of 1 Gbps. The buffer size with 32% utilization that is required to absorb the maximum FDV is 32000 bits while the total delay is 100.4 µs. The total delay violates the delay specification of the UPS (i.e. is larger than 75 µs).

In order for the total delay of the UPS with buffering to be less than the delay specification, the buffer can be designed so that only a percentage of the FDV is absorbed by the buffer. This allows to use FDV value less than the maximum FDV which leads to reduce the buffering delay and overall delay. However in implies that UPS traffic-carrying frames will be ignored (or dropped) for the current subframe. Fig. 5.18 shows a section (zoomed-in and annotated) of Fig. 5.17.

By using 97.4% of the FDV's CDF, the buffer size is reduced to a size of 48000 bits resulting in a total delay that is smaller than 75 µs. For the case of 64% utilization, however, the increased contention causes a higher average delay and maximum FDV for the UPS frames, and reduces the ability to absorb the FDV of the UPS traffic with respect to the delay specification. As shown in Fig. 5.18, with 64% utilization, only 96% of frames can be received within the requirements. On the other hand, with 16% and 8% utilization, 98% and 99% of frames can be received within the proposed requirements respectively.

Note that a significant percentage of the measured FDV is due to the baseline FDV variations. This is a result of the size variability of the transported frames, itself a result of variability in the traffic generation characteristics of the UPS-exposed control and user-plane traffic flows. The Ethernet mapping in this implementation is "overhead-optimized" and does not pad Ethernet frames to a fixed length. Padding would reduce (or eliminate) the baseline FDV but would lead to a reduction in achievable statistical multiplexing gains and an overall reduced efficiency in available capacity utilization. Considering just the excess value of the FDV (i.e. FDV values in excess of the baseline FDV), a significant improvement in the percentage of frames that can be received within the specifications is obtained, with all background traffic rates. For example, with a utilization of 64%, more than 99.9% of frames can be received within specification.

Table. V shows the achievable performance with 64% utilization considering different GbE technology link rates. The previous results up to this point have considered short fibre spans of 200m length.

With fibre link lengths less than 5 km, the percentage of frames that can be received within the requirements is higher than 93%. With 14 km fibre links, only 60% of the traffic is received within the specification. However, with 10 Gbps links, 100% of traffic can be transmitted within the specifications with a maximum 14 km fibre link length. This result shows how important reduced serialization delays are with overhead-optimized mapping techniques such as the one employed in this work.

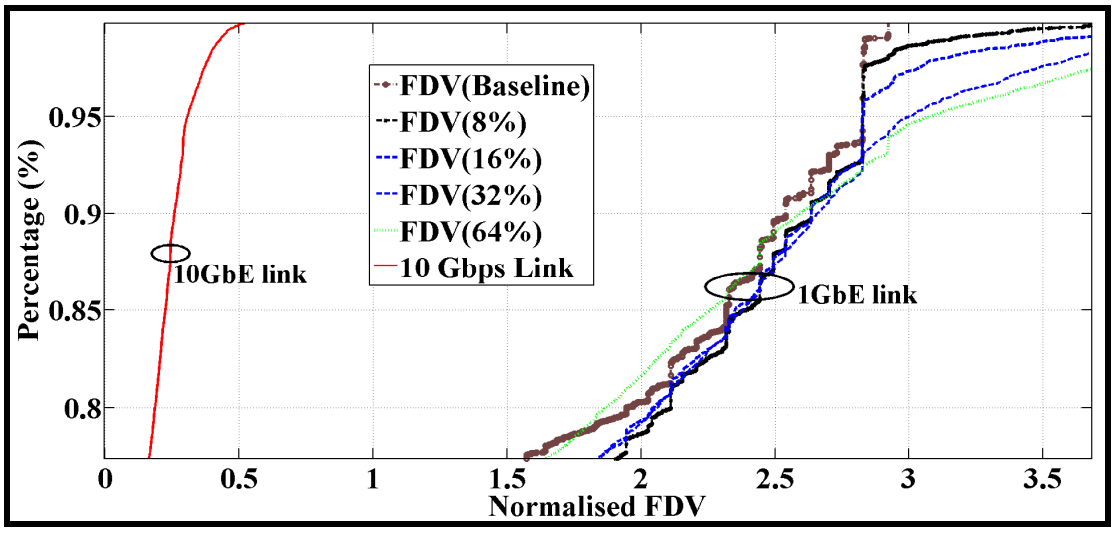

Figure.5.17. CDF of the UPS FDV in the Mixed Traffic with Different Time Sections Allocation scenario.

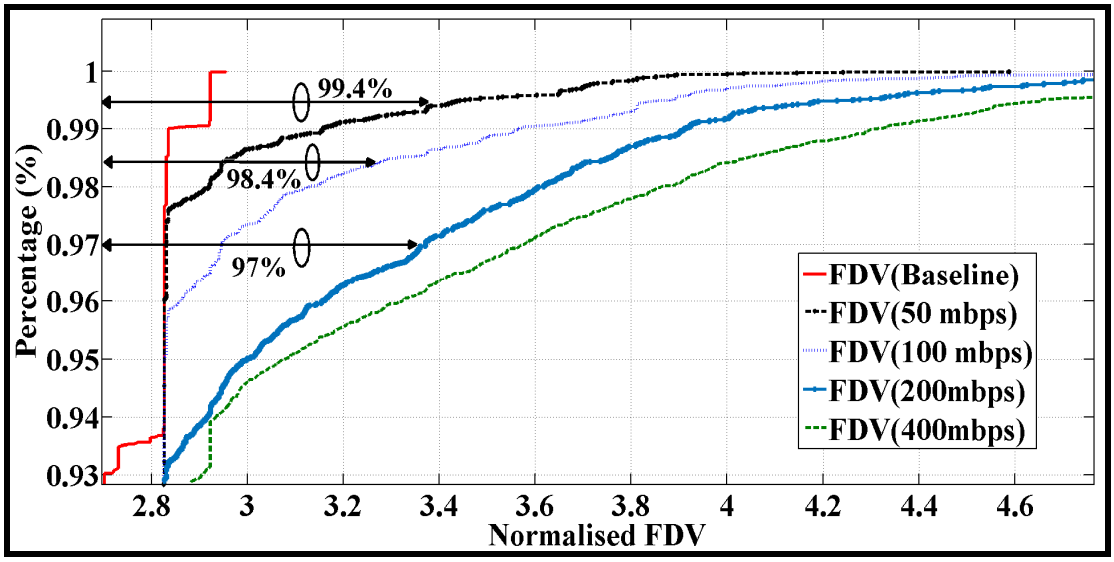

Figure.5.18. Zoomed UPS FDV's CDF results.

Table. V

Percentage Traffic within Specifications with Different Ethernet Links Lengths for 64% Utilization

Link Length (km)	Link Rate (1 Gbps)	Link Rate (10 Gbps)
0	97%	100%
0.2	96%	100%
1	95%	100%
5	93%	100%
13	60%	100%

5.4.5 Buffering in the Multi-Hop Ethernet Fronthaul

It has been shown in the previous subsection that using a 10Gbps links rate in a two hops network with 13 km overall links length can guarantee 100% of traffic to be transmitted within the specifications. Using more than two hops as shown in Fig. 5.19 with 13 km fronthaul can lead to a drop in the performance, as a percentage of traffic is transmitted outside the specifications due to the contention in each hop. The presented case considers that the UPS traffic transmitted alongside the same amount of traffic (background and CPRI traffic) in each hope and the incoming background traffic has

different transmission timing in each hop. The number of contention points C_N in the network is:

$$C_N = H_o - 1$$

where H_o is the number of hops in the network.

In Fig. 5.20, the CDF of the UPS FDV has been plotted for mixed traffic scenario with 13 km total links lengths, 10Gbps links rates and different numbers of contention points.

Table. VI shows the achievable performance with 64% utilization and 10 Gbps links considering different number of hops. The results show that with five hops and 13 km link lengths, less than 80% of UPS traffic can be received within the specifications. With 7 km link lengths, 100% of the traffic can be received within the specifications while with 10 km link lengths, 97% of the UPS traffic can be received within the specifications. Reducing the total Link lengths and/or the number of contention points or using higher link rates such as 40 Gbps or 100 Gbps links are the options to overcome the drop in the performance and guarantee that all the frames are transmitted according to the requirements.

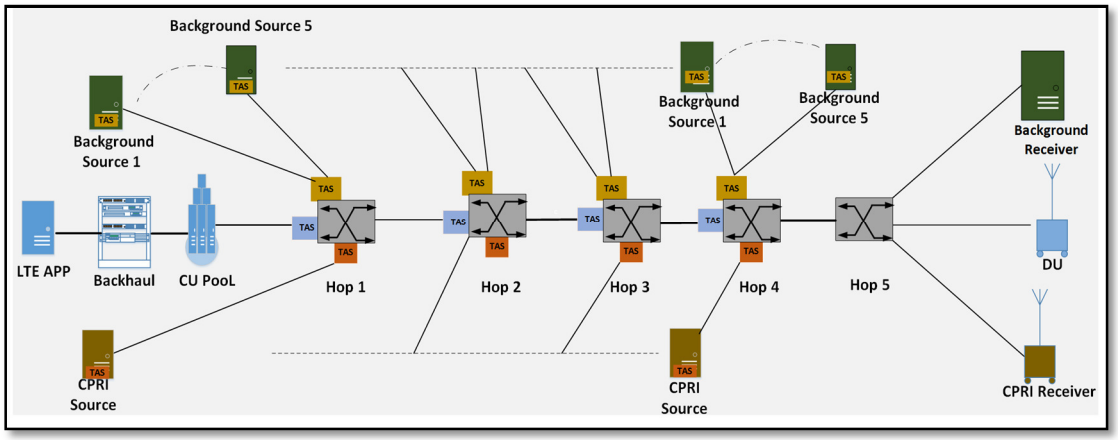

Figure.5.19. the simulation set-up of the Ethernet fronthaul with TAS and five hops.

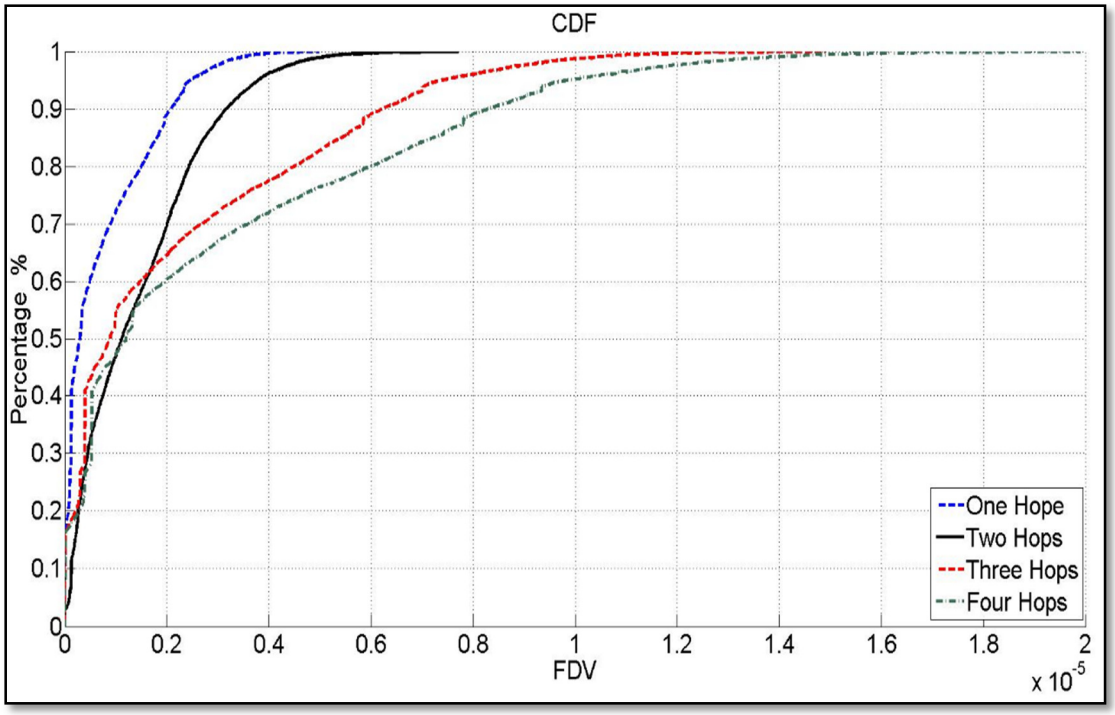

Figure.5.20. CDF of the UPS FDV in the mixed traffic with 10Gbps links, different Number of hops and 64% utilization.

Table. VI

Percentage Traffic within Specifications with Different Ethernet Links Lengths (13, 10 &7 Km) and Number of Hops for 64% utilization

Links Length (Km)	No of Contention points (no)	No of Hops (no)	Link Rate (1 Gbps)
13	1	2	100%
	2	3	99%
	3	4	83.5%
	4	5	76.3%
10	1	2	100%
	2	3	100%
	3	4	99%
	4	5	97%
7	1	2	100%
	2	3	100%
	3	4	100%
	4	5	100%

5.5 Conclusion

A model-based design, implemented in Riverbed-modeler, for an Upper Physical Split in an Ethernet fronthaul with mixed traffic and scheduling based on a TAS has been presented.

The model considered the proposed RoE frames, the encapsulation in the Ethernet frame and the transmission of the encapsulated UPS LTE traffic over an Ethernet network with two hops and small cell dimensions.

Contention in the Ethernet fronthaul is shown to cause a significant increase in the average and maximum FDV of UPS and CPRI-type traffic, leading to violation of FDV and delay specifications. In addition to contention-induced FDV, an overhead-optimized mapping approach to Ethernet and ROE, while leading to a particular increase in the statistical multiplexing gains, results in a finite (non-zero) baseline FDV, a result of variability in the traffic generation characteristics and encapsulation methods of the UPS-exposed flows.

TAS can remove the FDV for both traffic types when they are allocated to the PS. However, variability in the UPS traffic generation timings can cause frames to exceed their TAS allocation and be buffered for transmission to the next TW, violating delay specifications. This can be solved by either changing the traffic generation characteristic of the UPS traffic to a bursty one, for example, by having a CU that generates all physical channel data (for a subframe) at the start of a subframe (instead of following air interface timings), or by allocating the UPS traffic to the BES. The former will increase the complexity in the transmission and the implementation of the DU as the DU should play out the traffic according to the air interface timing. Allocating the UPS traffic to the BES can mitigate the delay problem but will cause an increase in the FDV due to contention with other traffic in the BES. Buffering is proposed to overcome this problem and to "absorb" the FDV. The buffer should be designed carefully so as not to violate the end-to-end delay requirements of the UPS and guarantee that most of the frames are received within delay specifications. The results show that while using low-rate Ethernet links limits the ability to use longer fibre links due to the limited delay threshold, using

10 Gigabit Ethernet links will potentially allow the use of longer fibre links (>10 km) with 100% of frames transmitted within the specifications. The results show as well that using multi-hops is challenging as the FDV can build up and as a result, the queuing at the end station should be reconsidered.

The performance of the solution with 10Gbps links reduced when increasing the number of hops in the Ethernet fronthaul network. The performance dropped by 22% with 13 km fronthaul and 5 hops. Reducing the overall link lengths or increasing the link rates in this case will overcome this problem and allow all of the UPS traffic to be transmitted according to the specifications.

6 Conclusions and Future Work

6.1 Conclusions

Comprehensive investigations for the queuing regimes in an Ethernet fronthaul have been undertaken in this work. Different traffic types with different rates, priorities and transmission patterns have been examined. The frame delay, frame inter-arrival delay and FDV of the different time-sensitive traffic types that are proposed to be transmitted in the Ethernet fronthaul are the focus of this thesis.

In Chapter 3, the performance of the SP and WRR queuing regimes in the proposed switched fronthaul for the future C-RAN were examined and reported. The transmission of emulated LTE base station and bursty background traffic and their contention in a two-hop switched network was investigated. The focus of the measurement was the LTE traffic. The results showed the importance of using a suitable queuing regime in the fronthaul network based on the priority and the time sensitivity of each individual stream. The WRR regime provides the capability to balance and distribute the available trunk capacity between different streams in the fronthaul network. The results demonstrated that the background traffic rate and Ethernet frame size of the background traffic affects the mean and STD values of the inter-arrival frame delay of the LTE traffic, with the mean of the inter-arrival frame delay increased by approximately 2.6% on average for each weight and the STD increased by approximately 13.7%. Using larger frame sizes (jumbo frames) will increase the mean and STD of the inter-arrival delay with the WRR regime. SP can be used with delay/jitter sensitive traffic where the mean and STD of inter-arrival frame delay is slightly increased. However, this regime does not guarantee that the time-sensitive traffic will not encounter higher delays and FDV, due to the lack of a pre-emptive mechanism. With SP, the frequency of occurrence of the contention has an important effect in increasing the mean and STD of the frame inter-arrival delay.

Equal-weight WRR and single queue (i.e. no-priority) regime cases have also shown that the equal-weight regime with small frame sizes results present a smaller mean frame inter-arrival delays than the no-priority case. When using Jumbo frames, the opposite behaviour is observed. This is significant as the number of available queues is generally limited to eight and might require two different traffic types to share the same queue.

In Chapter 4, an Opnet model design and implementation for the TAS based on the IEEE 802.1Qbv standard was presented. The Bridge-aware and Network-aware design of TAS were explained. The Bridge-aware TAS design considers the implementation of TAS in the Ethernet bridge ports. This design and implementation have the advantage of simplicity since it only considers applying the TAS in the Ethernet bridge ports and does not take into consideration any possible variations in the network timing due to various possible factors such as loss of synchronization. On the other hand, this design has many limitations such as dropping the frames that are transmitted outside the allocated time window and low immunity to timing variations in the network.

The Network-aware TAS design considers implementing TAS at the end stations as well as the Ethernet bridge ports. This design takes into account the time instability in the network and the frames that are received outside the allocated time window section. These frames will be queued at the end station ports and sent in the next time window. While the Network-aware TAS has more implementation and deployment complexity, it is more attractive for use as it has low frame loss and considers the timing variation and drifting in the network, which is one of the main concerns in the Ethernet fronthaul.

A number of scenarios with both design and implementation approaches are simulated to show the performance of the implemented TAS and compare it with the performance of the built in SP and WRR regimes in the Opnet/Riverbed simulation platform. The comparison focuses on the performance of the precision time protocol (PTP), in terms of FDV, when contention with background traffic takes place in an Ethernet fronthaul.

The simulation results show that the TAS is capable of minimising the contention-induced frame-delay variation for the high-priority traffic, while provisioning a guard period based on the maximum serialisation delay of a low-priority frame can lead to a complete removal of FDV.

Furthermore, the results show that the average and peak FDV of TAS are upper-bounded to the average and peak FDV of SP. This worst-case occurs when the GP in TAS is set to zero, but as the GP is increased both average and peak FDV reduce steadily, until FDV is completely eliminated. The GP that is required to eliminate FDV has a strong dependence on the statistical variations of the traffic sources. The stronger the variation, the closer the required GP needs to be to a full background traffic frame serialization delay. The obtained peak FDV results are extrapolated to worst-case PTP time stamping errors and it is shown how these errors reduce as the GP in TAS is increased. Allowing the buffering with TAS is fundamentally important to prevent dropping any high priority traffic frames which can instead be sent in the next time window. The buffering protection is important to prevent any continuous buffering at the end stations due to the limited time section. Even though the queuing here prevents any frame loss in the network, some traffic with very tight delay and FDV requirements such as CPRI (sub-section 2.2.1) might drop the frame due to long queuing time. The need for global scheduling to improve the use of the available network bandwidth with the buffering protection and manage the overall time section and sub-section allocation was discussed as well.

In Chapter 5, a model-based design, implemented in Riverbed-modeler, for an UPS in an Ethernet fronthaul with mixed traffic and scheduling based on a TAS was presented. The model considered the proposed RoE encapsulation, the framing in the Ethernet frame and the transmission of the encapsulated UPS LTE traffic over an Ethernet network with two hops and small cell dimensions.

Contention in the Ethernet fronthaul was shown to cause a significant increase in the average and maximum FDV of UPS and CPRI-type traffic, leading to violation of FDV and delay specifications. In addition to contention-induced FDV, an overhead-optimized mapping approach to Ethernet and RoE, while leading to a particular increase in the statistical multiplexing gains, was shown to result in a finite (non-zero) baseline FDV, a result of variability in the traffic generation characteristics and encapsulation methods of the UPS-exposed flows.

TAS can remove the FDV for both traffic types when they are allocated to the PS. However, variability in the UPS traffic generation timings can cause frames to exceed their TAS allocation and be buffered for transmission to the next TW, violating delay specifications. This can be solved by either changing the traffic generation characteristic of the UPS traffic to a bursty one, for example, by having a CU that generates all physical channel data (for a subframe) at the start of a subframe (instead of following air interface timings), or by allocating the UPS traffic to the BES. The former will increase the complexity in the transmission and the implementation of the DU as the DU should play out the traffic according to the air interface timing. Allocating the UPS traffic to the BES can mitigate the delay problem but will cause an increase in the FDV due to contention with other traffic in the BES. Buffering is proposed to overcome this problem and to absorb the FDV. The buffer should be designed carefully so that it does not violate the end-to-end delay requirements of the UPS and can guarantee that most of the frames are received within delay and FDV specifications. The results show that while using low-rate Ethernet links limits the ability to use longer fibre spans due to the limited delay threshold, using 10 Gigabit Ethernet links can potentially allow the use of longer fibre links (>10 km) with 100% of frames received within the specifications. Moreover, the results demonstrate that using multiple hops is challenging as the FDV can build up which makes reconsidering the queue size at the end stations in order to absorb the total induced FDV in the UPS traffic is essential. The performance in terms of FDV and delay (the amount of traffic that can be received within the delay and FDV specifications) of the solution with 10Gbps links has declined as a result of increasing the number of hops in the Ethernet fronthaul network since the FDV of each frame is increased and the amount of UPS traffic that can be sent within the specifications is reduced. The amount of traffic that can be received within the specifications is dropped by 22% with 13 km links and 5 hops. To overcome this decline in the delay and FDV performance and allow all the UPS traffic to be received according to the delay and FDV specifications, link lengths should be reduced to minimize the propagation delay or the link rates must be increased to reduce the serialization delay. Reducing the number of contention points in the fronthaul network can also improve the FDV and delay performance.

6.2 Main Contributions of the Thesis

The main contributions of the thesis are:

- Investigation of the advantages and the limitations of the traditional queuing regimes (SP, WRR) in the Ethernet fronthaul with emulated LTE traffic has been carried out for the first time.

In prior work [76], [77], the performance of both queuing regimes in controlling the delay was investigated, but not in an Ethernet fronthaul scenario where LTE I/Q samples traffic contend with background traffic.

Different use cases have been implemented by considering different factors such as the data rate and Ethernet frame size. These measurements considered, in addition to the standard Ethernet frames, jumbo frames, as these might be one of the options to handle the LTE and split traffic in the Ethernet fronthaul, as they can lead to high transport efficiency (a single header for a large chunk of data). Note, that SP is considered one of the scheduling profiles in 802.1 CM (see sub-section 2.4.1) and for that reason it has the potential to be used in the future fronthaul network. Both SP and WRR regimes are already implemented in the available Ethernet switches and can be used with low cost and complexity.

While fulfilling the time sensitive traffic delay and FDV requirements is important, other traffic types such as high layer split traffic (e.g., PDCP/RLC split traffic) have more relaxed requirements. SP and WRR can be potentially used with them in the Ethernet fronthaul network. Moreover, both queuing regimes can also be deployed with network slicing, where different traffic with differing requirements share the same physical links.

- Full modelling of the TAS based on 802.1Qbv standard in the Opnet/Riverbed simulation platform has been presented for the first time.

In previous work, limited implementation has been done for the TAS in the NS-3 simulation platform [65] by considering only the gating in the Ethernet switches. This implementation does not fully comply with the standard and the simulated scenarios

are limited to specific traffic types (CPRI, Background traffic) with specific rates and transmission patterns.

TAS has been selected to be modelled in this work due to the complexity and performance limitations of the frame pre-emption standard (see section 2.4.2). Different implementation approaches for this standard have been proposed, implemented and tested.

Testing TAS with PTP is very important due to the possible synchronization role of PTP in the future C-RAN. TAS performance with PTP has been tested with different traffic types, transmission patterns and rates which are transmitted alongside the PTP traffic in the Ethernet fronthaul for the first time. The time drifting due to different factors in the Ethernet network such as synchronization has been considered as well in the implementation of TAS. The importance of global scheduling has been investigated and discussed and the possible contribution of global scheduling in improving the statistical multiplexing gains is shown.

- For the first time, the implementation of the UPS in Opnet/Riverbed has been presented.

This split point (UPS) is important as it is the first split point in the physical layer that has the statistical multiplexing gain advantage. UPS requires limited amount of functionality to be moved from the CU to the DU. The implementation has considered the RoE as well, since it is proposed to be used as an intermediate sub-layer between LTE and Ethernet.

In the previous work [44] and [45], a software-emulated Option-6 split was presented, focusing on the latency performance [45], and the contribution of different transport channels in the Ethernet data rate [44]. In [16], a Mac/PHY split with CoMP was evaluated. In [41], PDCP-RLC split has been implemented in OAI and the increase in the throughput with different MCS has been shown.
To measure the effect of different traffic types on the Ethernet fronthaul, CPRI-type traffic has been modelled. The effect of CPRI-type traffic and other randomly generated traffic on the delay and FDV of the UPS has been measured and analysed.

- ❖ TAS has been used with the UPS traffic in the Ethernet fornthaul for the first time.

Thorough discussion and analysis for the performance of TAS with UPS has been carried out. Since UPS traffic is transmitted based on the air interface timing in this case, different time section sizes and allocation proposals have been used. Analysing and discussing a case where the high priority traffic has random transmission pattern through TAS is important as no guarantee that all the high priority traffic is temporally aligned with the TAS window in such a case is possible. Queueing at the end station has been proposed and analysed, which has not been presented in any prior work. UPS FDV with different link rates and number of hops which is suggested to be part of the network topology and structure in the Ethernet fronthaul network has been presented and discussed as well.

6.3 Future Work

For future work, further development for the TAS and UPS can be carried out in order to explore more of their potential as well as their limitations. In addition, more scenarios and use cases can be simulated, studied and compared. All of this will be discussed in the following paragraphs.

With the TAS model, dynamic windowing can be considered to overcome the loss of bandwidth due to the data rate variation to improve the overall statistical multiplexing gain in the network. Dynamic TAS can be implemented either in the same switching node or by implementing a global scheduler that updates the section sizes in the switching units in the fronthaul network based on the transmitted data rate and its transmission pattern during a specific time period.

Measurements for the delay and FDV for the traffic with different priorities can be performed in Opnet/Riverbed to show the effect of dynamic windowing in the fronthaul network on the transmitted frames in each traffic flow.

The loss of synchronization effects on the TAS is another area to be explored, as synchronization is one of the challenges for the implementation of TAS in the Ethernet

fronthaul network and generally in the use of Ethernet technology in the fronthaul network. In the current work, the time drifting has been considered in the downlink direction but more investigation can be done on the effect of the contention on the uplink and downlink, especially with PTP.

With UPS, the current scenarios can be extended with more traffic source types, DUs, receivers and Ethernet switches (hops) in the Ethernet fronthaul network to measure and examine the mutual effects between the different traffic types and the performance of TAS with such scenarios.

Improving the modelling of the UPS in Opnet/Riverbed to allow the UE to connect through the fronthaul to the DU instead of having the direct connection to the eNodeB in the current implementation can be undertaken. This requires a significant modification for the UE to recognize the implemented RRH and establish the connection with it. It also requires the RRH to provide the UE with some control information that usually in Opnet/riverbed is shared with the UE by direct memory access. A study for the contention effect in the Ethernet fronthaul bridges and switches on the different radio performance factors, such as retransmission and dropped packet rates can be done as soon as the UE is connected to the DU.

Different handover cases can also be tested to check the effect of fronthaul contention on the delay requirements of the handover. The current work considers the contention and the traffic requirements in the downlink only; the uplink direction can also be considered in any future work, especially when the UE is connected to the DU.

Implementing and testing cell stretching, where the size of the mobile cell shrinks or expands based on the location of the UE, density of the UEs and the requirements of each UE within the cell, with UPS can also be performed in Opnet/Riverbed. Cell stretching is one of the possible technique that can be used in the future mobile network.

Implementation of higher layers splits such as PDCP-RLC in Opnet/Riverbed can be done as the acquired experience is obtained. The performance of both splits with the Ethernet fronthaul can be measured and compared. The effect of the delay and FDV in the

Ethernet fronthaul on the requirements of both split traffic points and comparing the efficiency of TAS with each of them would be a beneficial investigation. The effect of the delay and FDV in the Ethernet fronthaul network on the radio performance with both split points is also an area to be explored.

Bibliography

[1] A. Radwan, K. M. S. Huq, S. Mumtaz, K. F. Tsang and J. Rodriguez, “Low-cost On-demand C-RAN based Mobile Small-cells,” IEEE Access, vol. 4, pp. 2331-2339, 2016.

[2] P. Chanclou, Z. Tayq, P. Turnbull, V. Jungnickel, L. Fernandez del Rosal, P. Assimakopoulos, N.Gomes, Y. Kai, H. Zhu, M. Parker, S. Walker, C. Magurawalage, K. Yang, H. Thomas, M. C. Torres, I. C. Rivera and F. J. H. Gonzales, “D2.1 iCIRRUS - Intelligent C-RAN Architecture,” 2015.

[3] C. Raack et al., “Centralised versus distributed radio access networks: Wireless integration into long reach passive optical networks,” in Proc.Conf. Telecommun., Media Internet Techno-Econ., Nov. 2015, pp. 1–8.

[4] M. Jaber, D. Owens, M. Imran, R. Tafazolli, and A. Tukmanov, "A joint backhaul and RAN perspective on the benefits of centralised RAN functions," in IEEE International Conference on Communications (ICC), Workshops, (Kuala Lumpur, Malaysia), May 2016.

[5] China Mobile Research Institute, “C-RAN The Road Towards Green RAN,” White Paper v.2.6, Sep.2013.

[6] M. HadZialic, B. Dosenovic, M. Dzaferagic, and J. Musovic. Cloud-RAN: Innovative radio access network architecture. In ELMAR, 2013 55th International Symposium, pages 115–120, Sept 2013.

[7] L. Fernandez del Rosal, V. Jungnickel, D. Muench, H. Griesser, P. Assimakopoulos, N. Gomes, Y.Kai, H. Thomas, M. Parker, C. Magurawalage, K. Wang, P. Chanclou and V. D, “D3.2 iCirrus -Preliminary Fronthaul Architecture Proposal,” 2016.

[8] Z. Tayq et al., “Real time demonstration of fronthaul transport over a mix 681 of analogue & digital RoF,” in Proc. Int. Conf. Transparent Opt. Netw., 682 Girona, Spain, 2017, pp. 1–4.

[9] N. Gomes, P. Chanclou, P. Turnbull, A. Magee and V.Jungnickel, “Fronthaul evolution: From CPRI to Ethernet,” Optical Fiber Technology, vol. 26, no. part A, p. OFC, 2015.

[10] P. Assimakopoulos, J. Zou, K. Habel, J.-P. Elbers, V. Jungnickel and N. J. Gomes, “A Converged Evolved Ethernet Fronthaul for the 5G Era,” IEEE Journal on Selected Areas in Communications , vol. 36 , no. 11, pp. 2528 - 2537, 2018.

[11] D. Chitimalla, K. Kondepu, L. Valcarenghi, M. Tornatore, and B.Mukherjee, “5G Fronthaul-Latency and Jitter Studies of CPRI Over Ethernet,” J. Opt. Commun. Netw. 9, 172-182, 2017.

[12] Open Base Station Architecture Initiative, “Reference Point 3 Specification,” [Online]. Available: http://www.obsai.com/specifications.htm.

[13] J. Duan, X. Lagrange, and F. Guilloud, “Performance analysis of several functional splits in C-RAN,” in Proc. IEEE 83rd Veh. Technol. Conf.,May 2016, pp. 1–5.

[14] I. Koutsopoulos, “Optimal functional split selection and scheduling policies in 5G radio access networks,” in Proc. IEEE Int. Conf. Commun.Workshops, May 2017, pp. 993–998.

[15] L. M. P. Larsen, A. Checko and H. L. Christiansen, “A Survey of the Functional Splits Proposed for 5G Mobile Crosshaul Networks,” IEEE COMMUN SURV TUT, pp. 1-24, 2018.

[16] 3GPP, "Radio access architecture and interfaces, (Release 15) 3GPP TR 38.801".

[17] Chih-Lin I; Jinri Huang; Ran Duan; Chunfeng Cui; Jiang, J.X.; Lei Li, ”Recent Progress on C-RAN Centralization and Cloudification,” Access, IEEE , vol.2, no., pp.1030,1039, 2014.

[18] NGMN Alliance, “5G White Paper,” 2015. [Online]. Available: https://www.ngmn.org/uploads/media/NGMN_5G_White_Paper_V1_0.pdf.

[19] China Mobile Research Institute, “White Paper of Next Generation Fronthaul Interface v1.0,” 2015.

[20] P. P.-H. Kuo and A. Mourad, “Millimeter wave for 5G mobile fronthaul and backhaul,” *2017 European Conference on Networks and Communications (EuCNC)*, 2017.

[21] D. Pliatsios, P. Sarigiannidis, S. Goudos, and G. K. Karagiannidis, ‘‘Realizing 5G vision through Cloud RAN: Technologies, challenges, and trends,’’ EURASIP J. Wireless Commun. Netw., vol. 2018, no. 1, p. 136, May 2018.

[22] A. Ericsson, H. T. Co.Ltd, N. Corporation, N. Networks and Alcatel-Lucent, “CPRI Specification V7.0 (2015-10-09): Common Public Radio Interface (CPRI); Interface Specification,,” [Online]. Available: http://www.cpri.info.

[23] L. Valcarenghi, K. Kondepu, and P. Castoldi, “Time- Versus Size-Based CPRI in Ethernet Encapsulation for Next Generation Reconfigurable Fronthaul,” J. Opt. Commun. Netw. 9, D64-D73, 2017.

[24] P. Turnbull, H. Thomas, D. Venmani, P. Chanclou, V. Jungnickel, L. Fernandez del Rosal, M.C. Parker, P.Assimakopoulos, M. K. Al-Hares, N. Gomes, D3.1 iCIRRUS: “Verification of Ethernet as transport protocol for fronthaul /midhaul", 2015.

[25] P. Assimakopoulos, M. K, A-Hares, N. Gomes., "Switched Ethernet fronthaul architecture for cloud-radio access networks", IEEE/OSA J. of Opt. Comm. Netw., vol. 8, no. 12, pp. B135-B146, 2016.

[26] IEEE, “IEEE 802.1Q-2018 - IEEE Standard for Local and Metropolitan Area Networks—Bridges and Bridged Networks,” IEEE, 2018. [Online]. Available: https://standards.ieee.org/standard/802_1Q-2018.html.

[27] N.J. Gomes et al., “Boosting 5G through Ethernet: How evolved fronthaul can take next-generation mobile to the next level,” IEEE Vehicular Technol. Mag., vol. 13, no. 1, pp. 74-84, 2018.

[28] N. J. Gomes, P. Assimakopoulos, J.-P. Elbers, D. Münch, P. Chanclou and V. Jungnickel, “Concepts and requirements for the Ethernet-based evolved fronthaul,” in 2017 IEEE Photonics Society Summer Topical Meeting Series (SUM), San Juan, 2017.

[29] ITU-T, Recommendation ITU-T G.8262/Y.1362 : Timing characteristics of synchronous Ethernet equipment slave clock.

[30] IEEE 1588-2008, "Standard for a Precision Clock Synchronization Protocol for Networked Measurement and Control Systems".

[31] I. Freire, I. Sousa and A. Klautau. Analysis and Evaluation of End-to-End PTP Synchronization for Ethernet-based Fronthaul. Dec. 2016 Global Communications Conference (GLOBECOM), 2016 IEEE.

[32] Standard for Radio Over Ethernet Encapsulations and Mappings,” IEEE Standard P1914.3 [Online]. Available: https://standards.ieee.org/content/ieee-standards/en/standard/1914_3-2018.html

[33] M. J. V. Monroy, “Latency and bit-error-rate evaluation for radio-over-ethernet in optical fiber front-haul networks,” Optical Switching and Networking, vol. 27, pp. 88-92, 2018.

[34] ETSI, “ETSI TS 136 300,” July 2010. [Online]. Available: https://www.etsi.org/deliver/etsi_ts/136300_136399/136300/09.04.00_60/ts_136300v090400p.pdf. [Accessed 15 January 2019].

[35] ETSI (Jan. 2011), “ETSI TS 136 300 V10.2.0, Evolved Universal Terrestrial Radio Access (E-UTRA) and Evolved Universal Terrestrial Radio Access Network (E-UTRAN); Overal description,” [Online]. Available: https://www.etsi.org/deliver/etsi_ts/136300_136399/136300/10.02.00_60/ts_136300v100200p.pdf.

[36] ETSI, “ETSI TS 136 201,” April 2009. [Online]. Available: https://www.etsi.org/deliver/etsi_ts/136200_136299/136201/08.03.00_60/ts_136201v080300p.pdf. [Accessed 22 October 2018].

[37] C.-Y. Chang et al., “FlexCRAN: A flexible functional split framework over ethernet fronthaul in Cloud-RAN,” in ICC 2017, IEEE International Conference on Communication, May 21-25, 2017, Paris, France, 2017.

[38] NGMN, "NGMN Overview on 5G RAN Functional Decomposition,"2018

[39] I. A. Alimi, A. L. Teixeira, and P. P. Monteiro, “Toward an efficient c-ran optical fronthaul for the future networks: A tutorial on technologies, requirements, challenges, and solutions,” IEEE Communications Surveys Tutorials, vol. 20, no. 1, pp. 708–769, Firstquarter 2018.

[40] U. Dotsch, M. Doll, H.-P. Mayer, F. Schaich, J. Segel, and P. Sehier,“Quantitative analysis of split base station processing and determination of advantageous architectures for LTE,” Bell Labs Tech. J., vol. 18, no. 1, pp. 105–128, Jun. 2013.

[41] N. Makrisy, P. Basarasy, T. Korakisy, N. Nikaein, and L. Tassiulas,“Experimental evaluation of functional splits for 5G Cloud-RANs,” in IEEE ICC, May 2017.

[42] M. Dryjanski and M. Rahnema, From LTE to LTE-Advanced Pro and 5G, Boston: Artech House, 2017.

[43] A. Maeder et al., “Towards a flexible functional split for cloud-RAN networks,” in Proc. Eur. Conf. Netw. Commun. (EuCNC), Bologna, Italy, Jun. 2014, pp. 1–5.

[44] G. S. Birring, P. Assimakopoulos, and N. J. Gomes, “An Ethernetbased fronthaul implementation with MAC/PHY split LTE processing,” in Proc. Global Commun. Conf., Singapore, Dec. 2017, pp. 1–6.

[45] G. Mountaser, M. Lema, T. Mahmoodi, and M. Dohler, ‘‘On the feasibility of MAC and PHY split in Cloud RAN,’’ in Proc. IEEE WCNC, Mar. 2017,p. 1.

[46] D. Harutyunyan and R. Riggio, “Flex5g: Flexible functional split in 5g networks,” IEEE Transactions on Network and Service Management, pp.1–1, 2018.

[47] M. Z. Chowdhury, M. T. Hossan, A. Islam, and Y. M. Jang, ‘‘A comparative survey of optical wireless technologies: Architectures and applications,’’ IEEE Access, vol. 6, pp. 9819–9840, 2018.

[48] Ge, X., Tu, S., Mao, G., et al.: ‘5G ultra-dense cellular networks’, IEEE Wirel. Commun., 2016, 23, (1), pp. 72–79.

[49] “N. J. Gomes et al., “The new flexible mobile fronthaul: Digital or analog, or both?” in Proc. ICTON, 2016”.

[50] “Small Cell Forum, “Crossing the Chasm: Small Cells Industry 2015,” 2015. [Online]. Available: http://scf.io/en/get_email.php?paper=2079. [Accessed 2019].

[51] ITU, “Recommendation ITU-T G.8261.1/Y.1361 : Packet delay variation network limits applicable to packet-based methods (Frequency synchronization).,” [Online].

[52] XENA Networks, “Measuring Frame Delay Variation (jitter),” [Online].Available: https://www.xenanetworks.com/wp-content/uploads/xenadocuments/app-notes/Measuring_Frame_Delay_Variation.pdf . [Accessed January 2019].

[53] Small Cell Forum, “Small Cell Virtualization Functional Splits and Use Cases,” June 2015. [Online]. Available: http://scf.io/en/get_email.php?doc=159.

[54] Microsemi, “Assisted Partial Timing Support (APTS,” Novemebr 2018. [Online]. Available: https://www.microsemi.com/document-portal/doc_view/1243879-assisted-partial-timing-support-apts-white-paper. [Accessed January 2019].

[55] I. Saidu, S. Subramaniam, A. Jaafar, and Z. A. Zukarnain, “A load-aware weighted round-robin algorithm for IEEE 802.16 networks,” EURASIP Journal on Wireless Communications and Networking, vol. 2014, no. 1, 2014.

[56] M. K. Al-Hares, P. Assimakopoulos, S. Hill, and N. J. Gomes “The effect of different queuing regime on a switched Ethernet fronthaul,” in Proc. Int. Conf. on Transp .Optic. Net. (ICTON), Trento, Italy, 2016, pp. 1-4.

[57] J. Segarra, V. Sales, and J. Prat: Queue Management and Priority Scheduling Disciplines for QoS Control in Wavelength Routed OBS (WROBS) Access Networks, in Proc. ICTON 2006, Nottingham,United Kingdom, pp. 207-214, 2006.

[58] Y. Qian, Z. Lu, and Q. Dou, “QoS Scheduling for NoCs: Strict Priority Queueing versus Weighted Round Robin”, In the Proceedings of the 28th International Conference on Computer Design (ICCD’10), pp. 52-59, Amerstedam, The Netherlands, 2010.

[59] IEEE, “802.1CM - Time-Sensitive Networking for Fronthaul,” [Online]. Available: http://www.ieee802.org/1/pages/802.1cm.html. [Accessed Dec 2018].

[60] IEEE Standard Association, “IEEE Standard for Local and metropolitan area networks,” 7 May 2018. [Online]. Available: https:// ieeexplore.ieee.org/stamp/stamp.jsp?tp=&arnumber=8376066. [Accessed December 2018].

[61] IEEE8021, IEEE P802.1Qbv Draft 3.1 Enhancement for scheduled traffic, 2015.

[62] M. K. Al-Hares, P. Assimakopoulos, D. Muench, and N. J. Gomes,“Modeling Time Aware Shaping in an Ethernet Fronthaul,” in Proc. IEEE Global. commun. Conf. (GLOBECOM), Singapore, 2017, pp.1-6.

[63] M. K. Al-Hares, P. Assimakopoulos, D. Muench and N. J. Gomes, “Scheduling in an Ethernet fronthaul network,” in Proc. Eoropean Conf. on Networks and Commun. (EUCNC), Oulu, Finland, 2017.

[64] T. Wan and P. Ashwood-Smith, “A Performance Study of CPRI over Ethernet with IEEE 802.1Qbu and 802.1Qbv Enhancements,” in Global Commun. Conf. (GLOBECOM), San Diego, CA, 2015, pp. 1-6

[65] ns-3, “ns-3,” ns-3, [Online]. Available: http://www.nsnam.org.

[66] J. Kim, B. Y. Lee, and J. Park, “Preemptive switched Ethernet for real-time process control system,” 2013 11th IEEE International Conference on Industrial Informatics (INDIN), 2013.

[67] W.-K. Jia, G.-H. Liu, and Y.-C. Chen, “Performance evaluation of ieee 802.1qbu: Experimental and simulation results,” in 38th IEEE Conference on Local Computer Networks (LCN 2013), Oct 2013, pp. 659–662.

[68] D. Thiele and R. Ernst "Formal worst-case performance analysis of time sensitive Ethernet with frame preemption", IEEE ETFA September 2016 in Berlin, Germany.

[69] Riverbed, “https://www.riverbed.com/gb/,” Riverbed, 2019. [Online]. Available: https://www.riverbed.com/gb/. [Accessed December 2018].

[70] 3GPP, "3GPP Specification series," 2016. [Online]. Available: http://www.3gpp.org/DynaReport/23-series.htm. [Accessed December 2018].

[71] 3GPP, “3GPP Specification series,” 2016. [Online]. Available: http://www.3gpp.org/dynareport/36-series.htm. [Accessed 22 January 2019].

[72] 3GPP, “3GPP Specification series,” 2016. [Online]. Available: https://portal.3gpp.org/desktopmodules/Specifications/SpecificationDetails.aspx?specificationId=1382. [Accessed December 2018].

[73] 3GPP, “Spatial channel model for Multiple Input Multiple Output (MIMO) simulations,” 4 July 2017. [Online]. Available: https://portal.3gpp.org/desktopmodules/Specifications/SpecificationDetails.aspx?specificationId=1382. [Accessed January 2019].

[74] 3GPP, “Non-Access-Stratum (NAS) protocol for Evolved Packet System (EPS); Stage 3,” 1 January 2015. [Online]. Available: https://portal.3gpp.org/desktopmodules/Specifications/SpecificationDetails.aspx?specificationId=1072. [Accessed 2 December 2018].

[75] IEEE, Standard and Associatition, “IEEE 802.3-2018 - IEEE Standard for Ethernet,” June 2018. [Online]. Available: https://standards.ieee.org/standard/802_3-2018.html. [Accessed December 2018].

[76] Y. Zhang and P.G. Harrison, “Performance of a Priority-Weighted Round Robin Mechanism for Differentiated Service Networks,” Proceedings of 16th International Conference on Computer Communications and Networks, 2007, pp. 1198-1203, Aug. 2007.

[77] J. Diemer, D. Thiele, and R. Ernst, “Formal worst-case timing analysis of Ethernet topologies with strict-priority and AVB switching,” in Industrial Embedded Systems (SIES), 2012 7th IEEE International Symposium on. IEEE, 2012, pp. 1–10.

[78] Hp, “3Com® Switch 5500 Family,” [Online]. Available: https://support.hpe.com/hpsc/doc/public/display?docId=emr_na-c02582204

[79] A. Astarloa, J. Lazaro, U. Bidarte, J. A. Araujo, and N. Moreira, “FPGA implemented cut-through vs store-and-forward switches for reliable ethernet networks,” Design of Circuits and Integrated Systems, 2014.

[80] R. Veisllari, et al., “Experimental demonstration of 100Gb/s optical packet network for mobile fronthaul with load-independent ultra-low latency”, ECOC 2017.

[81] C.-Y. Chang, N. Nikaein, and T. Spyropoulos, “Impact of Packetization and Scheduling on C-RAN Fronthaul Performance,” 2016 IEEE Global Communications Conference (GLOBECOM), 2016.

[82] C. Cox, An Introduction to LTE: LTE, LTE-Advanced, SAE, VoLTE and 4G Mobile Communications, India: Wiley, 2014.